OPEN ACCESS

Repository of the Max Delbrück Center for Molecular Medicine (MDC) in the Helmholtz Association

http://edoc.mdc-berlin.de/21411/

Downregulation of odd-skipped related 2, a novel regulator of epithelial-mesenchymal transition, enables efficient somatic cell reprogramming

Anh L.P.H., Nishimura K., Kuno A., Nguyen T.L., Kato T., Ohtaka M., Nakanishi M., Sugihara E., Sato T.A., Hayashi Y., Fukuda A., Hisatake K.

This is the final version of the accepted manuscript.

This is a pre-copyedited, author-produced PDF of an article accepted for publication in *Stem Cells* following peer review. The version of record

Le Phuong Hoang Anh, Ken Nishimura et al., Downregulation of Odd-Skipped Related 2, a Novel Regulator of Epithelial-Mesenchymal Transition, Enables Efficient Somatic Cell Reprogramming, Stem Cells, Volume 40, Issue 4, April 2022, Pages 397–410

is available online at: https://academic.oup.com/stmcls/article-abstract/40/4/397/6536984 or 10.1093/stmcls/sxac012 .

Stem Cells
2022 APR 29 ; 40(4): 397-410
2022 FEB 25 (first published online: final publication)
doi: 10.1093/stmcls/sxac012

Publisher: Oxford University Press

Copyright © The Author(s) 2022. Published by Oxford University Press. All rights reserved. For permissions, please email: journals.permissions@oup.com.

Downregulation of Odd-Skipped Related 2, a Novel Regulator of Epithelial-Mesenchymal Transition, Enables Efficient Somatic Cell Reprogramming

Le Phuong Hoang Anh[1], Ken Nishimura[1], Akihiro Kuno[2,3], Nguyen Thuy Linh[1,9], Tetsuo Kato[1], Manami Ohtaka[4], Mahito Nakanishi[4,5], Eiji Sugihara[6,7], Taka-Aki Sato[6], Yohei Hayashi[8], Aya Fukuda[1], Koji Hisatake[1]

[1]Laboratory of Gene Regulation, Faculty of Medicine, University of Tsukuba, Tsukuba, Ibaraki 305-8575, Japan.

[2]Department of Anatomy and Embryology, Faculty of Medicine, University of Tsukuba, Tsukuba, Ibaraki 305-8575, Japan.

[3]Ph.D. Program in Human Biology, School of Integrative and Global Majors, University of Tsukuba, Tsukuba, Ibaraki 305-8575, Japan

[4]TOKIWA-Bio, Inc. Tsukuba, Ibaraki 305-0047, Japan

[5]National Institute of Advanced Industrial Science and Technology (AIST), Tsukuba, Ibaraki 305-8562, Japan

[6]Research and Development Center for Precision Medicine, University of Tsukuba, Tsukuba, Ibaraki 305-8550, Japan.

[7]Center for Joint Research Facilities Support, Research Promotion and Support Headquarters, Fujita Health University, Toyoake, Aichi 470-1192, Japan

[8]iPS Cell Advanced Characterization and Development Team, Bioresource Research Center, RIKEN, Tsukuba, Ibaraki 305-0074, Japan

[9]Max Delbrück Center for Molecular Medicine, 13125 Berlin, Germany; Humboldt-University of Berlin, Institute of Biology, 10115 Berlin, Germany

Author contributions

Le Phuong Hoang Anh: Collection and assembly of data, Data analysis and interpretation

Ken Nishimura: Conception and design, Financial support, Collection and assembly of data, Data analysis and interpretation, Manuscript writing

Akihiro Kuno: Data analysis and interpretation

Nguyen Thuy Linh: Collection and assembly of data, Data analysis and interpretation

Tetsuo Kato: Collection and assembly of data, Data analysis and interpretation

Manami Ohtaka: Provision of material

© The Author(s) 2022. Published by Oxford University Press. All rights reserved. For permissions, please email: journals.permissions@oup.com.

Mahito Nakanishi: Provision of material

Eiji Sugihara: Collection and assembly of data

Taka-Aki Sato: Collection and assembly of data

Yohei Hayashi: Collection and assembly of data

Aya Fukuda: Financial support, Manuscript writing

Koji Hisatake: Conception and design, Financial support, Manuscript writing, Final approval of manuscript

Correspondence

Ken Nishimura, PhD, and Koji Hisatake, MD, PhD, 1-1-1 Tennodai, Tsukuba, Ibaraki 305-8575, Japan

Email: ken-nishimura@md.tsukuba.ac.jp (K.N.) and kojihisa@md.tsukuba.ac.jp (K.H.)

Funding information

JSPS KAKENHI Grant Numbers JP16K07244 (to K.N), JP19H03203 (to K.N), JP19K22945 (to K.N), JP19K07343 (to A.F.), P17H04036 (to K.H.), and JP21H02678 (to K.H.); Takeda Science Foundation (to K.N.)

Abstract

Somatic cell reprogramming proceeds through a series of events to generate induced pluripotent stem cells (iPSCs). The early stage of reprogramming of mouse embryonic fibroblasts (MEFs) is characterized by rapid cell proliferation and morphological changes, which are accompanied by downregulation of mesenchyme-associated genes. However, the functional relevance of their downregulation to reprogramming remains poorly defined. In this study, we have screened transcriptional regulators that are downregulated immediately upon reprogramming, presumably through direct targeting by reprogramming factors. To test if these transcriptional regulators impact reprogramming when expressed continuously, we generated an expression vector that harbors human cytomegalovirus upstream open reading frame 2 (uORF2), which reduces translation to minimize the detrimental effect of an expressed protein. Screening of transcriptional regulators with this expression vector revealed that downregulation of odd-skipped related 2 (*Osr2*) is crucial for efficient reprogramming. Using a cell-based model for epithelial-mesenchymal transition (EMT), we show that *Osr2* is a novel EMT regulator that acts through induction of TGF-β signaling. During reprogramming, *Osr2* downregulation not only diminishes TGF-β signaling but also allows activation of Wnt signaling, thus promoting mesenchymal-epithelial transition (MET) toward acquisition of pluripotency. Our results illuminate the functional significance of *Osr2* downregulation in erasing the mesenchymal phenotype at an early stage of somatic cell reprogramming.

Key words

Osr2, reprogramming, Epithelial-Mesenchymal Transition, TGF-β, Wnt

Graphical abstract

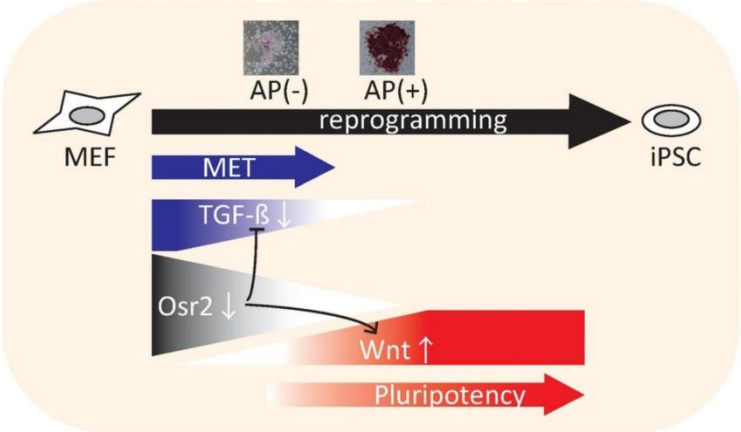

Significance Statement

Reprogramming of mouse embryonic fibroblasts (MEFs) is underpinned by gene expression changes, which include downregulation of mesenchyme-associated genes to eliminate the somatic cell identity. This study shows that downregulation of a mesenchyme-associated transcriptional regulator, *Osr2*, is critical for efficient reprogramming. *Osr2* is a novel regulator of epithelial-mesenchymal transition (EMT) and acts through induction of TGF-β signaling. During somatic cell reprogramming, *Osr2* downregulation permits reduction of TGF-β signaling and activation of Wnt signaling, both of which lead to more efficient mesenchymal-epithelial transition (MET) and acquisition of pluripotency.

1) INTRODUCTION

Somatic cells are reprogrammed by four transcription factors, OCT4, SOX2, KLF4, and c-MYC, to induced pluripotent stem cells (iPSCs), which give rise to all types of cells in the body.[1,2] iPSCs avoid ethical issues associated with derivation of embryonic stem cells (ESCs) and hold a great promise for applications in regenerative medicine, disease modeling, and drug development.[3,4] Somatic cell reprogramming is apparently a prolonged and complex process that proceeds through a series of events. Upon introduction of the reprogramming factors, somatic cells start to proliferate rapidly and undergo morphological changes to lose their cell identity. Subsequently, a subset of the cells establish the pluripotency network to achieve the fully pluripotent state.[5-7]

Somatic cell reprogramming is regarded as a reversal of differentiation that is driven by key transcriptional regulators expressed in tissue or cell-type specific manners.[8] Thus, reprogramming of mouse embryonic fibroblasts (MEFs) into iPSCs should by necessity encompass downregulation of transcriptional regulators associated with a mesenchymal phenotype. Indeed, MEFs at an early reprogramming stage downregulate many mesenchymal genes, which are believed to underlie dramatic morphological changes characterized by mesenchymal-epithelial transition (MET).[6,7,9-11] MET is a reverse process of epithelial-mesenchymal transition (EMT) that plays critical roles during embryonic development.[12] Thus, genes that are downregulated in MET during reprogramming include mesenchyme-associated genes that are induced in EMT during differentiation.[6]

EMT is characterized by morphological changes, loss of cell-cell contacts, and increased cell motility, and constitutes an integral process of embryogenesis, organ development, and cancer progression.[12,13] The best characterized inducer of EMT is transforming growth factor-β (TGF-β),[14] which by itself induces EMT in model epithelial cell lines such as normal murine mammary gland (NMuMG) cells.[15] In EMT, the effect of TGF-β is mediated by a transcription factor *Sox4*, which is induced strongly in NMuMG cells in response to TGF-β. SOX4 then elicits EMT-related gene expression changes by modifying chromatin structure via a polycomb component, *Ezh2*.[16] The TGF-β signaling ultimately links to SNAI1/2 and ZEB1/2, which form a core EMT regulatory network together with TWIST.[17] Subsequently, the EMT core regulatory network downregulates epithelial genes and upregulates mesenchymal genes to induce EMT-associated phenotypes.[12]

MET induced by reprogramming factors occurs through downregulation of TGF-β, which then leads to downregulation of *Snai1/2* and *Zeb1/2*.[18,19] However, overexpression of *Snai1* does not delay but rather facilitates reprogramming.[20] Moreover, even after initial downregulation, EMT-associated transcriptional regulators such as *Snai2*, *Zeb1*, and *Zeb2* remain expressed, albeit at lower levels, until a late reprogramming stage.[6] Thus, the functional relevance of downregulation of mesenchymal genes to progression of reprogramming remains to be better defined. Moreover, the early reprogramming stage is not self-sustaining, and if the reprogramming factors are removed, the cells revert to slower proliferation and flattened morphology[5,7,21] with concomitant reversion of the gene expression pattern.[6] A reversible and elastic nature of the early reprogramming stage also points to the importance of uncovering mesenchyme-associated transcriptional regulators, which should be downregulated for irreversibly disintegrating the mesenchymal cell identity.

Here, we sought to identify mesenchyme-associated transcriptional regulators whose downregulation at an early reprogramming stage is functionally relevant to the progression of reprogramming. We found that downregulation of *Osr2* is critical for efficient progression through MET at an early reprogramming stage.

Using NMuMG cells as a cell-based model, we found that *Osr2* induces EMT by activating TGF-β signaling. During reprogramming, *Osr2* downregulation is required for reduction of TGF-β signaling to induce MET as well as for upregulation of Wnt signaling to promote acquisition of pluripotency. Our results reveal *Osr2* as a critical transcriptional regulator whose immediate downregulation facilitates efficient reprogramming of MEFs.

2) MATERIAL AND METHODS

2.1) Cell culture

Mouse embryonic fibroblasts (MEFs) were isolated from embryos obtained from 13.5-day-pregnant C57BL/6NCrSlc mice or mice carrying the *Nanog*-GFP-IRES-Puro^r reporter construct[22] (provided by the RIKEN BioResource Center) (hereafter termed cMEF or nMEF, respectively). MEFs, PLAT-E, NIH3T3, and BHK/T7/151M cells were maintained as described previously.[23]

Normal murine mammary gland (NMuMG) cells were cultured in DMEM medium supplemented with 1 μg/mL insulin (Sigma) at 37°C with 5% CO_2. Epithelial-mesenchymal transition was induced with 5 ng/mL recombinant TGF-β1 (BioLegend) for 3 days. TGF-β signaling was inhibited by addition of SB431542 (Calbiochem; 10 μM), RepSox (Santa Cruz; 10 μM), SB203580 (Wako; 5 μM), or PD0325901 (Wako; 1 μM). CHIR99021 (Wako; 3 μM) was used for activation of Wnt signaling.

SNL feeder cells were generated from SNL76/7 harboring the puromycin resistance gene[24] by treatment with 10 μg/mL mitomycin C (Sigma) for 2.5 hours.

2.2) Production of retroviral vectors

The cDNAs encoding mesenchyme-associated transcriptional regulators fused with 3xFLAG-tag were amplified from MEF cDNA and inserted into pMCsΔYY1-IRES-Puro plasmid[23] to construct retroviral vectors expressing each protein. Annealed DNA oligonucleotides (89 nucleotides) encoding upstream Open Reading Frame 2 (uORF2) (Table S1) were placed 20 nucleotides before the inserted gene in pMCsΔYY1-IRES-Puro plasmid to reduce expression from the retroviral vectors. For expression of shRNA against *Osr2*, DNA oligonucleotides listed in Table S1 were annealed and inserted into pMXs-U6-Puro plasmid (Cambridge bioscience). Retrovirus stocks were prepared as described previously.[25]

2.3) Production of SeVdp vectors

The SeVdp vector genomic cDNA and SeVdp vector stock were prepared as described previously.[26] The cDNA for SeVdp(KOSMaB) was constructed by insertion of the Blasticidin S resistance gene together with the T2A peptide sequence after the *c-Myc* gene of SeVdp(KOSM).[27]

2.4) Cell reprogramming

MEFs were first transduced with a retroviral vector and then reprogrammed by infection with SeVdp(KOSM) or SeVdp(KOSMaB) as described previously.[23] For knockdown of *Osr2* during reprogramming, siRNA against *Osr2* was transfected into MEFs by using Lipofectamine RNAiMAX Transfection Reagent (Invitrogen) two days before reprogramming. Target sequences of the siRNAs are listed in Table S2. For feeder-free culture, SeVdp(KOSMaB)-infected cells were seeded onto a gelatin-coated plate with SNL-conditioned medium, which

was derived from the supernatant of SNL feeder cells cultured for two days. SeVdp(KOSMaB)-infected cells were selected by treatment with 2 μg/mL Blasticidin S (Nacalai Tesque) for 4 days. Alkaline phosphatase staining was performed using VECTOR Red Alkaline Phosphatase Substrate Kit (Vector).

2.5) Cell proliferation assay

Cell proliferation was quantified by XTT cell proliferation kit (Biological Industries) using five hundred cells seeded into a 96-well plate. At indicated time points, the cells were treated with activated XTT reagent and incubated at 37°C, 5% CO_2 before absorbance (OD_{450}) of the culture medium was measured by Infinite F200 (TECAN).

2.6) Quantitative RT-PCR

Total RNA extraction, reverse transcription, and quantitative PCR (qPCR) were performed as described previously.[28] The expression levels were normalized against that of TATA-box binding protein (TBP). The DNA sequences of the primers are listed in Table S3.

2.7) Detection and determination of protein expression

Immunofluorescence staining was performed as described previously[27] using anti-SeV NP antibody (1:1,000).[29] Whole cell extracts were isolated and subjected to SDS-PAGE and western blot analysis as described previously[25] using the following primary antibodies; anti-FLAG (1:4,000, M2, Sigma) and anti-α-TUBULIN (1:10,000, ab7291, Abcam).

2.8) Cell migration assay

3.0×10^4 of NMuMG cells were added to the top chamber of Transwell 6.5 mm with 8.0 μm Pore Polycarbonate Membrane Insert (CORNING). After 16 hours of culture, cells were removed from the upper side of the membrane by using a cotton swab. Cells migrated to the lower side of the membrane were fixed and stained with Staining solution (0.05% crystal violet, 1% formaldehyde, 1% methanol in PBS(-)) for 20 min at R.T. The migrated cells were counted under a microscope.

2.9) Transcriptome analyses

For analysis of EMT induction in NMuMG cells, two replicates of extracted total RNAs were used for library construction, and RNA-seq was performed with Illumina using sequencing platform (Annoroad Gene Technology). Sequence reads were mapped to the mouse genome (GRCm38.p6) using STAR aligner (v2.7.3a) with default parameters.[30] The read counts were calculated by featureCounts (v2.0.0)[31] with the gene model from Ensemble (Mus_musculus GRCm38.75.gtf) at the gene level to obtain TPM (Transcripts Per Million). The gene count data was normalized by variance stabilizing transformations (VST) using DESeq2 (v1.26.0).[32] The VST-normalized value was used to show the transcriptome similarity through the heatmap with Ward's method and PCA. Differentially expressed genes (DEGs) were selected by the Likelihood ratio test using DESeq2. Pathway analysis of the DEGs was performed by using WikiPathway[33] through Enrichr.[34]

For analysis of reprogrammed MEFs, a single replicate of total RNA was used for library prep and sequence as described previously.[35] Read mapping and quantification of gene expression were done as described above. The genes whose TPM changed over 3-fold were selected as DEGs.

2.10) Statistical analysis

Student's t-tests were employed to determine a statistically significant difference between data sets, except for RNA-seq data. A value of $P < 0.05$ was regarded as statistically significant.

3) RESULTS

3.1) Downregulation of *Osr2* is important for efficient reprogramming of MEFs

To identify critical factors that should be downregulated for efficient reprogramming, we prepared MEFs reprogrammed by SeVdp(KOSM), which is derived from a defective and persistent Sendai virus (SeVdp)-based expression vector.[26] SeVdp(KOSM) expresses OCT4, SOX2, KLF4, and c-MYC and generates iPSCs efficiently from a wide range of somatic cells.[36-38] We used the DNA microarray expression data of iPSCs reprogrammed from MEFs[25] and identified 1,787 DEGs that reduced expression by over 2-fold throughout reprogramming (namely: day 2, day 8, and fully reprogrammed iPSCs versus MEFs) (Figure S1A). Gene ontology analysis of 1,787 DEGs selected 150 transcriptional regulators, which were further narrowed down to 37 genes by presumed direct regulation by reprogramming factors, based upon the experimentally confirmed occupancies of OCT4, SOX2, KLF4, and c-MYC[39] or OCT4 and SOX2[40] in the vicinity of genes during iPSC generation or in ESCs, respectively. Moreover, given the prominent roles of cell cycle, mesenchymal-epithelial transition (MET), and de-differentiation at an early reprogramming stage,[41-46] we identified 10 mesenchyme-associated transcriptional regulators, which are related to the reverse cellular functions; namely, cell cycle arrest, EMT, and differentiation. Quantitative RT-PCR of the 10 genes showed that 8 genes (*Ebf1*, *Ebf3*, *Meox1*, *Meox2*, *Osr2*, *Prrx1*, *Smarcd3*, and *Zic1*) were downregulated throughout the first 8 days of reprogramming of MEFs (Figure S1B).

To assess the functional relevance of their downregulation to reprogramming, we expressed each transcriptional regulator in MEFs using a silencing-resistant retroviral vector, MCsΔYY1,[23] to avoid reduction of its expression by retroviral silencing during reprogramming.[25] The MEFs were then reprogrammed by SeVdp(KOSM), and the number of alkaline phosphatase-positive (AP(+)) colonies was counted after 10 days of reprogramming (Figure 1A). As shown in Figure S1C, the AP(+) colony number was reduced significantly when *Ebf1*, *Ebf3*, *Meox2*, *Osr2*, *Prrx1*, and *Smarcd3* were expressed in MEFs, suggesting that their continued expression reduces the efficiency of reprogramming. We noted, however, that expression of some of the transcriptional regulators reduced the viability of MEFs even without reprogramming (Figure S1D), which implicated that the reduction of the AP(+) colony number may have been overestimated.

To minimize the cytotoxic effect of overexpressed transcriptional regulators on cell viability, we constructed an MCsΔYY1-based expression vector that harbors an upstream open reading frame 2 (uORF2) before the protein-coding region (Figure 1A). The uORF2, derived from the human cytomegalovirus (CMV) virion glycoprotein gpUL4 (gp48), reduces translation of a heterologous gene when inserted in its 5' untranslated region.[47] Using this uORF2-containing expression vector, we expressed each of the 8 transcriptional regulators in MEFs and found that their protein levels were lowered to 1~60% of those by the original MCsΔYY1-based vectors albeit with smaller changes of their mRNA levels (Figure S2A). As expected, the cytotoxic effect of expressed transcriptional regulators on the cell viability and proliferation rate could be minimized (Figures 1B and 1C).

We then re-assessed the effect of their continued expression during reprogramming of MEFs by SeVdp(KOSM). In contrast to the results in Figure S1C, expression of only *Ebf1*, *Ebf3*, and *Osr2* reduced the AP(+) colony number at day 10 of reprogramming, whereas *Meox1*, *Meox2*, *Prrx1*, *Smarcd3*, and *Zic1* showed no such effects (Figure 1D). These results suggest that failure to downregulate *Ebf1*, *Ebf3*, and *Osr2* reduces the efficiency of reprogramming. Although *Ebf1* and *Ebf3* apparently showed greater effects than *Osr2*, MEFs expressing *Ebf1* or *Ebf3* failed to proliferate after initiation of reprogramming and underwent massive cell death (Figures S2B and S2C), which precluded the analysis of their functional relevance to reprogramming. Thus, in the subsequent analyses, we focused on the effect of *Osr2* that clearly impaired the efficiency of reprogramming when expressed continuously.

Mouse *Osr2* gene encodes a zinc-finger protein related to *Drosophila* odd-skipped and produces two isoforms, OSR2A and OSR2B, which differ in their C-terminal regions due to alternative splicing.[48] OSR2B, which was used in Figure 1D, is the predominant form that possesses three zinc fingers whereas OSR2A is the minor form that possesses two additional zinc fingers[49] (Figure S3A). OSR2A and OSR2B show opposite transcriptional activities that may vary depending on the employed assays.[49] As shown in Figure S3B, both OSR2A and OSR2B reduced the AP(+) colony number, but the effect was more marked for OSR2B, which indicates that downregulation of the predominant isoform OSR2B has a stronger effect on the efficiency of reprogramming. Because of its stronger effect and predominant expression in MEFs, we used OSR2B for further analyses.

3.2) *Osr2* hinders progression of MET during reprogramming

Given that *Osr2* reduces the number of colonies with positive AP staining, an early-stage marker of reprogramming (Figures 1D), we analyzed the effect of *Osr2* on the expression of SSEA1, an intermediate-stage marker of reprogramming.[5] At day 12 of reprogramming, the number of SSEA1(+) colonies was reduced markedly, with a sharp increase in the percentage of SSEA1(-) colonies (Figure 2A). This result indicates that *Osr2* hampers reprogramming at a relatively early stage in both quantitative and qualitative manners. Consistent with this diminished quality caused by exogenous *Osr2* expression, iPSCs derived from *Osr2*-expressing MEFs failed to grow after the first passage at day 27 (Figure 2B), which likely reflects their poor capacity of proliferation and self-renewal. On the other hand, when MEFs were reprogrammed after *Osr2* was knocked down by two independent siRNAs, higher numbers of AP(+) and Nanog(+) colonies were generated, and the expression of pluripotency markers (*Fbxo15* and *Rex1*) also increased as compared with MEFs treated with control siRNA (Figures S4A-D). Together, these results suggest that *Osr2* lowers both quantity and quality of iPSCs by negatively impacting reprogramming at a relatively early stage.

One major event at an early reprogramming stage is MET, in which mesenchymal cells undergo morphological changes to acquire the epithelial phenotype. In fact, *Osr2* is expressed in the regions where epithelial and mesenchymal cells interact during palatal development,[45] when palatal fusion requires proper EMT.[50] This suggests a likely role for *Osr2* in EMT during palatal development and, by extension, in MET during reprogramming. We therefore asked if *Osr2* downregulation is required for MET during reprogramming. To accurately assess changes in cell morphology and gene expression, we used a new Sendai virus vector, SeVdp(KOSMaB), that harbors the Blasticidin S resistance gene to eliminate MEFs not infected with the reprogramming vector (Figure 2C). *Osr2*-expressing MEFs, infected with SeVdp(KOSMaB), were selected with Blasticidin S and then allowed to undergo reprogramming. *Osr2*-expressing MEFs generated only small or incomplete colonies (Figure 2D), which contained more elongated cells that lacked clear cell-cell adhesion (Figure 2E). Although *Osr2*-expressing cells downregulated some mesenchymal genes such as *Cdh2* and *Snai2*,

other mesenchymal genes such as *Zeb2*, *Fn1*, and *Vim* were downregulated to a far lesser extent as compared with control MEFs (Figure 2F). In addition, upregulation of epithelial genes, *Cdh1* and *Ocln*, were severely reduced (Figure 2F). Collectively, these results suggest that *Osr2* downregulation is a prerequisite for proper MET at an early reprogramming stage.

3.3) *Osr2* induces EMT-like changes through TGF-β signaling

To clarify the mechanistic relationship between *Osr2* and MET/EMT, we employed NMuMG cells, an EMT model cell line that is used widely for analyzing factors and mechanisms of EMT.[15] NMuMG cells are epithelial cells that exhibit rapid and synchronous transition into a mesenchymal state upon TGF-β addition, as opposed to heterogeneous and unsynchronized MET during reprogramming. We expressed *Osr2* in NMuMG cells or added TGF-β as control, and observed changes in cell morphology, cell migration, and gene expression pattern (Figure 3A). Upon expression of *Osr2*, NMuMG cells became flattened and spindle-shaped with reduced cell-cell contacts (Figure 3B, middle panels), displaying morphological changes similar to those of TGF-β-treated NMuMG cells (Figure 3B, bottom panels). These morphological changes, however, required longer time (over 7 days) than TGF-β-treated cells (3 days), providing a window of time for the cells to proliferate before they cease cell division. In cell migration assays, *Osr2*-expressing NMuMG cells displayed enhanced migration akin to TGF-β-treated cells (Figure 3C). Furthermore, *Osr2* upregulated *Snai1*, *Snai2*, *Vim*, *Tgfb3*, *Zeb2*, and *Cdh2* while downregulating *Cdh1* and *Epcam* (Figure 3D). These results show that *Osr2* induces changes in cell morphology, cell motility, and gene expression typically observed in EMT induced by TGF-β treatment.

To further explore the mechanism by which *Osr2* induces EMT in NMuMG cells, we performed RNA-seq analyses of *Osr2*-expressing and TGF-β-treated NMuMG cells. Hierarchical clustering and principal component analysis (PCA) indicated that expression of *Osr2* for 3 or 9 days elicits a gene expression pattern distinct from that by TGF-β treatment (Figures 4A and 4B). Differentially expressed genes (DEGs) were grouped into clusters that are shared or distinct between *Osr2*-expressing and TGF-β-treated NMuMG cells (Figure 4C, Table S4). Genes in Cluster 3-2 whose expression were upregulated by both *Osr2* (Day 3) and TGF-β treatment are enriched in pathways related to EMT (Figures 4C and S5, Table S5). This enrichment is more pronounced at day 9 of exogenous *Osr2* expression (Cluster 9-3) (Figures 4C and S5, Table S5), consistent with a slow and prolonged progression of EMT by exogenous *Osr2* expression. Indeed, Clusters 3-2 and 9-3 include EMT-related regulatory genes (*Snai1*, *Tgfb1*, *Wnt7a*, *Zeb2*, *Foxq1*, and *Smad3*) as well as their downstream structural genes (*Nrp2*, *Pkp1*, *Cldn4*, *Fn1*, *Fzd1/2*, and *Notch2*) (Figure 4C). Clusters 3-6 and 9-5, which include genes downregulated by both exogenous *Osr2* expression and TGF-β treatment, are enriched in pathways related to cellular metabolism including oxidative phosphorylation (Figures 4C and S5, Table S5), which is consistent with metabolic changes during EMT.[51] Together, these results demonstrate that *Osr2* induces EMT in NMuMG cells, albeit in a delayed manner as compared with TGF-β treatment. Interestingly, genes upregulated by exogenous *Osr2* expression (Day 3) but not by TGF-β treatment (Cluster 3-1) is enriched in pathways related to DNA replication, transcription, and translation (Figure S5, Table S5), which are no longer enriched at day 9 (Cluster 9-4) (Figure S5, Table S5). Thus, the results from RNA-seq analyses are consistent with the observation that *Osr2* promotes transient proliferation of NMuMG cells before their subsequent progression through EMT (Figure 3B).

Given the similar roles of *Osr2* and TGF-β in EMT, we next examined their causal relationship. First, we expressed shRNA to knock down *Osr2* in NMuMG cells, which were then treated by TGF-β . As shown in Figures S6A and S6B, *Osr2* knockdown showed little effect on EMT induced by TGF-β treatment, consistent

with RNA-seq data that detected almost no expression of *Osr2* in NMuMG cells with or without TGF-β treatment (Figure S6C). Next, we expressed *Osr2* in NMuMG cells and then inhibited the TGF-β pathway with two different TGF-β inhibitors, SB431542[52] or RepSox.[53] As shown in Figure 5A, SB431542 and RepSox prevented *Osr2* from inducing changes in cell morphology and cell-cell contacts. In addition, both TGF-β inhibitors reduced expression of EMT-associated genes (*Snai1*, *Snai2*, and *Zeb2*) (Figure 5B) and cell migration (Figure 5C), both of which were otherwise enhanced by exogenous *Osr2* expressed in NMuMG cells. Finally, RNA-seq analysis of *Osr2*-expressing NMuMG cells showed that *Osr2* induces genes related to TGF-β signaling (Figure S7). Together, these results suggest that *Osr2* induces EMT in NMuMG cells, at least in part, through TGF-β signaling.

3.4) *Osr2* downregulation reduces TGF-β signaling to facilitate reprogramming through MET

TGF-β was previously demonstrated to impair reprogramming by preventing MET, and inhibition of TGF-β signaling was shown to enhance reprogramming.[18] Given that *Osr2* promotes EMT by upregulating TGF-β signaling in NMuMG cells, we wondered if *Osr2* downregulation is a prerequisite for subsequent reduction of TGF-β signaling during reprogramming. As reported previously,[9] TGF-β family genes (*Tgfb1*, *Tgfb2*, and *Tgfb3*) were downregulated at day 3 and day 5 of reprogramming of control MEFs. However, *Osr2*-expressing MEFs attenuated downregulation of *Tgfb1* or even upregulated expression of *Tgfb2* and *Tgfb3* (Figure 6A, upper panels). By contrast, the effects of *Osr2* on the expression of TGF-β receptors were largely unremarkable as compared with three TGF-β family genes except that expression of *Tgfbr2* remained higher in *Osr2*-expressing MEFs than control MEFs (Figure 6A, lower panels). These results suggest that expression of *Osr2* maintains TGF-β signaling, at least in part, by counteracting downregulation of the TGF-β family members (*Tgfb1*, *Tgfb2*, and *Tgfb3*) during reprogramming. Next, we tested the functional role for *Osr2* in regulating TGF-β signaling during reprogramming of *Osr2*-expressing MEFs in the presence of a TGF-β inhibitor, SB431542. As shown in Figures 6B and 6C, SB431542 showed little impact on the number of colonies generated from control MEFs. By contrast, SB431542 increased the number of colonies generated from *Osr2*-expressing MEFs. We noticed, however, that a substantial proportion of colonies generated from *Osr2*-expressing MEFs in the presence of SB431542 consisted of less tightly packed cells that were negative for alkaline phosphatase (AP(-)) (Figure 6B, insets), and it appeared that SB431542 mostly increased AP(-) colonies consisting of less pluripotent iPSCs (Figure 6C).

TGF-β signaling is mediated through the canonical Smad pathway as well as non-Smad pathways within a cell.[54] In EMT models using human keratinocytes (HaCaT cells) and murine NMuMG cells, MAPK activation was identified as one of the non-Smad pathways of TGF-β signaling.[55,56] To test if non-Smad pathways mediate TGF-β signaling downstream of *Osr2*, we performed reprogramming in the presence of p38 or MEK inhibitor (SB203580 or PD0325901, respectively) instead of SB431542 that blocks both Smad and non-Smad pathways[57] (Figure 6D). As shown in Figure 6E, neither SB203580 nor PD0325901 counteracted the negative effect of *Osr2* on reprogramming, indicating that p38 and MEK in non-Smad pathways do not mediate the TGF-β signaling by *Osr2* during reprogramming. These results suggest that *Osr2* hinders reprogramming by augmenting TGF-β signaling mediated mainly through the Smad pathway in a cell.

3.5) *Osr2* downregulation increases Wnt signaling to facilitate reprogramming toward pluripotency

Because TGF-β inhibitors could only partially block the effect of *Osr2* and generated incompletely reprogrammed AP(-) iPSCs, we sought for additional effectors that mediate the signaling downstream of *Osr2*. We reasoned that the hypothetical downstream effector genes would be enriched in a set of genes that change their expression level by *Osr2*. Moreover, their expression levels would not be changed by the TGF-β inhibitor SB431542, regardless of exogenous *Osr2* expression. We therefore performed RNA-seq of MEFs reprogrammed under four different conditions: 1) MEFs reprogrammed without SB431542, 2) *Osr2*-expressing MEFs reprogrammed without SB431542, 3) MEFs reprogrammed with SB431542, and 4) *Osr2*-expressing MEFs reprogrammed with SB431542 (Figure 7A). First, we selected genes that changed expression by *Osr2* in the absence of SB431542 (Figure 7B, upper). Second, we selected genes that changed expression by *Osr2* in the presence of SB431542 (Figure 7B, bottom). After pathway analyses of each gene set, the common pathways enriched in both gene sets were found to include DNA replication, gene expression, cell cycle, PluriNetWork as well as Wnt Signaling Pathway (Figure 7B). Consistent with the results in Figures 6B and 6C, the RNA-seq data showed that SB431542 did not promote reprogramming effectively when added to *Osr2*-expressing MEFs (Figure S8).

We were intrigued by inclusion of Wnt Signaling Pathway in the common pathways because Wnt signaling was previously reported to facilitate reprogramming[58,59] and play an important role in maintaining pluripotency of ESCs.[60] In agreement with these studies, *Osr2* lowered the expression of key components in the Wnt signaling pathway, *Axin2* and *Tcf7*, during reprogramming (Figure 7C). Functionally, a Wnt pathway activator CHIR99021 increased the number of colonies generated from control MEFs in the presence of SB431542 (Figures 7D and 7E). Although addition of CHIR99021 did not increase the number of colonies generated from *Osr2*-expressing MEFs in the presence of SB431542, they generated a higher proportion of AP(+) colonies under this condition (Figures 7D and 7E). Indeed, in the presence of SB431542, *Osr2*-expressing cells restored the expression of pluripotency markers, *Cdh1*, *Fbxo15*, endogenous *Oct4*, and *Nanog* when the Wnt pathway is activated by CHIR99021 (Figure 7F). Consistently, expression of TGF-β-related genes (*Tgfb2*, *Tgfb3*, and *Zeb2*), reduced by SB431542 in *Osr2*-expressing cells, remained unchanged by CHIR99021; however, expression of Wnt-related genes (*Axin2*, *Lef1*, and *Tcf7*) were completely restored under this condition (Figure S9). Thus, Wnt signaling promotes reprogramming by driving *Osr2*-expressing MEFs toward pluripotency even when it does not necessarily increase the number of reprogrammed cells. Taken together, *Osr2* downregulation is a prerequisite for subsequent reduction of TGF-β signaling and activation of Wnt signaling, both of which combine to facilitate progression through MET toward acquisition of pluripotency.

4) DISCUSSION

In this study, we have shown that *Osr2* downregulation is crucial for promoting progression through MET to permit efficient reprogramming. Previous studies implicated a role for *Osr2* in EMT, the reversal of MET, during tooth development.[61,62] In the analyses using NMuMG cells, we found that *Osr2* induces EMT by upregulating genes involved in TGF-β signaling and that this indirect induction of EMT enables transient cell proliferation before EMT is firmly established. The transient cell proliferation in *Osr2*-expressing NMuMG cells is consistent with our own RNA-seq analysis and an earlier observation that *Osr2* regulates genes involved in cell proliferation.[63] EMT preceded by cell proliferation is suited for a developmental process such as palatal

growth and patterning,[61] in which cells increase in number before they undergo EMT for terminal differentiaion.[45]

In reprogramming, MET is initiated by the cooperative actions of reprogramming factors that ultimately reduce TGF-β signaling.[9] MET is an early event of reprogramming MEFs and is essential for progression of reprogramming toward pluripotency.[9] However, except for upregulation of the miR-200 family by OCT4 and SOX2 to suppress *Zeb2*,[64] the functional links between reprogramming factors and TGF-β signaling/MET remained obscure. Given that its downregulation precedes MET, *Osr2* is likely to be a key molecule that links the reprogramming factors with reduced TGF-β signaling. Because of their binding near the *Osr2* gene, reprogramming factors probably downregulate *Osr2* directly at an early reprogramming stage. Downregulation of *Osr2* may then diminish the mesenchymal phenotype and provide a permissive cue for subsequent MET during reprogramming of MEFs.

In addition to TGF-β signaling, our study suggests a regulatory role for *Osr2* in Wnt signaling during reprogramming. *Osr2* was reported to upregulate Wnt antagonists, *Dkk2* and *Sfrp2* in the dental mesenchymal cells during tooth development.[62] Moreover, *Osr1*, an *Osr* family member closely related to *Osr2*, reduces Wnt signaling by inhibiting SOX9 and β-catenin to suppress proliferation and invasion of lung cancer cells.[65] Thus, in mesenchymal cells such as MEFs, *Osr2* may regulate genes related to the Wnt pathway to reduce its signaling; conversely, *Osr2* downregulation during reprogramming may allow subsequent upregulation of Wnt signaling. It is well known that Wnt signaling is part of a key regulatory network that controls self-renewal and maintenance of pluripotency in ESCs.[60,66,67] Consistent with the roles of Wnt signaling in ESCs, small-molecule compounds that activate Wnt signaling enhance reprogramming.[58,59] Despite its role in self-renewal and differentiation of ESCs, however, detailed mechanistic analyses revealed that Wnt signaling operates at an unexpectedly early stage of reprogramming.[68] Thus, besides maintaining iPSCs in the pluripotent state, Wnt signaling may act at an earlier reprogramming stage for progression toward pluripotency, for which reducing *Osr2* expression is a prerequisite.

Reprogramming of somatic cells to iPSCs can be promoted not only by overexpression of transcription factors but also by modulation of signaling pathways. Given that small-molecule compounds that target signaling pathways have been demonstrated to substitute reprogramming factors,[69] transcription factors and signaling pathways appear to have close functional linkage during reprogramming. However, how transcription factors and signaling pathways converge, crosstalk, and cooperate during reprogramming remains to be better defined.[70] Large-scale collaborative analyses of sea urchin development revealed that transcription factors and intercellular signaling form gene regulatory networks (GRNs) that control developmental processes.[71] Analogously, *Osr2* and the TGF-β signaling pathway may constitute a part of the GRN that governs the mesenchymal state in MEFs. Disintegration of this GRN probably requires downregulation of *Osr2* to permit reduction of TGF-β signaling, and subsequent activation of Wnt signaling may lead to a distinct GRN that governs a more advanced stage of reprogramming. Thus, our study underscores the importance of identifying key components of GRNs that alternate during reprogramming to understand how cells convert their identity.

5) CONCLUSION

We found that downregulation of *Osr2* is crucial for efficient reprogramming of MEFs. *Osr2* functions as an EMT regulator through activation of TGF-β signaling, which is inhibitory for progression of MET during reprogramming. Moreover, downregulation of *Osr2* is required for activation of Wnt signaling, which promotes acquisition of pluripotency. These results show that *Osr2* is one of key transcriptional regulators that are downregulated for efficient reprogramming by disintegrating the somatic cell identity.

ACKNOWLEDGMENTS

We thank Y. Okita for technical advice on cell invasion and migration assays. We also thank T. Nishimura for technical assistance.

CONFLICT OF INTERESTS

The authors declare no competing interests.

AUTHOR CONTRIBUTIONS

K.N. and K.H. designed the research. L.P.H.A., K.N., N.T.L., T.K., E.S, T.S., and Y.H. collected and analyzed the data. K.N. and A.K. analyzed microarray and RNA-seq data. L.P.H.A., K.N., M.O. and M.N. prepared the materials. K.N., A.F., and K.H. wrote the paper.

DATA AVAILABILITY STATEMENT

The data that support the findings of this study are available from the corresponding author upon reasonable request.

REFERENCES

1. Takahashi K, Tanabe K, Ohnuki M, et al. Induction of pluripotent stem cells from adult human fibroblasts by defined factors. *Cell*. 2007;131(5):861-872.

2. Takahashi K, Yamanaka S. Induction of Pluripotent Stem Cells from Mouse Embryonic and Adult Fibroblast Cultures by Defined Factors. *Cell*. 2006;126(4):663-676.

3. Stadtfeld M, Hochedlinger K. Induced pluripotency: History, mechanisms, and applications. *Genes Dev*. 2010;24(20):2239-2263.

4. Takahashi K, Yamanaka S. A decade of transcription factor-mediated reprogramming to pluripotency. *Nat Rev Mol Cell Biol*. 2016;17(3):183-193.

5. Brambrink T, Foreman R, Welstead GG, et al. Sequential expression of pluripotency markers during direct reprogramming of mouse somatic cells. *Cell Stem Cell*. 2008;2(2):151-159.

6. Samavarchi-Tehrani P, Golipour A, David L, et al. Functional genomics reveals a BMP-Driven mesenchymal-to-Epithelial transition in the initiation of somatic cell reprogramming. *Cell Stem Cell*. 2010;7(1):64-77.

7. Stadtfeld M, Maherali N, Breault DT, Hochedlinger K. Defining Molecular Cornerstones during Fibroblast to iPS Cell Reprogramming in Mouse. *Cell Stem Cell*. 2008;2(3):230-240.

8. Spitz F, Furlong EE. Transcription factors: from enhancer binding to developmental control. *Nat Rev Genet*. 2012;13(9):613-626.

9. Li R, Liang J, Ni S, et al. A mesenchymal-to-epithelial transition initiates and is required for the nuclear reprogramming of mouse fibroblasts. *Cell Stem Cell*. 2010;7(1):51-63.

10. Mikkelsen TS, Hanna J, Zhang X, et al. Dissecting direct reprogramming through integrative genomic analysis. *Nature*. 2008;454(7200):49-55.

11. Polo JM, Anderssen E, Walsh RM, et al. A molecular roadmap of reprogramming somatic cells into iPS cells. *Cell*. 2012;151(7):1617-1632.

12. Nieto MA, Huang RY, Jackson RA, Thiery JP. Emt: 2016. *Cell*. 2016;166(1):21-45.

13. Thiery JP, Acloque H, Huang RY, Nieto MA. Epithelial-mesenchymal transitions in development and disease. *Cell*. 2009;139(5):871-890.

14. Chen T, You Y, Jiang H, Wang ZZ. Epithelial-mesenchymal transition (EMT): A biological process in the development, stem cell differentiation, and tumorigenesis. *J Cell Physiol*. 2017;232(12):3261-3272.

15. Miettinen PJ, Ebner R, Lopez AR, Derynck R. TGF-beta induced transdifferentiation of mammary epithelial cells to mesenchymal cells: involvement of type I receptors. *J Cell Biol*. 1994;127(6 Pt 2):2021-2036.

16. Tiwari N, Tiwari VK, Waldmeier L, et al. Sox4 is a master regulator of epithelial-mesenchymal transition by controlling Ezh2 expression and epigenetic reprogramming. *Cancer Cell*. 2013;23(6):768-783.

17. Moes M, Le Bechec A, Crespo I, et al. A novel network integrating a miRNA-203/SNAI1 feedback loop which regulates epithelial to mesenchymal transition. *PLoS One*. 2012;7(4):e35440.

18. Shu X, Pei D. The function and regulation of mesenchymal-to-epithelial transition in somatic cell reprogramming. *Curr Opin Genet Dev*. 2014;28:32-37.

19. Wang Y, Mah N, Prigione A, Wolfrum K, Andrade-Navarro MA, Adjaye J. A transcriptional roadmap to the induction of pluripotency in somatic cells. *Stem Cell Rev Rep*. 2010;6(2):282-296.

20. Unternaehrer JJ, Zhao R, Kim K, et al. The epithelial-mesenchymal transition factor SNAIL paradoxically enhances reprogramming. *Stem Cell Rep*. 2014;3(5):691-698.

21. Woltjen K, Michael IP, Mohseni P, et al. piggyBac transposition reprograms fibroblasts to induced pluripotent stem cells. *Nature*. 2009;458(7239):766-770.

22. Okita K, Ichisaka T, Yamanaka S. Generation of germline-competent induced pluripotent stem cells. *Nature*. 2007;448(7151):313-317.

23. Nishimura K, Aizawa S, Nugroho FL, et al. A Role for KLF4 in Promoting the Metabolic Shift via TCL1 during Induced Pluripotent Stem Cell Generation. *Stem Cell Rep*. 2017;8(3):787-801.

24. Tran THY, Fukuda A, Aizawa S, et al. Live cell imaging of X chromosome reactivation during somatic cell reprogramming. *Biochem Biophys Rep*. 2018;15:86-92.

25. Bui PLL, Nishimura K, Seminario Mondejar G, et al. Template Activating Factor-I alpha Regulates Retroviral Silencing during Reprogramming. *Cell Rep*. 2019;29(7):1909-1922.

26. Nishimura K, Sano M, Ohtaka M, et al. Development of defective and persistent Sendai virus vector: A unique gene delivery/expression system ideal for cell reprogramming. *J Biol Chem*. 2011;286(6):4760-4771.

27. Nishimura K, Kato T, Chen C, et al. Manipulation of KLF4 expression generates iPSCs paused at successive stages of reprogramming. *Stem Cell Rep*. 2014;3(5):915-929.

28. Nishimura K, Ishiwata H, Sakuragi Y, Hayashi Y, Fukuda A, Hisatake K. Live-cell imaging of subcellular structures for quantitative evaluation of pluripotent stem cells. *Sci Rep*. 2019;9(1):1777.

29. Nishimura K, Segawa H, Goto T, et al. Persistent and stable gene expression by a cytoplasmic RNA replicon based on a noncytopathic variant sendai virus. *J Biol Chem*. 2007;282(37):27383-27391.

30. Dobin A, Davis CA, Schlesinger F, et al. STAR: ultrafast universal RNA-seq aligner. *Bioinformatics*. 2013;29(1):15-21.

31. Liao Y, Smyth GK, Shi W. featureCounts: an efficient general purpose program for assigning sequence reads to genomic features. *Bioinformatics*. 2014;30(7):923-930.

32. Love MI, Huber W, Anders S. Moderated estimation of fold change and dispersion for RNA-seq data with DESeq2. *Genome Biol*. 2014;15(12):550.

33. Slenter DN, Kutmon M, Hanspers K, et al. WikiPathways: a multifaceted pathway database bridging metabolomics to other omics research. *Nucleic Acids Res*. 2018;46(D1):D661-D667.

34. Kuleshov M V, Jones MR, Rouillard AD, et al. Enrichr: a comprehensive gene set enrichment analysis web server 2016 update. *Nucleic Acids Res*. 2016;44(W1):W90-7.

35. Aizawa S, Nishimura K, Mondejar GS, et al. Early reactivation of clustered genes on the inactive X chromosome during somatic cell reprogramming. *Stem Cell Rep*. 2022;17(1):53-67.

36. Kyttälä A, Moraghebi R, Valensisi C, et al. Genetic Variability Overrides the Impact of Parental Cell Type and Determines iPSC Differentiation Potential. *Stem Cell Rep*. 2016;6(2):200-212.

37. Matsumoto T, Fujimori K, Andoh-Noda T, et al. Functional Neurons Generated from T Cell-Derived Induced Pluripotent Stem Cells for Neurological Disease Modeling. *Stem Cell Rep*. 2016;6(3):422-435.

38. Nishimura T, Kaneko S, Kawana-Tachikawa A, et al. Generation of rejuvenated antigen-specific T cells by reprogramming to pluripotency and redifferentiation. *Cell Stem Cell*. 2013;12(1):114-126.

39. Sridharan R, Tchieu J, Mason MJ, et al. Role of the murine reprogramming factors in the induction of pluripotency. *Cell*. 2009;136(2):364-377.

40. Sharov AA, Masui S, Sharova L V., et al. Identification of Pou5f1, Sox2, and Nanog downstream target genes with statistical confidence by applying a novel algorithm to time course microarray and genome-wide chromatin immunoprecipitation data. *BMC Genomics*. 2008;9:1-19.

41. Douville JM, Cheung DY, Herbert KL, Moffatt T, Wigle JT. Mechanisms of MEOX1 and MEOX2 regulation of the cyclin dependent kinase inhibitors p21 and p16 in vascular endothelial cells. *PLoS One*. 2011;6(12):e29099.

42. Gan L, Chen S, Zhong J, et al. ZIC1 is downregulated through promoter hypermethylation, and functions as a tumor suppressor gene in colorectal cancer. *PLoS One*. 2011;6(2):e16916.

43. Garcia-Dominguez M, Poquet C, Garel S, Charnay P. Ebf gene function is required for coupling neuronal differentiation and cell cycle exit. *Development*. 2003;130(24):6013-6025

44. Jordan N V, Prat A, Abell AN, et al. SWI/SNF chromatin-remodeling factor Smarcd3/Baf60c controls epithelial-mesenchymal transition by inducing Wnt5a signaling. *Mol Cell Biol*. 2013;33(15):3011-3025.

45. Lan Y, Ovitt CE, Cho ES, Maltby KM, Wang Q, Jiang R. Odd-skipped related 2 (Osr2) encodes a key intrinsic regulator of secondary palate growth and morphogenesis. *Development*. 2004;131(13):3207-3216.

46. Ocana OH, Corcoles R, Fabra A, et al. Metastatic colonization requires the repression of the epithelial-mesenchymal transition inducer Prrx1. *Cancer Cell*. 2012;22(6):709-724.

47. Degnin CR, Schleiss MR, Cao J, Geballe AP. Translational inhibition mediated by a short upstream open reading frame in the human cytomegalovirus gpUL4 (gp48) transcript. *J Virol*. 1993;67(9):5514-5521.

48. Lan Y, Kingsley PD, Cho ES, Jiang R. Osr2, a new mouse gene related to Drosophila odd-skipped, exhibits dynamic expression patterns during craniofacial, limb, and kidney development. *Mech Dev*. 2001;107(1-2):175-179.

49. Kawai S, Kato T, Inaba H, Okahashi N, Amano A. Odd-skipped related 2 splicing variants show opposite transcriptional activity. *Biochem Biophys Res Commun*. 2005;328(1):306-311.

50. Nakajima A, C FS, Gulka AOD, Hanai JI. TGF-beta Signaling and the Epithelial-Mesenchymal Transition during Palatal Fusion. *Int J Mol Sci*. 2018;19(11):3638.

51. Kang H, Kim H, Lee S, Youn H, Youn B. Role of Metabolic Reprogramming in Epithelial−Mesenchymal Transition (EMT). *Int J Mol Sci*. 2019;20(8):2042.

52. Inman GJ, Nicolas FJ, Callahan JF, et al. SB-431542 is a potent and specific inhibitor of transforming growth factor-beta superfamily type I activin receptor-like kinase (ALK) receptors ALK4, ALK5, and ALK7. *Mol Pharmacol*. 2002;62(1):65-74.

53. Ichida JK, Blanchard J, Lam K, et al. A small-molecule inhibitor of tgf-Beta signaling replaces sox2 in reprogramming by inducing nanog. *Cell Stem Cell*. 2009;5(5):491-503.

54. Zhang YE. Non-Smad Signaling Pathways of the TGF-β Family. *Cold Spring Harb Perspect Biol*. 2017;9(2):a022129.

55. Zavadil J, Bitzer M, Liang D, et al. Genetic programs of epithelial cell plasticity directed by transforming growth factor-beta. *Proc Natl Acad Sci U S A*. 2001;98(12):6686-6691.

56. Xie L, Law BK, Chytil AM, Brown KA, Aakre ME, Moses HL. Activation of the Erk pathway is required for TGF-beta1-induced EMT in vitro. *Neoplasia*. 2004;6(5):603-610.

57. Halder SK, Beauchamp RD, Datta PK. A specific inhibitor of TGF-beta receptor kinase, SB-431542, as a potent antitumor agent for human cancers. *Neoplasia*. 2005;7(5):509-521.

58. Lluis F, Pedone E, Pepe S, Cosma MP. Periodic activation of Wnt/beta-catenin signaling enhances somatic cell reprogramming mediated by cell fusion. *Cell Stem Cell*. 2008;3(5):493-507.

59. Marson A, Foreman R, Chevalier B, et al. Wnt signaling promotes reprogramming of somatic cells to pluripotency. *Cell Stem Cell*. 2008;3(2):132-135.

60. Sokol SY. Maintaining embryonic stem cell pluripotency with Wnt signaling. *Development*. 2011;138(20):4341-4350.

61. Greene RM, Pisano MM. Palate morphogenesis: current understanding and future directions. *Birth Defects Res C Embryo Today*. 2010;90(2):133-154.

62. Jia S, Kwon HJE, Lan Y, Zhou J, Liu H, Jiang R. Bmp4-Msx1 signaling and Osr2 control tooth organogenesis through antagonistic regulation of secreted Wnt antagonists. *Dev Biol*. 2016;420(1):110-119.

63. Kawai S, Abiko Y, Amano A. Odd-skipped related 2 regulates genes related to proliferation and development. *Biochem Biophys Res Commun*. 2010;398(2):184-190.

64. Wang G, Guo X, Hong W, et al. Critical regulation of miR-200/ZEB2 pathway in Oct4/Sox2-induced mesenchymal-to-epithelial transition and induced pluripotent stem cell generation. *Proc Natl Acad Sci U S A*. 2013;110(8):2858-2863.

65. Wang Y, Lei L, Zheng YW, et al. Odd-skipped related 1 inhibits lung cancer proliferation and invasion by reducing Wnt signaling through the suppression of SOX9 and β-catenin. *Cancer Sci*. 2018;109(6):1799-1810.

66. Sato N, Meijer L, Skaltsounis L, Greengard P, Brivanlou AH. Maintenance of pluripotency in human and mouse embryonic stem cells through activation of Wnt signaling by a pharmacological GSK-3-specific inhibitor. *Nat Med*. 2004;10(1):55-63.

67. Cole MF, Johnstone SE, Newman JJ, Kagey MH, Young RA. Tcf3 is an integral component of the core regulatory circuitry of embryonic stem cells. *Genes Dev*. 2008;22(6):746-755.

68. Zhang P, Chang WH, Fong B, et al. Regulation of induced pluripotent stem (iPS) cell induction by Wnt/β-catenin signaling. *J Biol Chem*. 2014;289(13):9221-9232.

69. Hou P, Li Y, Zhang X, et al. Pluripotent stem cells induced from mouse somatic cells by small-molecule compounds. *Science*. 2013;341(6146):651-654.

70. Lluis F, Cosma MP. Somatic cell reprogramming control: signaling pathway modulation versus transcription factor activities. *Cell Cycle*. 2009;8(8):1138-1144.

71. Peter IS. Regulatory states in the developmental control of gene expression. *Brief Funct Genomics*. 2017;16(5):281-287.

FIGURE LEGENDS

Figure 1. Screening of mesenchyme-associated transcriptional regulators that reduces the efficiency of reprogramming MEFs. A, Experimental outline for testing the effect of expressed mesenchyme-associated transcriptional regulators on reprogramming. ψ; Packaging signal. NP, P/C, and L; Sendai virus-derived genes. B, Reduced cytotoxicity and enhanced cell viability by lowered expression of mesenchyme-associated transcriptional regulators. cMEFs were transduced with uORF2-containing retroviral vector expressing each transcriptional regulator for two days and selected by puromycin for two days. Cells were photographed after 4 days of transduction. Scale bars, 100 μm. C, Proliferation of MEFs expressing each mesenchyme-associated transcriptional regulator. Proliferation of cells prepared as B was quantified at the indicated days after transduction. Data represent mean ± SEM from three independent experiments. **P* < 0.05, ***P* < 0.01, ****P* < 0.001 versus Day 0. D, AP(+) colonies generated from reprogrammed MEFs that express a mesenchyme-associated transcriptional regulator. cMEFs were transduced as described in B and then reprogrammed by SeVdp(KOSM), and iPSC colonies were stained for AP and counted at day 10 of reprogramming. Data represent mean ± SEM from three independent experiments. ***P* < 0.01, ****P* < 0.001 versus control retroviral vector. Left panels; photos of iPSC colonies after AP staining.

Figure 2. Inhibitory effect of exogenous *Osr2* expression on MET during reprogramming. A, Expression of SSEA1. cMEFs were transduced with or without uORF2-containing retroviral vector expressing *Osr2* and then reprogrammed by SeVdp(KOSM). SSEA1 was detected by immunofluorescence staining at day 12, and SSEA1-positive and -negative colonies were counted. Scale bars, 100 μm. Data represent mean ± SEM from three independent experiments. **P* < 0.05, ****P* < 0.001. B, Growth of iPSC colonies before and after passage. cMEFs were reprogrammed as described in A, and the programmed cells were stained by crystal violet before (Day 22) or after (Day 27) passage. Data represent mean ± SEM from three independent experiments. ***P* < 0.01. C, Structure of SeVdp(KOSMaB) expressing the four reprogramming factors as well as Blasticidin S resistance gene (Bs^r). D, Selection of reprogrammed cells harboring SeVdp(KOSMaB). cMEFs were transduced with a uORF2-containing retroviral vector that expresses *Osr2*. The cells infected with SeVdp(KOSMaB) vector were selected by Blasticidin S. Five days after reprogramming, SeVdp vector-infected cells were immunostained with anti-SeV NP antibody. Scale bars, 100 μm. E, Morphology of reprogrammed cells expressing *Osr2*. Cells prepared in D were observed at day 5. Scale bars, 100 μm. F, Changes in the mRNA expression level of EMT-related genes. cMEFs were reprogrammed as described in D, and the mRNA levels of indicated genes were determined at days 3 and 5 of reprogramming. Data represent mean ± SEM from three independent experiments. **P* < 0.05, ***P* < 0.01, ****P* < 0.001 versus MEF or mouse iPSCs (miPSCs). $^{\#}P$ < 0.05, $^{\#\#}P$ < 0.01 versus control reprogramming in each date.

Figure 3. Induction of EMT in NMuMG cells by OSR2. A, Experimental outline for analyzing the effects of exogenous *Osr2* expression in NMuMG cells. B, Morphology of NMuMG cells expressing *Osr2*. NMuMG cells were transduced with *Osr2*-expressing retroviral vector or treated with 5 ng/mL recombinant TGF-β1. Cell morphology was observed at indicated days. Scale bars, 100 μm. C, Cell migration assay of NMuMG cells expressing *Osr2*. Seven days after transduction of *Osr2*-expressing vector or one day after TGF-β treatment, NMuMG cells were cultured in a Transwell chamber for 16 h. Migrating cells were stained by crystal violet.

Scale bars, 100 μm. D, mRNA expression level of EMT-related genes. NMuMG cells were transduced with *Osr2*-expressing retroviral vector or treated with TGF-β. mRNA levels were determined 10 days after infection or 2 days after TGF-β treatment. Data represent mean ± SEM from three independent experiments. **P* < 0.05, ***P* < 0.01, ****P* < 0.001 versus control NMuMG cells.

Figure 4. Global gene expression profiles of NMuMG cells expressing *Osr2*. A, Hierarchical clustering of NMuMG cells expressing *Osr2* or treated with TGF-β, based on expression profiles from RNA-seq. Samples used for RNA-seq are NMuMG cells transduced with *Osr2*-expressing retroviral vector for 3 days (Day3) or 9 days (Day9) as well as those treated with or without TGF-β (TGFβ or Control, respectively) for 2 days. B, PCA of NMuMG cells expressing *Osr2* or treated with TGF-β. The expression profiles of DEGs among Control, Day3 or Day9, and TGFβ samples (*P* < 0.05) were used for the PCA. C, Hierarchical clustering of DEGs. DEGs among Control, Day3 or Day9, and TGFβ samples were clustered based on expression profiles, and six clusters are indicated in each group. EMT-related genes induced both by exogenous *Osr2* expression and TGF-β treatment are shown on the right side of each panel. The data is deposited in the Gene Expression Omnibus (GEO) with accession number GSE180471 (https://www.ncbi.nlm.nih.gov/geo/query/acc.cgi?acc=GSE180471).

Figure 5. EMT induced by exogenous *Osr2* expression is mediated by TGF-β signaling. A, Morphology of *Osr2*-expressing NMuMG cells treated with TGF-β inhibitor. NMuMG cells were transduced with the retroviral vector expressing *Osr2* or treated with 5 ng/mL TGF-β1. Five days after retroviral transduction or on the same day in case of TGF-β treatment, 10 μg/mL SB431542, or 10 μg/mL RepSox was added to the culture medium. Cell morphology was observed 2 days after treatment with the TGF-β inhibitor. Scale bars, 100 μm. B, mRNA expression level of EMT-related genes. mRNA levels in the cells prepared as described in A were determined 2 days after treatment with TGF-β inhibitor. Data represent mean ± SEM from three independent experiments. **P* < 0.05, ***P* < 0.01 versus control NMuMG cells. $^{\#}P$ < 0.05, $^{\#\#}P$ < 0.01 versus cells without TGF-β inhibitor treatment. C, Effect of TGF-β inhibitor on cell migration of *Osr2*-expressing cells. Cells prepared as described in A were cultured in a Transwell chamber for 16 h. Migrating cells were stained by crystal violet and counted. Scale bars, 100 μm. Data represent mean ± SEM from three independent experiments. **P* < 0.05 versus control NMuMG cells. $^{\#}P$ < 0.05, $^{\#\#}P$ < 0.01 versus cells without TGF-β inhibitor treatment.

Figure 6. Regulation of TGF-β signaling by OSR2 during reprogramming. A, Changes in the mRNA expression level of genes related to TGF-β signaling. *Osr2*-expressing cMEFs were reprogrammed by SeVdp(KOSMaB), and the mRNA levels of indicated genes were determined at days 3 and 5 of reprogramming. Data represent mean ± SEM from three independent experiments. **P* < 0.05, ***P* < 0.01 versus MEF. $^{\#}P$ < 0.05, $^{\#\#}P$ < 0.01 versus control reprogramming at each day. B, Generation of iPSC colonies from MEFs expressing *Osr2* in the presence of TGF-β inhibitor. cMEFs were transduced with the *Osr2*-expressing retroviral vector for 2 days, followed by puromycin selection for 2 days and reprogramming by SeVdp(KOSM). 10 μg/mL SB431542 was added 3 days before reprogramming. iPSC colonies were stained for AP and counted at day 10 of reprogramming. Insets; enlarged images of representative colonies. Scale bars, 100 μm. C, AP staining of iPSC colonies induced by exogenous *Osr2* expression and TGF-β inhibitor. cMEFs expressing *Osr2* were

reprogrammed with or without SB431542 treatment (10 μg/mL) for indicated days. Ten days after reprogramming, the iPSC colonies were stained for AP. Based on the AP staining, the number of the AP-positive and -negative colonies were counted separately. Bottom graph; percentage of AP(+) colonies. Data represent mean ± SEM from three independent experiments. **P* < 0.05, ***P* < 0.01. D, Smad or non-Smad pathway of TGF-β signaling pathway and their inhibitors. E, AP staining of iPSC colonies induced by exogenous *Osr2* expression and TGF-β inhibitors. cMEFs expressing *Osr2* were treated with 10 μg/mL SB431542, 5 μM SB203580, or 1 μM PD0325901 from 3 days before reprogramming by SeVdp(KOSM). The colonies were stained for AP at day 10 of reprogramming. Data represent mean ± SEM from three independent experiments. **P* < 0.05, ***P* < 0.01.

Figure 7. Functional relevance of OSR2 to Wnt signaling during reprogramming. A, Scheme of collecting 4 kinds of cells for RNA-seq. *Osr2*-expressing or control MEFs were treated with or without 10 μg/mL SB431542 from 3 days before reprogramming by SeVdp(KOSMaB). Total RNAs were collected at day 5 of reprogramming. B, Highly enriched pathways in DEGs by exogenous *Osr2* expression. The genes whose TPM changed over 3-fold by exogenous *Osr2* expression were selected as DEGs. Common pathways found in both analyses are highlighted. The data is deposited in GEO with accession number GSE180428 (https://www.ncbi.nlm.nih.gov/geo/query/acc.cgi?acc=GSE180428). C, Changes in the mRNA expression level of genes related to Wnt signaling. *Osr2*-expressing cMEFs were reprogrammed by SeVdp(KOSMaB), and the mRNA levels of indicated genes were determined at days 3 and 5 of reprogramming. Data represent mean ± SEM from three independent experiments. **P* < 0.05 versus MEF. $^{\#}P$ < 0.05 versus control reprogramming at each day. D, Generation of iPSC colonies from MEFs expressing *Osr2* in the presence of TGF-β inhibitor and Wnt activator. cMEFs, transduced with *Osr2*-expressing retroviral vector for 2 days, were selected with puromycin for 2 days and then reprogrammed by SeVdp(KOSM). 10 μg/mL SB431542 and/or 3 μM CHIR99021 was added from 3 days before reprogramming. iPSC colonies were stained for AP and counted at day 10 of reprogramming. Insets; enlarged images of representative colonies. Scale bars, 100 μm. E, Number of iPSC colonies induced in the presence of TGF-β inhibitor and/or Wnt activator. cMEFs were reprogrammed as described in D. Ten days after reprogramming, iPSC colonies were stained for AP. Based on the AP staining, the number of the AP-positive and -negative colonies were counted separately. Data represent mean ± SEM from three independent experiments. **P* < 0.05, ***P* < 0.01, ****P* < 0.001. F, Changes in the mRNA expression level of pluripotency-related genes. cMEFs were reprogrammed as described in D using SeVdp(KOSMaB), then the mRNA levels of indicated genes were determined at day 10 of reprogramming. Data represent mean ± SEM from three independent experiments. **P* < 0.05, ***P* < 0.01, ****P* < 0.001 versus control reprogramming neither with SB431542 or CHIR99021. $^{\#}P$ < 0.05, $^{\#\#}P$ < 0.01 versus control reprogramming under each condition.

LEGEND FOR GRAPHICAL ABSTRACT

This study shows that downregulation of *Osr2* is crucial for efficient reprogramming of mesenchymal cells. The *Osr2* downregulation has an important role both for a progression of mesenchymal-epithelial transition (MET) and an acquisition of pluripotency in somatic cell reprogramming through TGF-β and Wnt signaling, respectively.

Figure 1

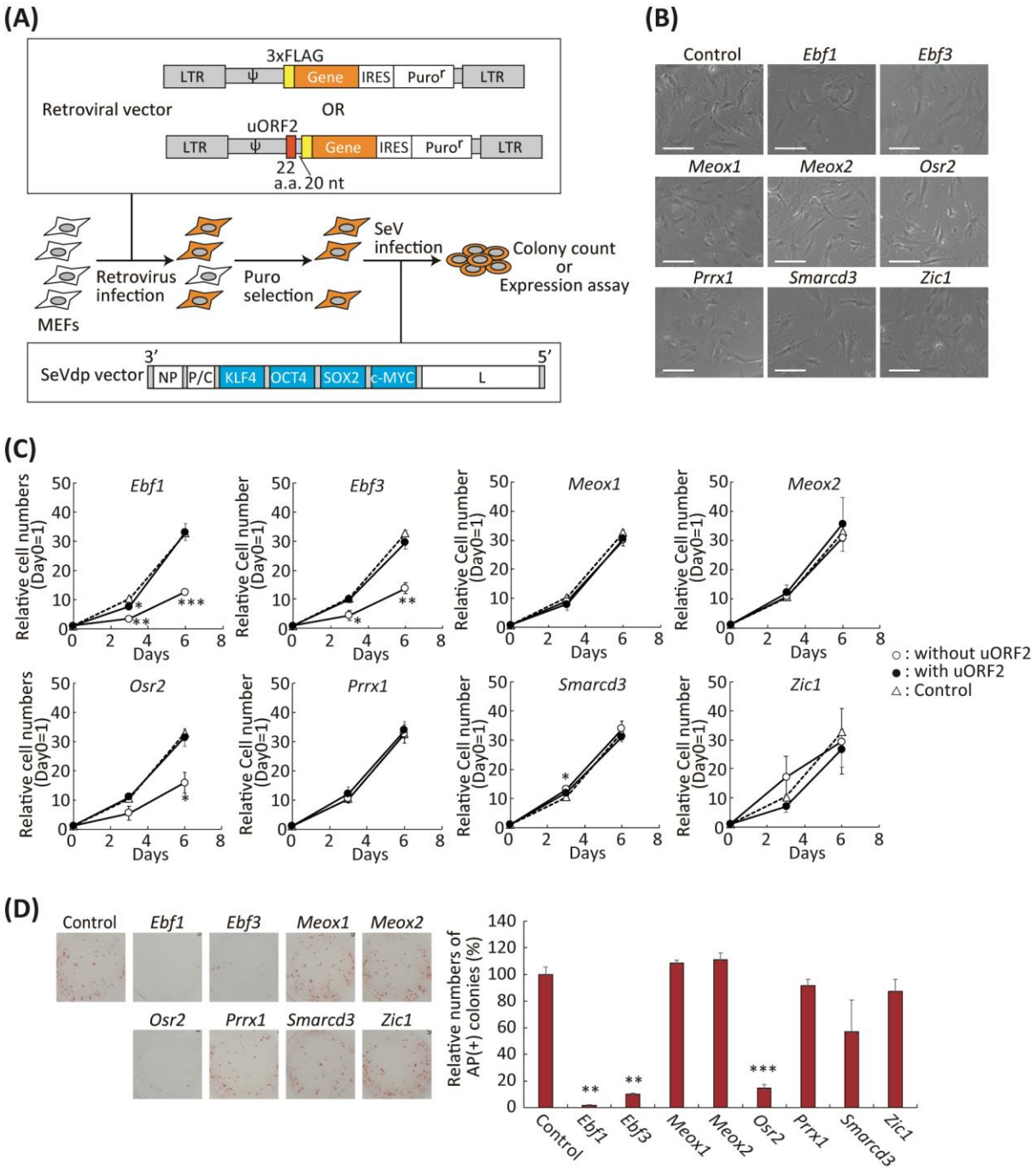
(A)
3xFLAG
LTR
Ψ
Gene
IRES
Puroʳ
LTR
Retroviral vector
OR
uORF2
22 a.a. 20 nt
MEFs
Retrovirus infection
Puro selection
SeV infection
Colony count or Expression assay
SeVdp vector
3′
5′
NP
P/C
KLF4
OCT4
SOX2
c-MYC
L
(B)
Control
Ebf1
Ebf3
Meox1
Meox2
Osr2
Prrx1
Smarcd3
Zic1
(C)
Relative cell numbers (Day0=1)
Relative Cell number (Day0=1)
Days
○ : without uORF2
● : with uORF2
△ : Control
(D)
Relative numbers of AP(+) colonies (%)

Figure 2

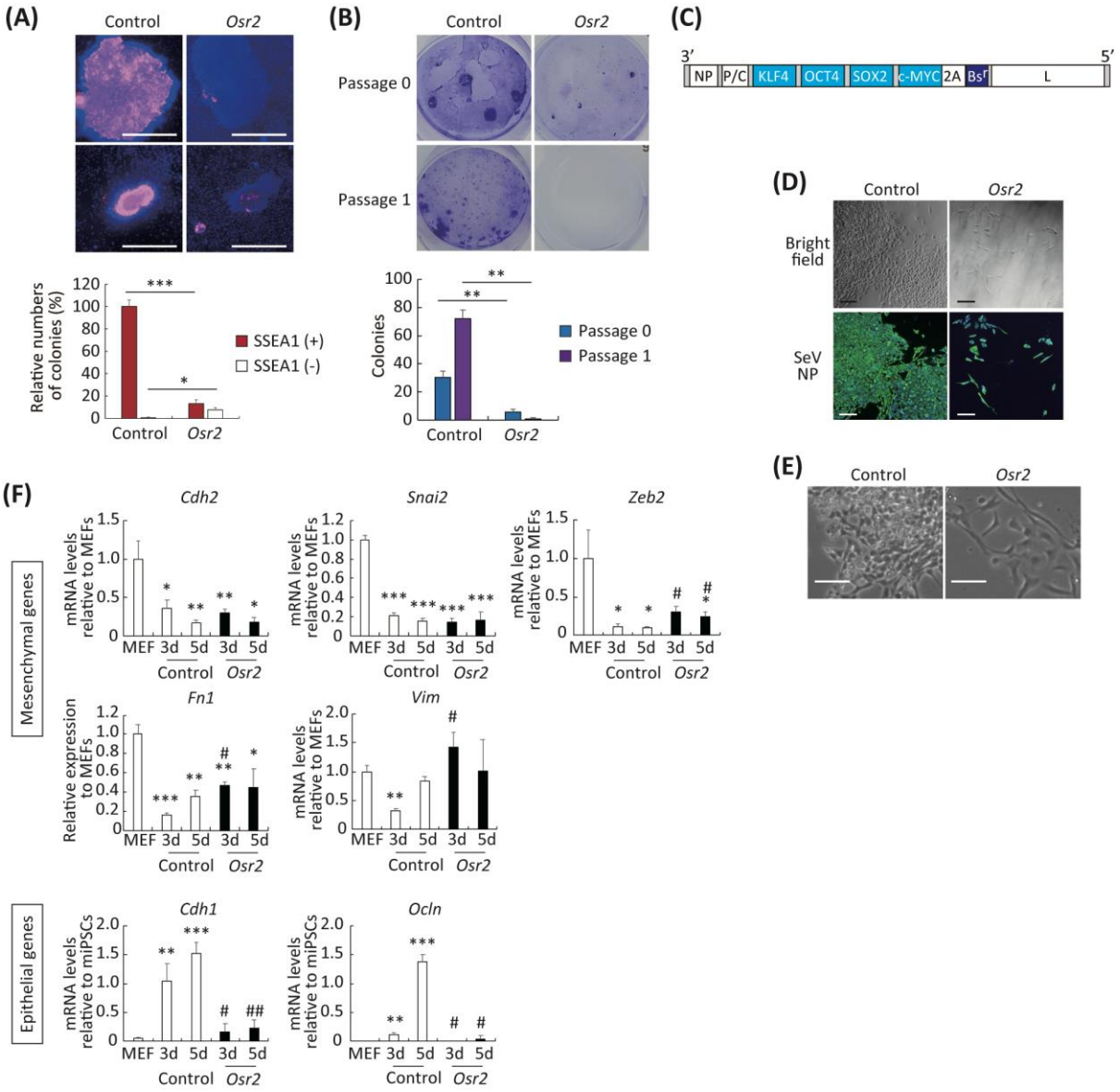
(A)
Control
Osr2
Relative numbers of colonies (%)
SSEA1 (+)
SSEA1 (-)
(B)
Passage 0
Passage 1
Colonies
(C)
3′
5′
NP
P/C
KLF4
OCT4
SOX2
c-MYC
2A
Bsr
L
(D)
Bright field
SeV NP
(E)
(F)
Mesenchymal genes
Epithelial genes
Cdh2
Snai2
Zeb2
Fn1
Vim
Cdh1
Ocln
mRNA levels relative to MEFs
Relative expression to MEFs
mRNA levels relative to miPSCs
MEF
3d
5d

Figure 3

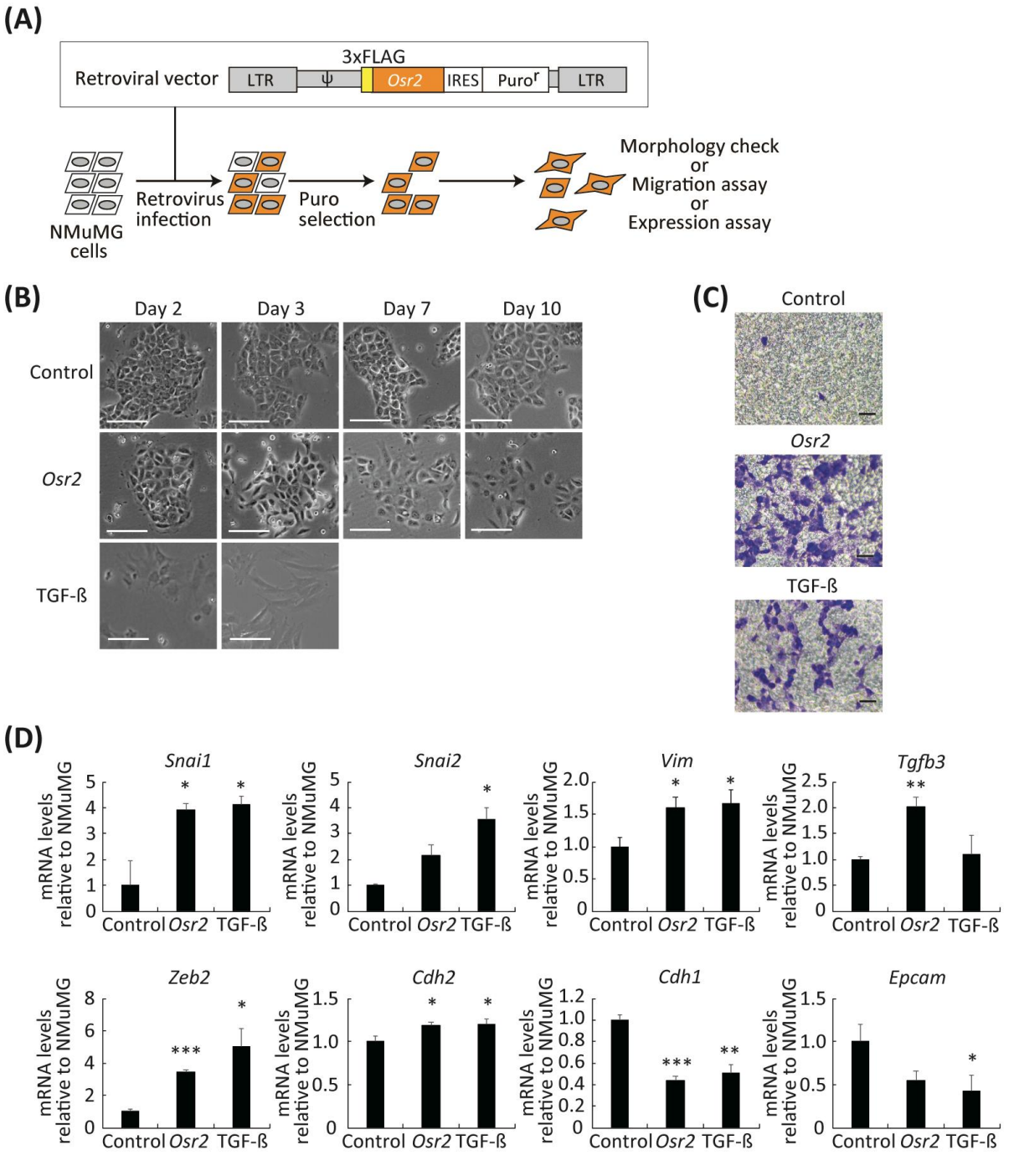
(A)
Retroviral vector
3xFLAG
LTR
Ψ
Osr2
IRES
Puro^r
LTR
NMuMG cells
Retrovirus infection
Puro selection
Morphology check or Migration assay or Expression assay
(B)
Day 2
Day 3
Day 7
Day 10
Control
Osr2
TGF-ß
(C)
Control
Osr2
TGF-ß
(D)
Snai1
Snai2
Vim
Tgfb3
Zeb2
Cdh2
Cdh1
Epcam
mRNA levels relative to NMuMG
Control
Osr2
TGF-ß

Figure 4

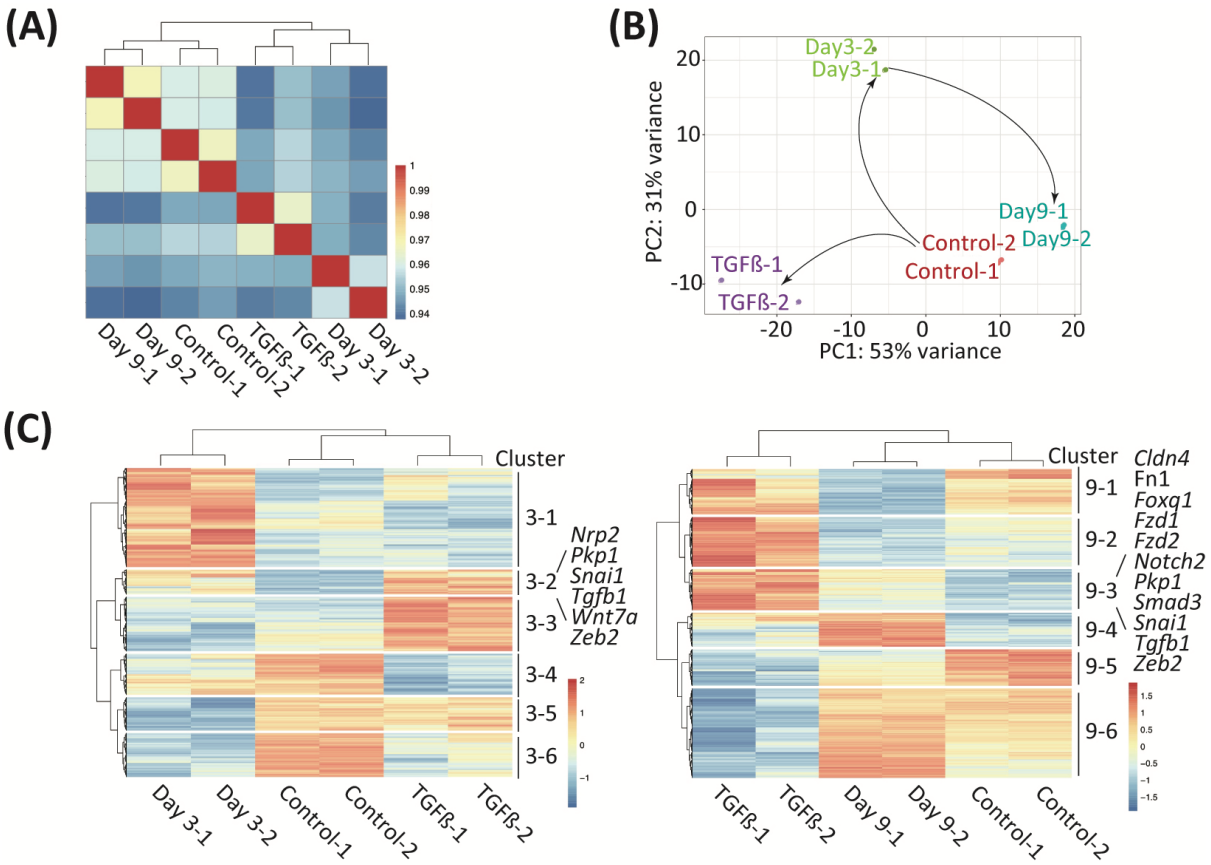
(A)
Day 9-1
Day 9-2
Control-1
Control-2
TGFß-1
TGFß-2
Day 3-1
Day 3-2
(B)
PC2: 31% variance
PC1: 53% variance
Day3-2
Day3-1
Day9-1
Day9-2
Control-2
Control-1
TGFß-1
TGFß-2
(C)
Cluster
3-1
3-2
3-3
3-4
3-5
3-6
Nrp2
Pkp1
Snai1
Tgfb1
Wnt7a
Zeb2
Day 3-1
Day 3-2
Control-1
Control-2
TGFß-1
TGFß-2
Cluster
9-1
9-2
9-3
9-4
9-5
9-6
Cldn4
Fn1
Foxq1
Fzd1
Fzd2
Notch2
Pkp1
Smad3
Snai1
Tgfb1
Zeb2
TGFß-1
TGFß-2
Day 9-1
Day 9-2
Control-1
Control-2

Figure 5

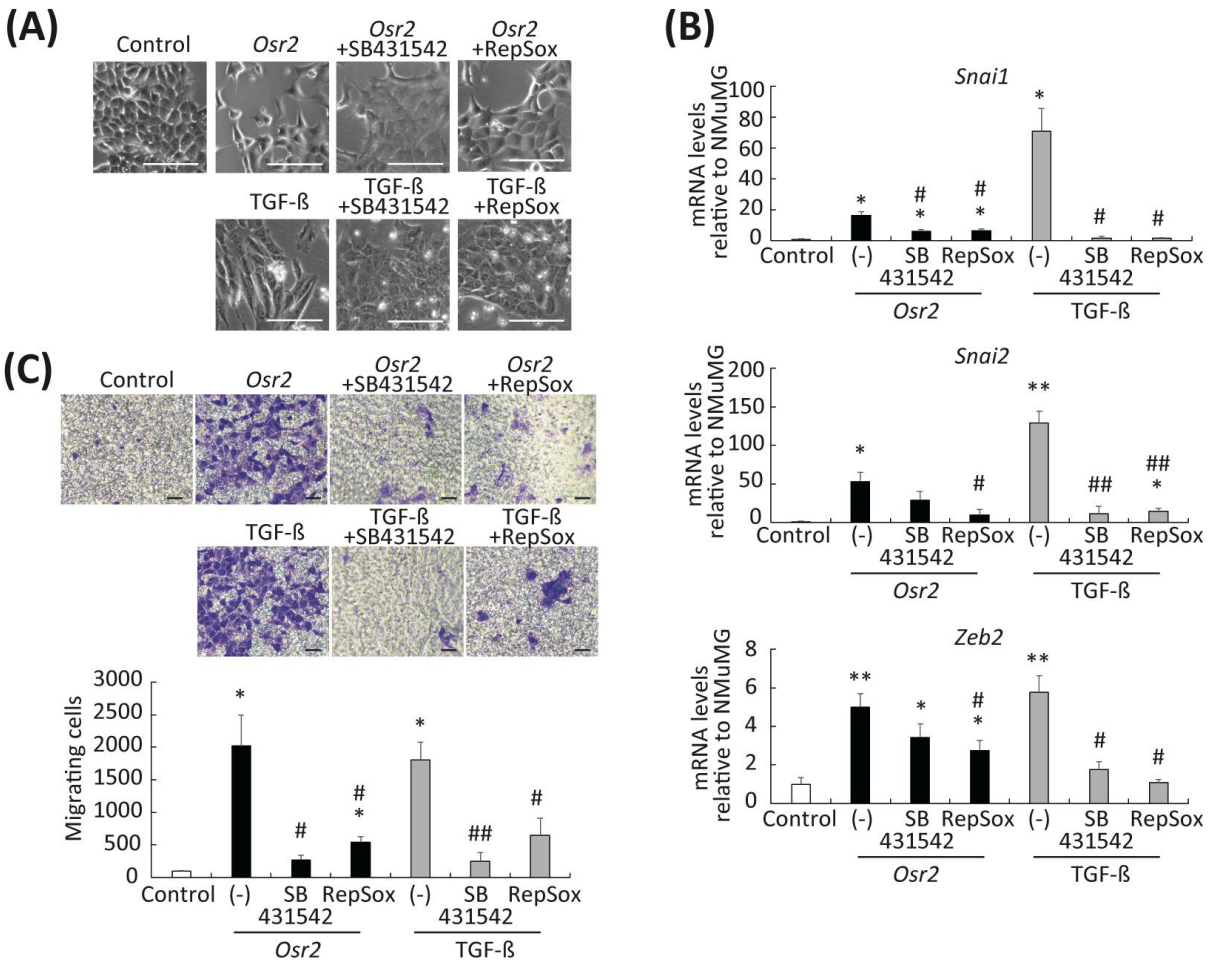
(A)
Control
Osr2
Osr2 +SB431542
Osr2 +RepSox
TGF-ß
TGF-ß +SB431542
TGF-ß +RepSox
(B)
Snai1
Snai2
Zeb2
mRNA levels relative to NMuMG
Control
(-)
SB 431542
RepSox
Osr2
TGF-ß
(C)
Migrating cells

Figure 6

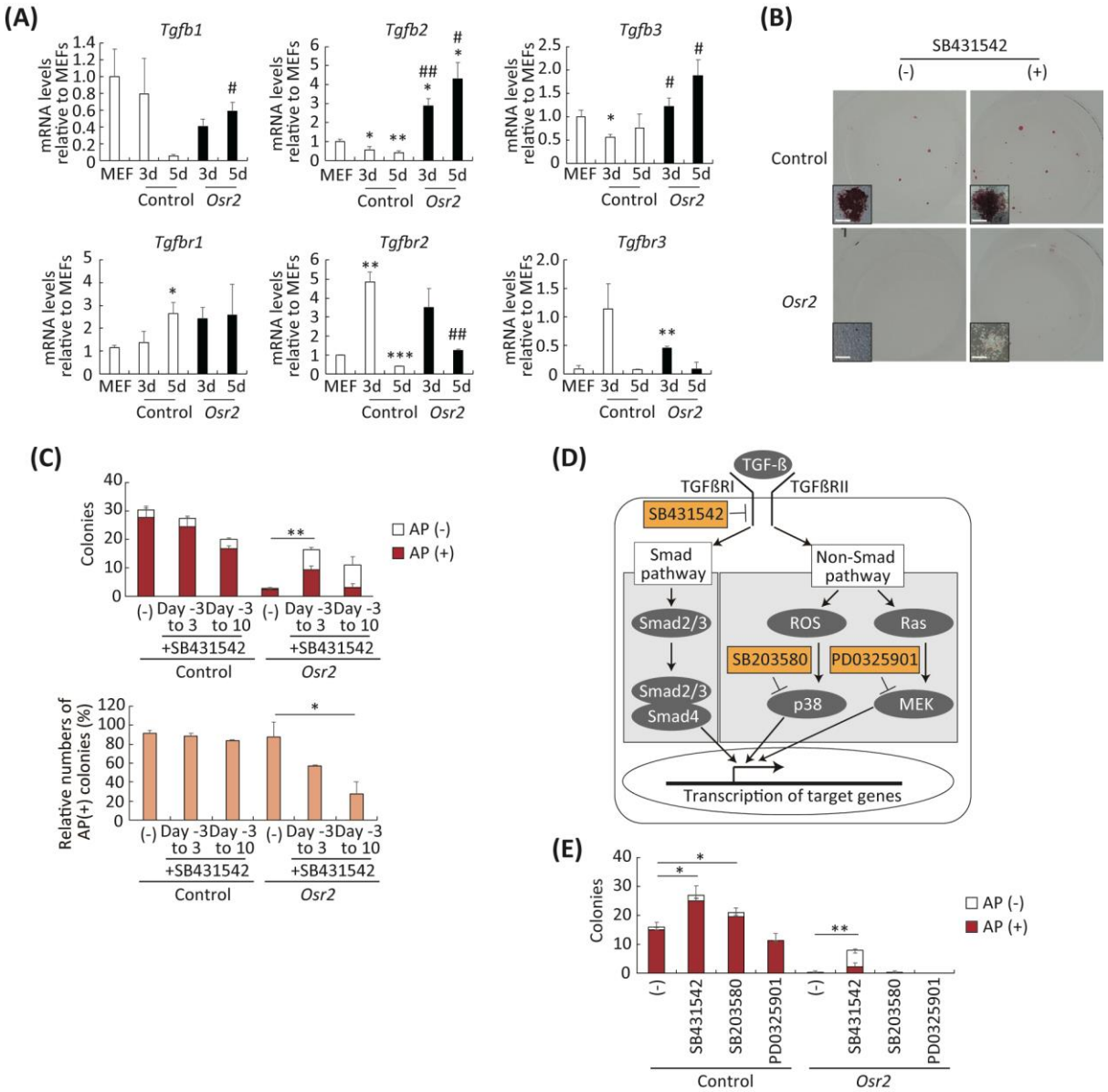
(A)
Tgfb1
Tgfb2
Tgfb3
Tgfbr1
Tgfbr2
Tgfbr3
mRNA levels relative to MEFs
MEF 3d 5d 3d 5d
Control Osr2
(B)
SB431542
(-) (+)
Control
Osr2
(C)
Colonies
AP (-)
AP (+)
(-) Day -3 to 3 Day -3 to 10
+SB431542
Control Osr2
Relative numbers of AP(+) colonies (%)
(D)
TGF-ß
TGFßRI
TGFßRII
SB431542
Smad pathway
Non-Smad pathway
Smad2/3
ROS
Ras
SB203580
PD0325901
Smad2/3
Smad4
p38
MEK
Transcription of target genes
(E)
Colonies
AP (-)
AP (+)
(-) SB431542 SB203580 PD0325901
Control Osr2

Figure 7

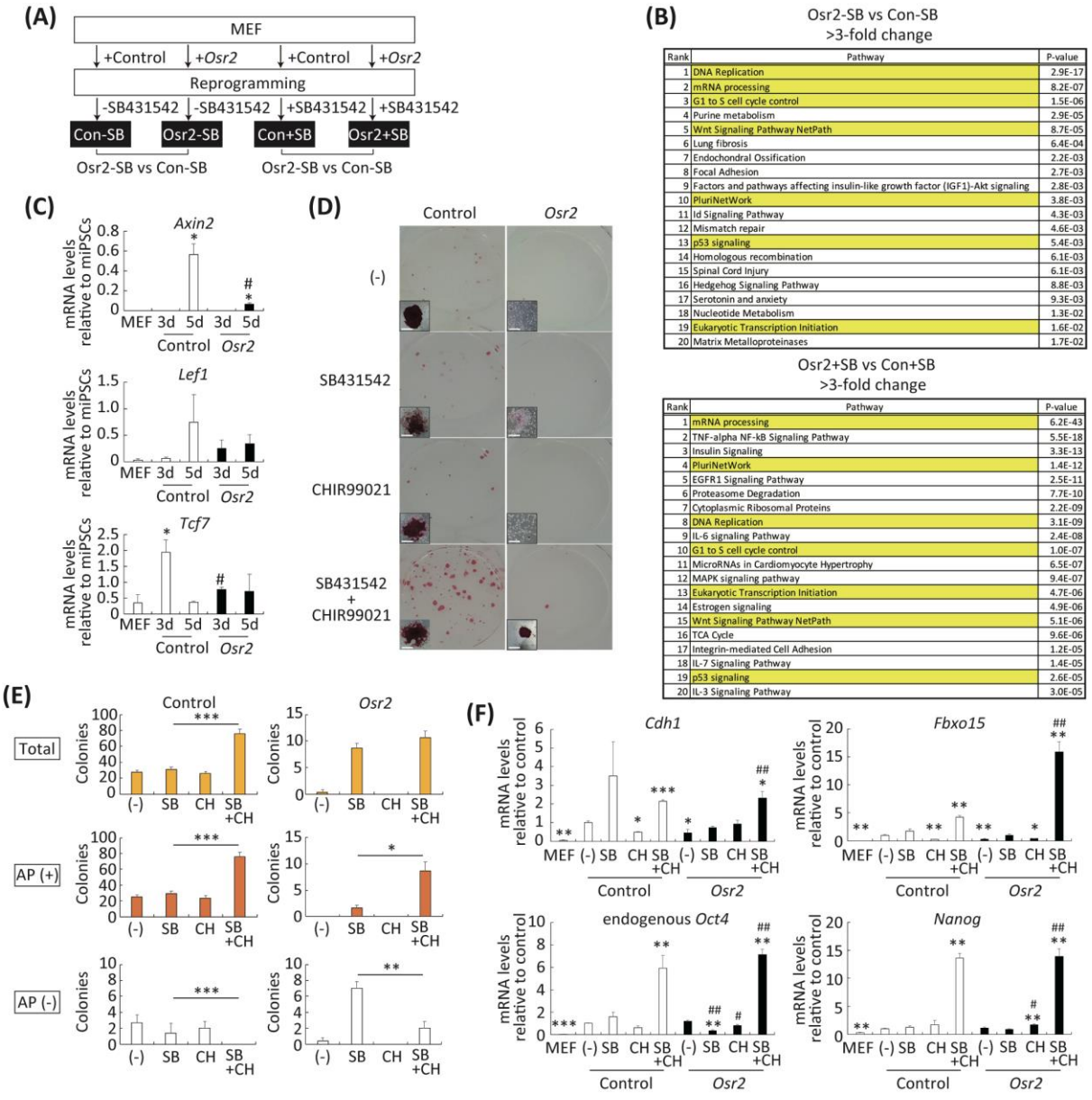
(A)
MEF
+Control
+Osr2
+Control
+Osr2
Reprogramming
-SB431542
-SB431542
+SB431542
+SB431542
Con-SB
Osr2-SB
Con+SB
Osr2+SB
Osr2-SB vs Con-SB
Osr2-SB vs Con-SB
(B)
Osr2-SB vs Con-SB
>3-fold change
Rank Pathway P-value
1 DNA Replication 2.9E-17
2 mRNA processing 8.2E-07
3 G1 to S cell cycle control 1.5E-06
4 Purine metabolism 2.9E-05
5 Wnt Signaling Pathway NetPath 8.7E-05
6 Lung fibrosis 6.4E-04
7 Endochondral Ossification 2.2E-03
8 Focal Adhesion 2.7E-03
9 Factors and pathways affecting insulin-like growth factor (IGF1)-Akt signaling 2.8E-03
10 PluriNetWork 3.8E-03
11 Id Signaling Pathway 4.3E-03
12 Mismatch repair 4.6E-03
13 p53 signaling 5.4E-03
14 Homologous recombination 6.1E-03
15 Spinal Cord Injury 6.1E-03
16 Hedgehog Signaling Pathway 8.8E-03
17 Serotonin and anxiety 9.3E-03
18 Nucleotide Metabolism 1.3E-02
19 Eukaryotic Transcription Initiation 1.6E-02
20 Matrix Metalloproteinases 1.7E-02
Osr2+SB vs Con+SB
>3-fold change
Rank Pathway P-value
1 mRNA processing 6.2E-43
2 TNF-alpha NF-kB Signaling Pathway 5.5E-18
3 Insulin Signaling 3.3E-13
4 PluriNetWork 1.4E-12
5 EGFR1 Signaling Pathway 2.5E-11
6 Proteasome Degradation 7.7E-10
7 Cytoplasmic Ribosomal Proteins 2.2E-09
8 DNA Replication 3.1E-09
9 IL-6 signaling Pathway 2.4E-08
10 G1 to S cell cycle control 1.0E-07
11 MicroRNAs in Cardiomyocyte Hypertrophy 6.5E-07
12 MAPK signaling pathway 9.4E-07
13 Eukaryotic Transcription Initiation 4.7E-06
14 Estrogen signaling 4.9E-06
15 Wnt Signaling Pathway NetPath 5.1E-06
16 TCA Cycle 9.6E-06
17 Integrin-mediated Cell Adhesion 1.2E-05
18 IL-7 Signaling Pathway 1.4E-05
19 p53 signaling 2.6E-05
20 IL-3 Signaling Pathway 3.0E-05
(C)
Axin2
Lef1
Tcf7
mRNA levels relative to miPSCs
MEF 3d 5d 3d 5d
Control Osr2
(D)
Control
Osr2
(-)
SB431542
CHIR99021
SB431542 + CHIR99021
(E)
Control
Osr2
Total
AP (+)
AP (-)
Colonies
(-) SB CH SB +CH
(F)
Cdh1
Fbxo15
endogenous Oct4
Nanog
mRNA levels relative to control
MEF (-) SB CH SB +CH (-) SB CH SB +CH
Control
Osr2

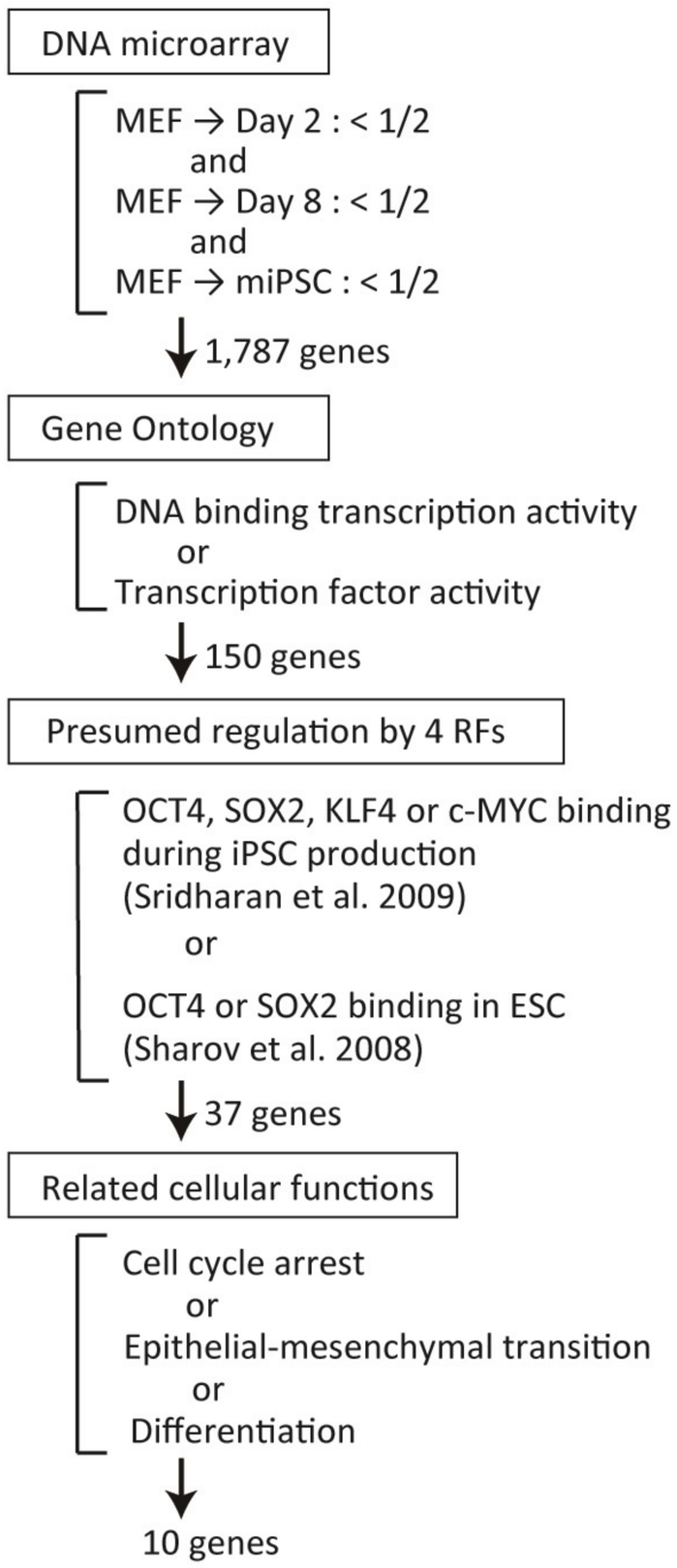

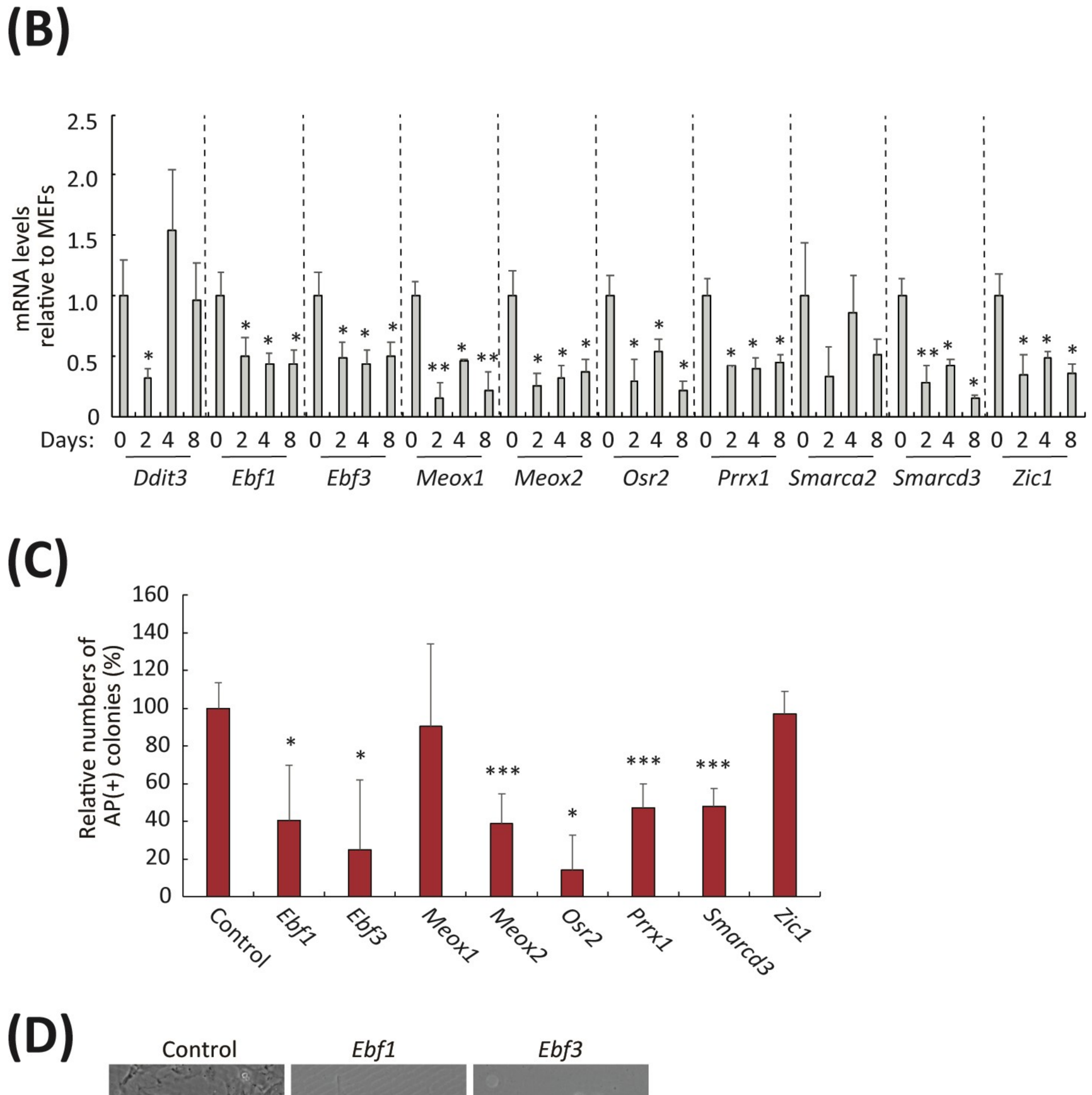

Figure S1. Screening of mesenchyme-associated transcriptional regulators that reduce the reprogramming efficiency of MEFs

A, Flowchart of the screening. Genome-wide gene expression data sets (GSE134847) were used to select 1,787 genes whose expression were downregulated over 2-fold at day 2 and day 8 of reprogramming by SeVdp(KOSM) as well as in mouse iPSCs compared with MEFs. Ten genes were selected as mesenchyme-associated transcriptional regulators by presumed function as a transcriptional regulator, binding near the gene, and presumed functional role in cell cycle, mesenchymal-epithelial transition, or differentiation.

B, Changes in the mRNA expression level of 10 mesenchyme-associated transcriptional regulators during first 8 days of iPSC generation. cMEFs were reprogrammed by SeVdp(KOSM) and their mRNA levels were determined at days 0, 2, 4, and 8. Data represent mean ± SEM from three independent experiments. *$P < 0.05$, **$P < 0.01$ versus MEF.

C, Generation of alkaline phosphatase-positive (AP(+)) colonies from MEFs expressing each mesenchyme-associated transcriptional regulator. cMEFs were transduced with the retroviral vector for 2 days, followed by puromycin selection for 2 days. Selected cells were then reprogrammed by SeVdp(KOSM), and iPSC colonies were stained for AP and counted at day 10 of reprogramming. Data represent mean ± SEM from three independent experiments. *$P < 0.05$, ***$P < 0.001$ versus control reprogramming.

D, Growth of MEFs expressing mesenchyme-associated transcriptional regulator. cMEFs were transduced with the retroviral vector that expresses each transcriptional regulator. Cell proliferation was observed at day 4. Scale bars, 100 μm.

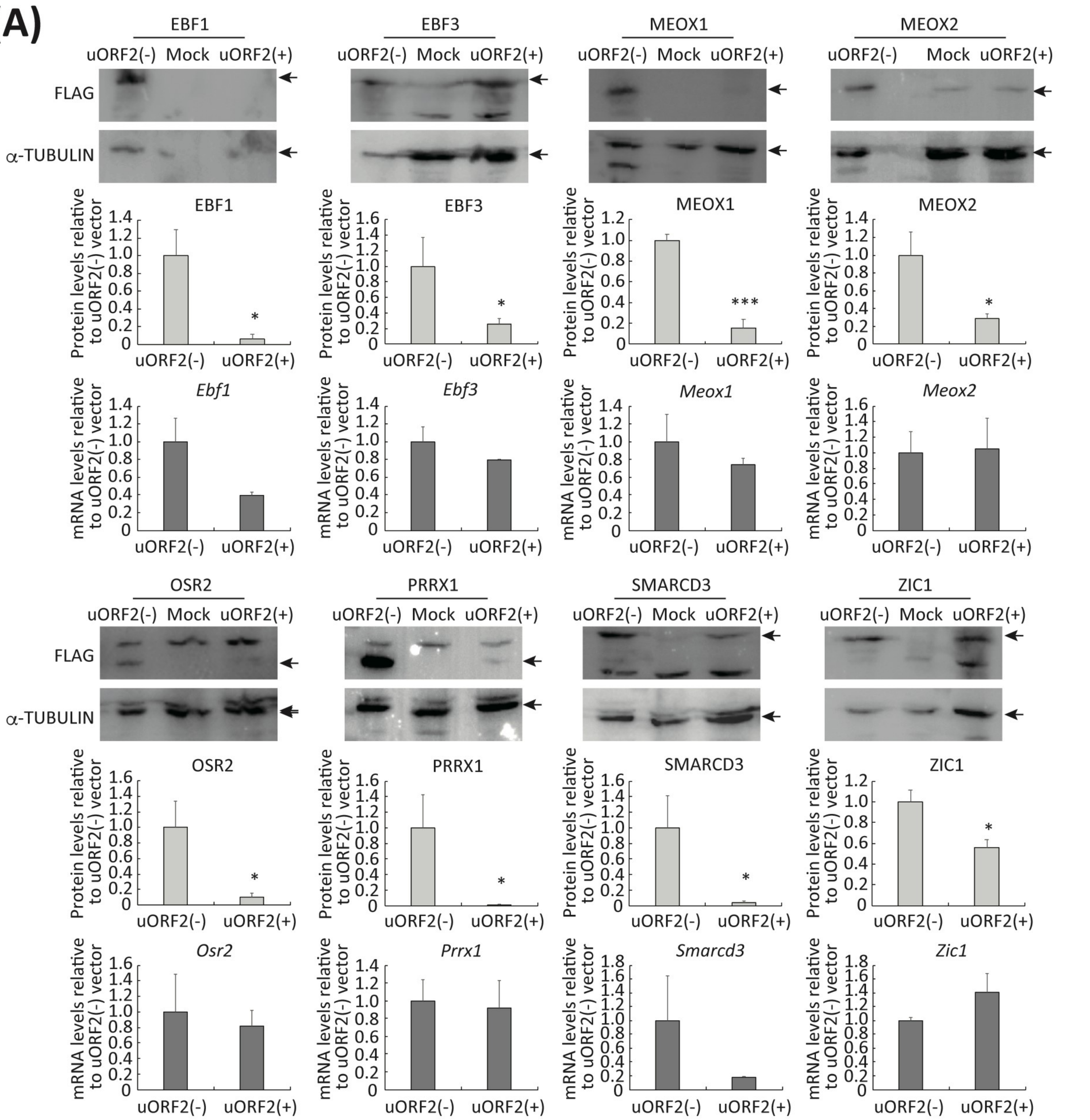

Figure S2. Reduced translation by uORF2

A, Changes in protein and mRNA levels by insertion of uORF2. NIH3T3 cells were transduced with standard (uORF2(-)) or uORF2-containing retroviral vector (uORF2(+)) that expresses each transcriptional regulator. Whole cell extracts and total RNAs were prepared from NIH3T3 cells 3 days after transduction with standard or uORF2-containing retroviral vector. Protein levels were determined by western blotting using anti-FLAG (upper panels) or anti-α-TUBULIN (lower panels) antibody for the whole cell extracts. mRNA levels were determined by RT-qPCR of the total RNAs. Arrows indicate the positions of quantified bands. Data represent mean ± SEM from three independent experiments. $*P < 0.05$, $***P < 0.001$ versus standard retroviral vector.

B, Cell death of MEFs expressing *Ebf1, Ebf3*, or *Osr2* upon reprogramming. cMEFs were transduced with uORF2-containing retroviral vector that expresses control hKO, *Ebf1, Ebf3*, or *Osr2*. After puromycin selection for 2 days, the selected cells were infected with or without SeVdp(KOSMaB) vector. Cells were observed 5 days after SeVdp vector infection. Scale bars, 100 μm.

C, Proliferation of MEFs expressing *Ebf1, Ebf3*, or *Osr2* upon reprogramming. Proliferation of cMEFs transduced with uORF2-containing retroviral vector expressing control hKO, *Ebf1, Ebf3*, or *Osr2* were quantified before or 3 days after reprogramming. Data represent mean ± SEM from three independent experiments. $***P < 0.001$ versus control retroviral vector.

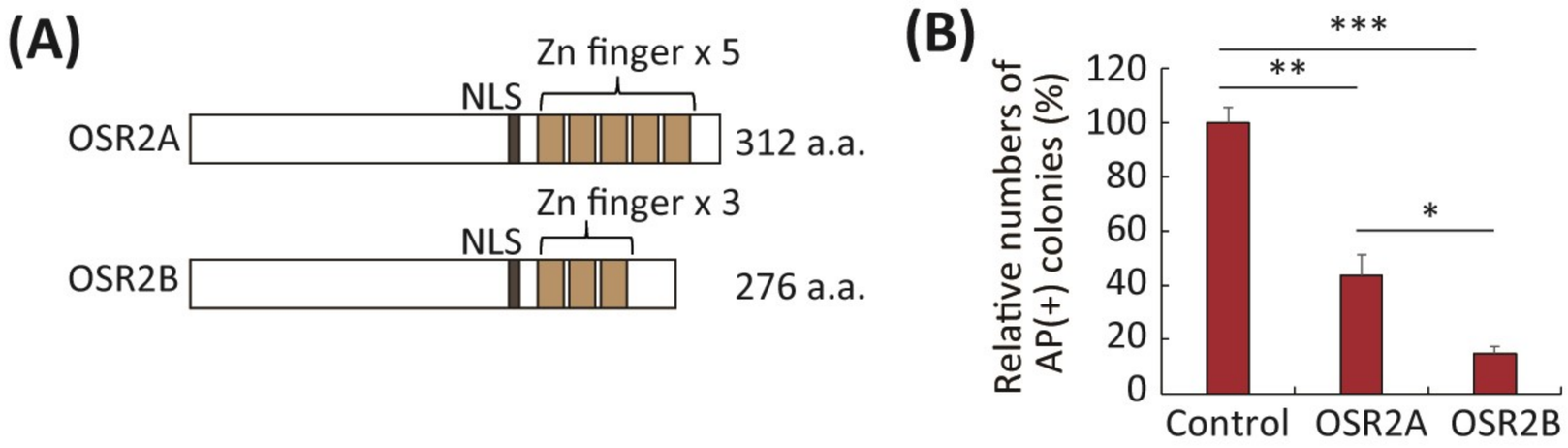

Figure S3. Inhibitory effect of OSR2 isoforms on iPSC generation.

A, Structures of OSR2 isoforms. NLS; nuclear localization signal.

B, Induction of AP(+) colonies from MEFs expressing each OSR2 isoform. cMEFs were transduced with uORF2-containing retroviral vector that expresses either OSR2A or OSR2B and then reprogrammed by SeVdp(KOSM). After 10 days of reprogramming, colonies were stained for AP and counted. Data represent mean ± SEM from three independent experiments. $*P < 0.05$, $**P < 0.01$, $***P < 0.001$.

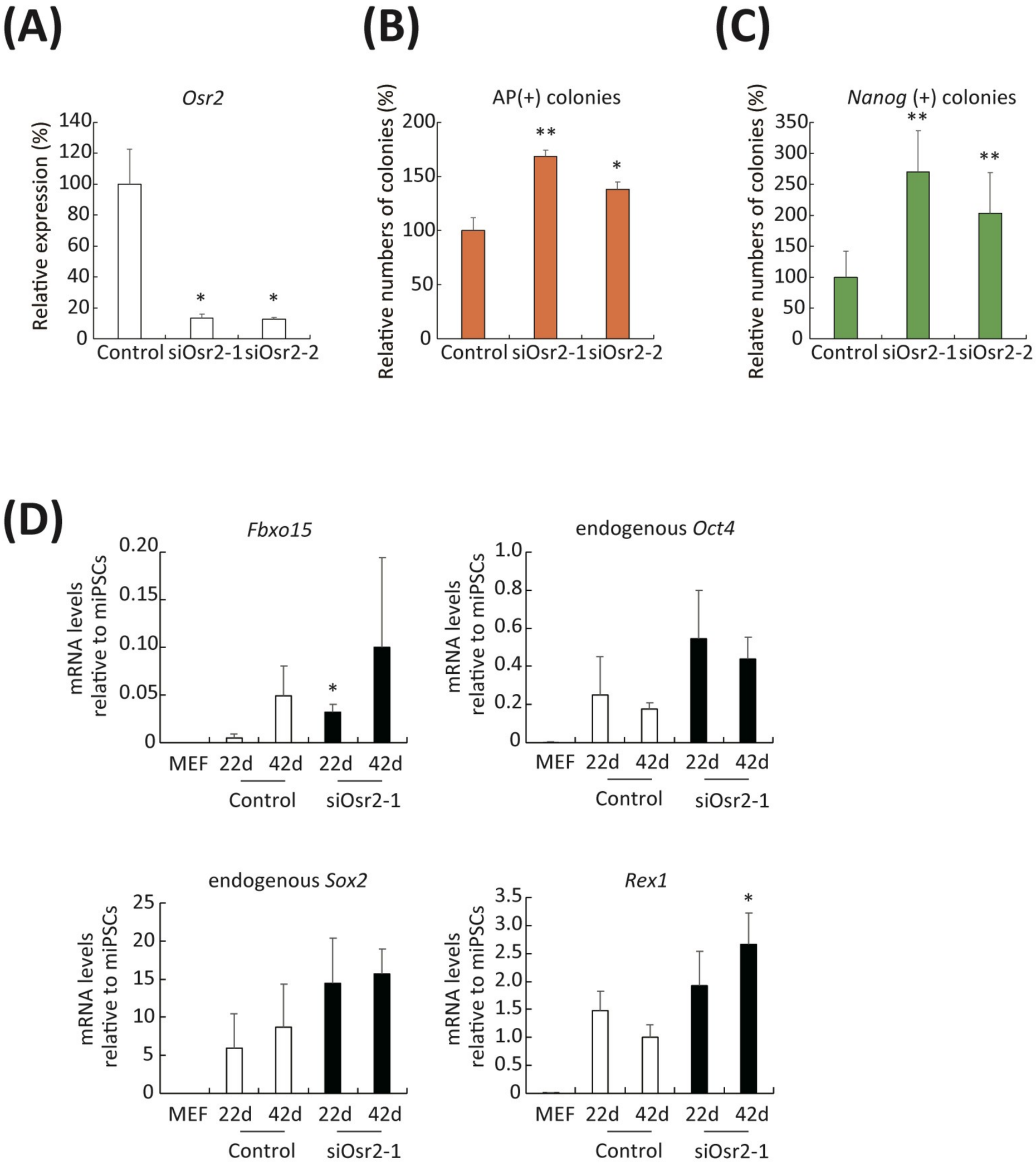

Figure S4. iPSC generation after *Osr2* knockdown

A, Expression of *Osr2* after its knockdown. cMEFs were transfected with each siOsr2 for 2 days, and the expression level of *Osr2* was determined by RT-qPCR.

B and C, Increased number of AP(+) or *Nanog* (+) colonies by knockdown of *Osr2*. siOsr2-treated nMEFs as described in A were reprogrammed by SeVdp(KOSM). AP(+) (B) or *Nanog*-GFP (+) (C) iPSC colonies were counted at day 10 or 23 of reprogramming, respectively. All of the data represent mean ± SEM from three independent experiments. * $P < 0.05$, ** $P < 0.01$ versus reprogramming without *Osr2* knockdown.

D, Changes in the mRNA expression level of pluripotency-related genes. nMEFs were reprogrammed as described in B, and then the mRNA levels of indicated genes were determined at days 22 or 42 of reprogramming. Data represent mean ± SEM from three independent experiments. * $P < 0.05$ versus control reprogramming in each date.

Osr2 Day 3

<Cluster 3-2> +Osr2 & TGFß: High

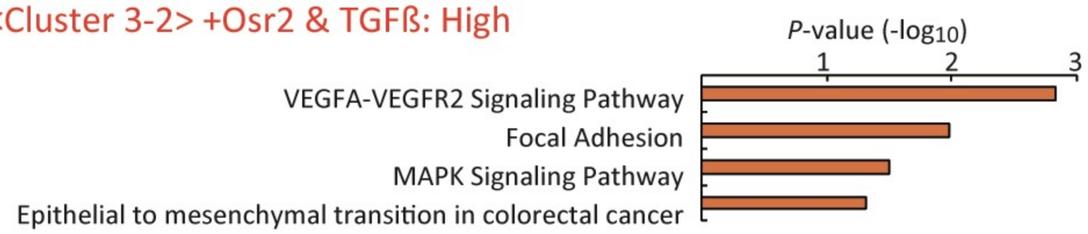

<Cluster 3-1> +Osr2 only: High

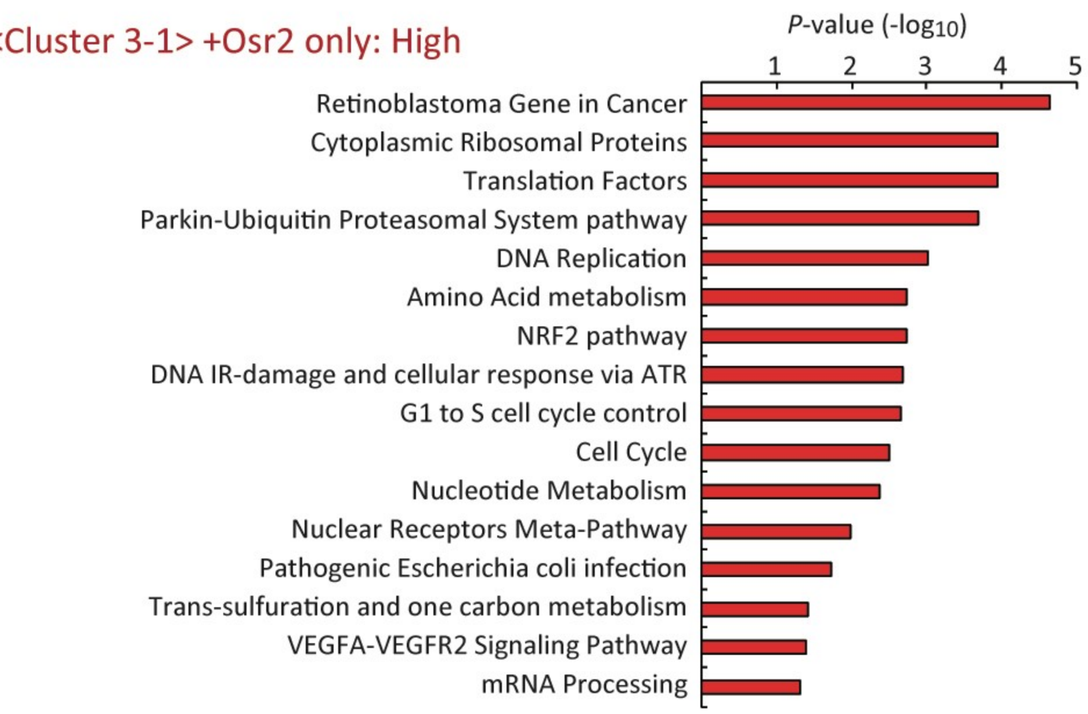

<Cluster 3-6> +Osr2 & TGFß: Low

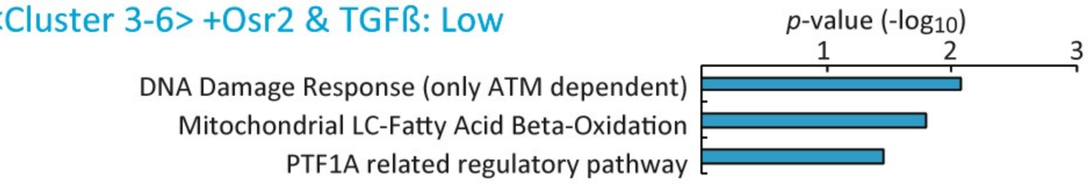

<Cluster 3-5> +Osr2 only: Low

No highly enriched pathway

Osr2 Day 9

<Cluster 9-3> +Osr2 & TGFß: High

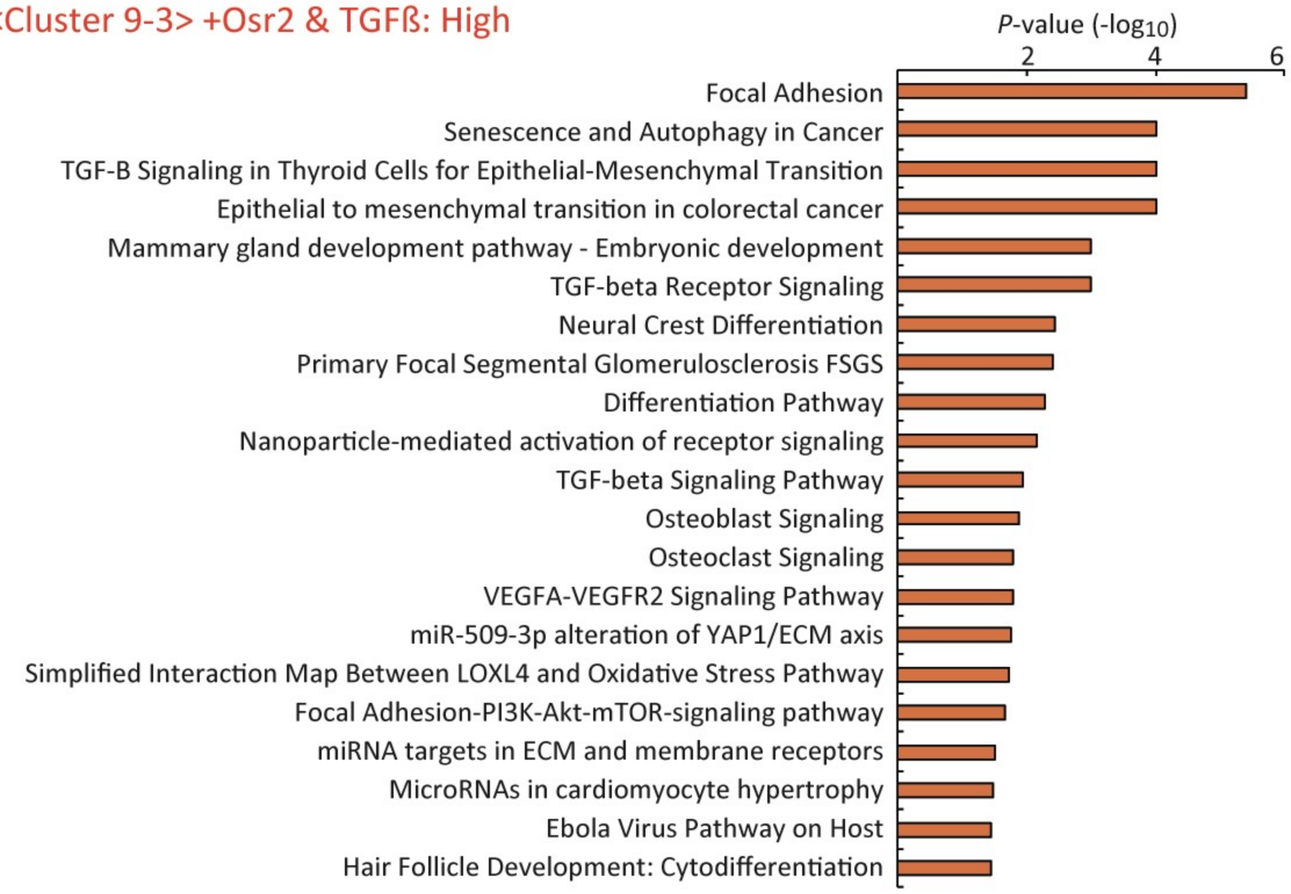

<Cluster 9-4> +Osr2 only: High

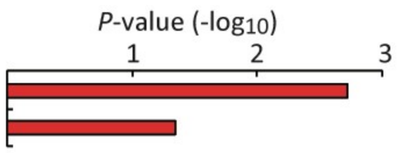

<Cluster 9-5> +Osr2 & TGFß: Low

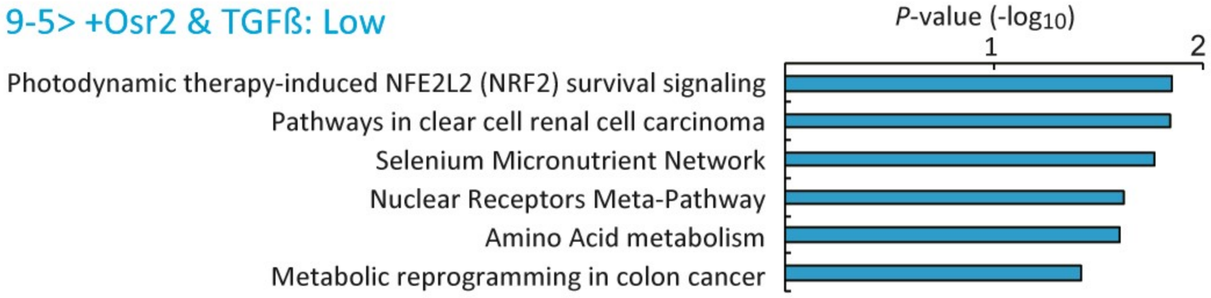

<Cluster 9-1> +Osr2 only: Low

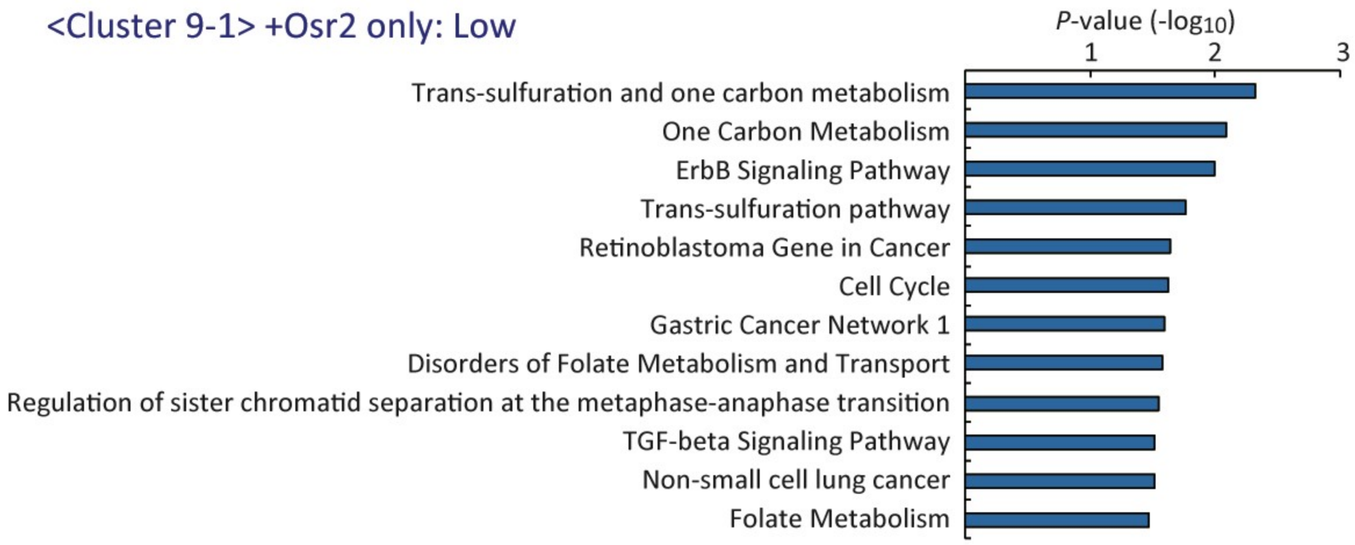

Figure S5. Enriched pathways in the selected cluster

Highly enriched pathways ($P < 0.05$) in clusters 3-1, 3-2, 3-5, 3-6, 9-1, 9-3, 9-4, or 9-5 in Figure 4C are shown.

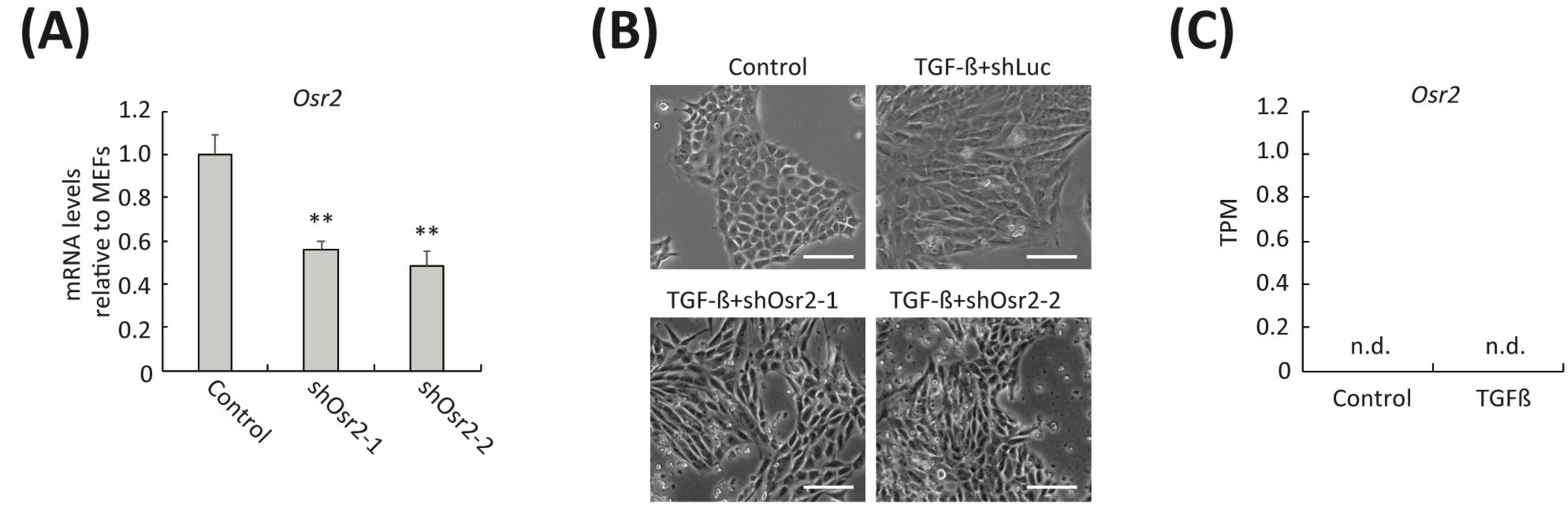

Figure S6. Relationship between TGF-ß and *Osr2* expression

A, Suppression of *Osr2* expression by shRNA against *Osr2*. NIH3T3 cells were transduced with retroviral vector that expresses the indicated shRNA against *Osr2*, followed by puromycin selection. mRNA levels of *Osr2* were determined 2 days after transduction. Data represent mean ± SEM from three independent experiments. $^{**}P < 0.01$ versus control NIH3T3 cells.

B, Morphology of NMuMG cells treated with TGF-ß after *Osr2* knockdown. NMuMG cells were transduced with retroviral vector that expresses shRNA against *Osr2* and selected by puromycin. The selected cells were then treated with 5 ng/mL TGF-ß1. Cell morphology was observed 2 days after TGF-ß treatment. Scale bars, 100 µm.

C, *Osr2* expression in NMuMG cells after TGF-ß treatment. Average TPM values of *Osr2* mRNA levels were extracted from RNA-seq data in Figure 4. n.d.; not detected.

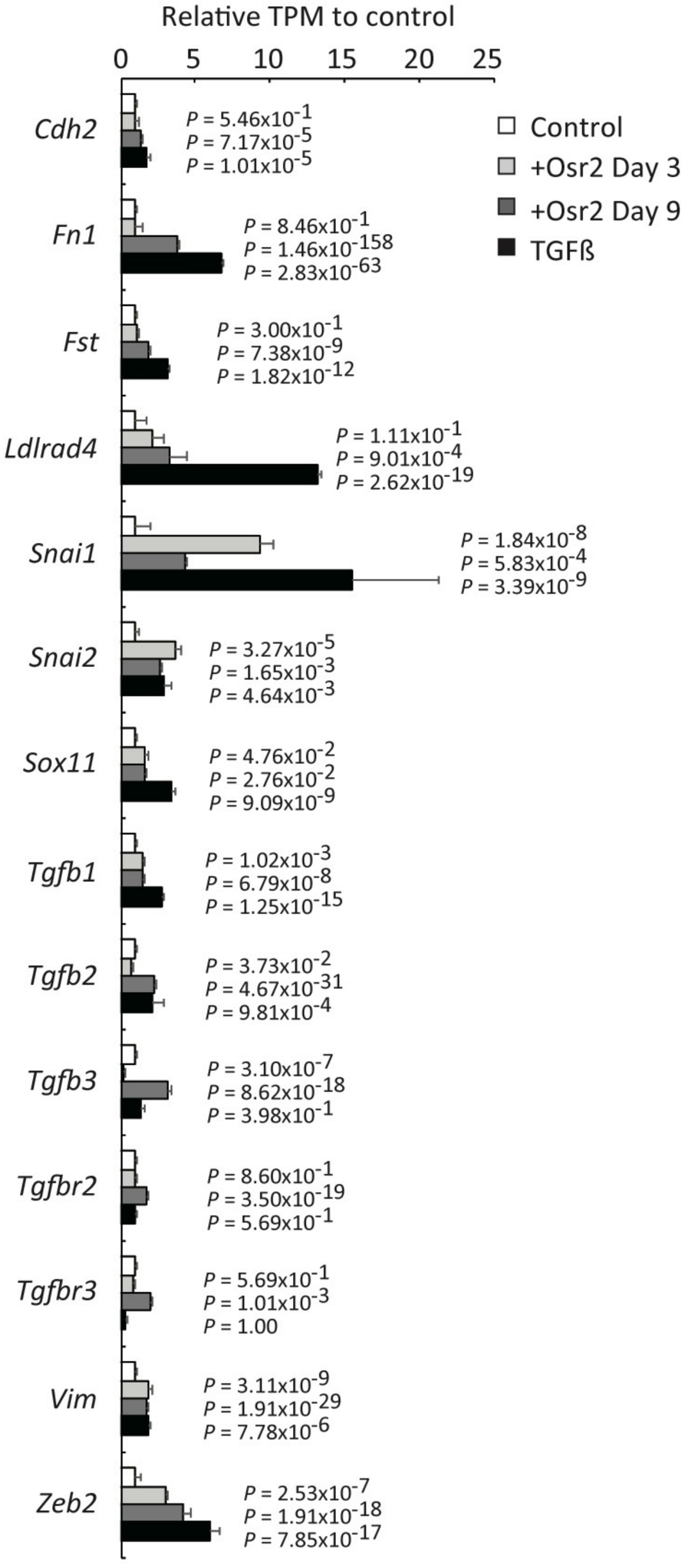

Figure S7. Expression of genes related to the TGF-ß signaling pathway in NMuMG cells upon expression of *Osr2*

Average of TPM values of the mRNA levels of indicated genes were extracted from RNA-seq data in Figure 4 and normalized to those in control NMuMG cells. *P*-values versus control cells, calculated by DESeq2, are shown.

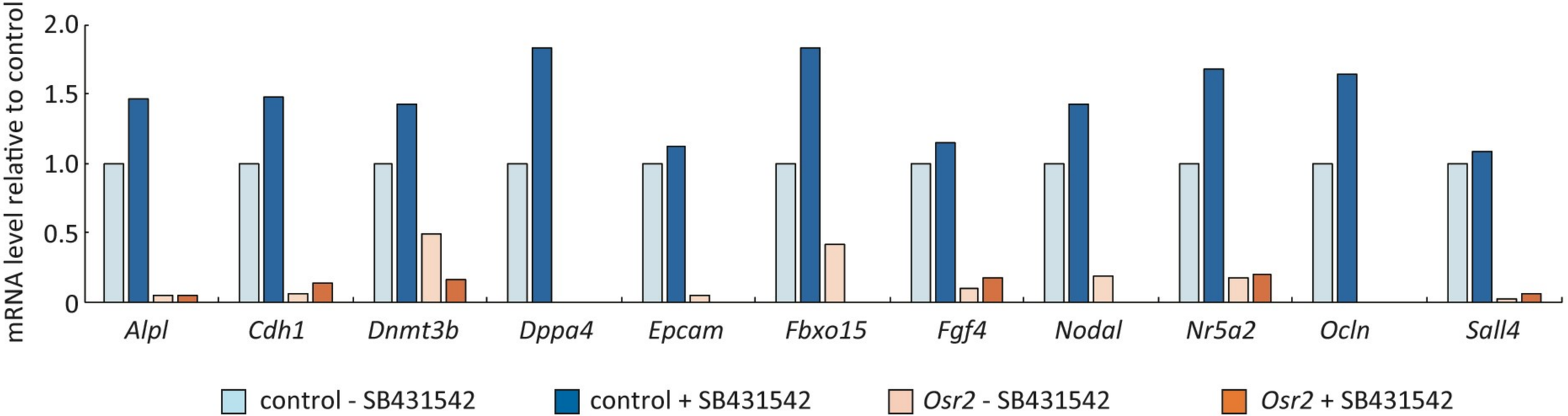

Figure S8. Expression of genes related to progression of reprogramming in *Osr2*-expressing MEFs treated with or without TGF-ß inhibitor

mRNA levels of indicated genes were extracted from RNA-seq data in Figure 7 and normalized to those in control reprogramming without treatment of SB431542.

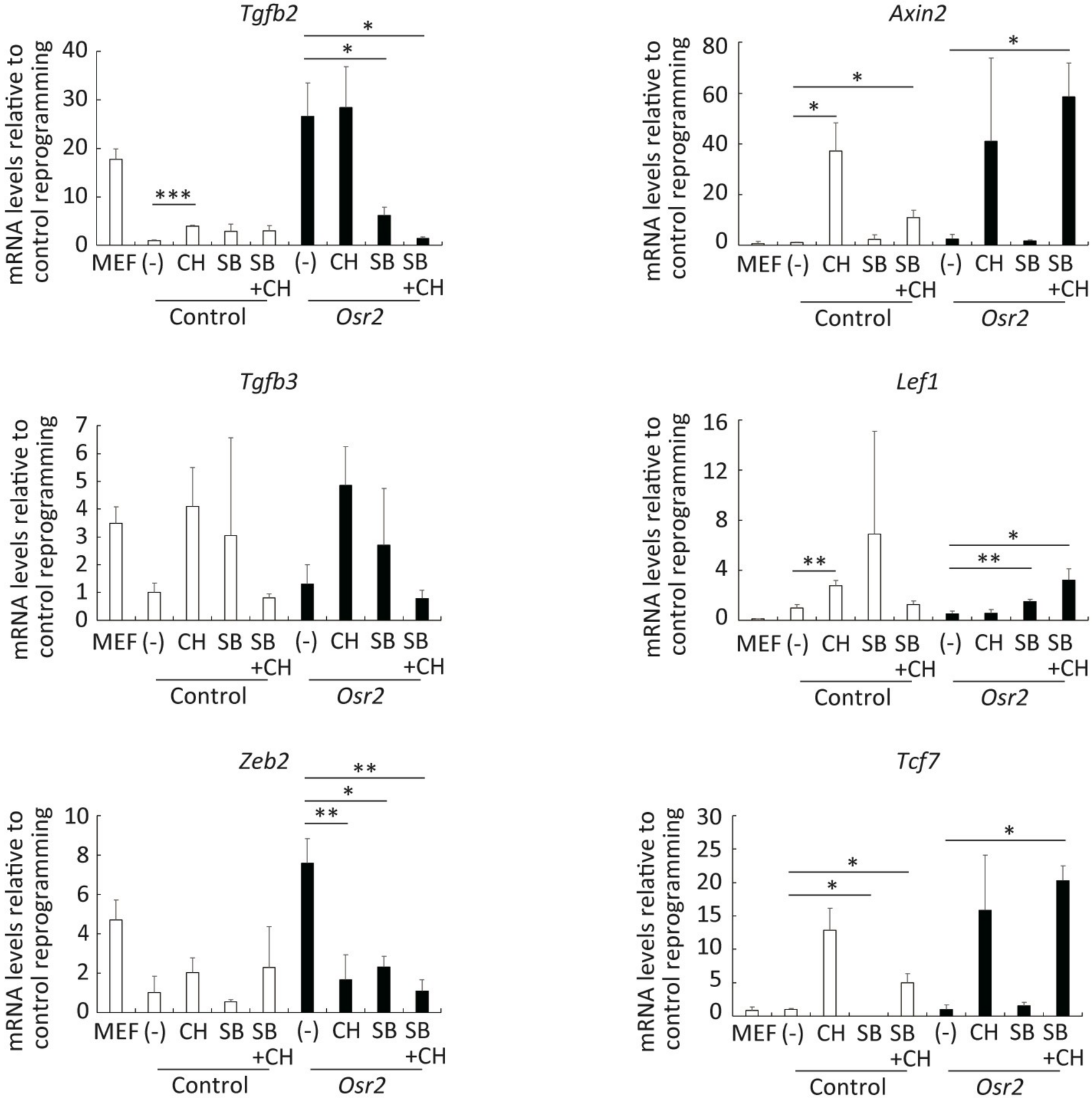

Figure S9. Changes in the mRNA expression level of genes related to TGF-ß or Wnt signaling

cMEFs, transduced with *Osr2*-expressing retroviral vector for 2 days, were selected with puromycin for 2 days and then reprogrammed by SeVdp(KOSMaB). 10 μg/mL SB431542 and/or 3 μM CHIR99021 was added from 3 days before reprogramming. The mRNA levels of indicated genes were determined at day 5 of reprogramming. Data represent mean ± SEM from three independent experiments. **P* < 0.05, ***P* < 0.01, ****P* < 0.001.

Table S1. Oligonucleotide sequences for construction of plasmids

< upstream ORF2 >

shRNA	Sequence
upstream ORF2	aatcagttgccggccttgtgATGCAGCCGCTGGTTCTCTCGGCGAAAAAACTGTCGTCTTTGCTGACTTGCAAATACATCCCGCCTTAA
	TTAAGGCGGGATGTATTTGCAAGTCAGCAAAGACGACAGTTTTTTCGCCGAGAGAACCAGCGGCTGCATcacaaggccggcaactgatt

< shRNA >

shRNA	Sequence
shOsr2-1	gatccGTTCACAAAACTTTACATATGttcaagagaACATATGTAAAGTTTTGTGAACttttttggaaag
	aattctttccaaaaaGTTCACAAAACTTTACATATGtctcttgaaCATATGTAAAGTTTTGTGAACg
shOsr2-2	gatccATATCCATTCCAAAGAAAAGCttcaagagaGCTTTTCTTTGGAATGGATAttttttggaaag
	aattctttccaaaaaTATCCATTCCAAAGAAAAGCtctcttgaaGCTTTTCTTTGGAATGGATATg

Table S2. Target sequences of siRNA for *Osr2*

Name	Target sequences
siOsr2-1	CAGACACTTTACCAAATCATACA
siOsr2-2	CAGTTCACAAAACTTTACATATG

Table S3. Oligonucleotide sequences for quantitative RT-PCR analyses

Gene	Sequence
Axin2	ATGGAGTCCCTCCTTACCGCAT
	GTTCCACAGGCGTCATCTCCTT
Cdh1	ACGTCCCCCTTTACTGCTG
	TATCCGCGAGCTTGAGATG
Cdh2	ATCAACCCCATCTCAGGACA
	CAATGTCAATGGGGTTCTCC
Ddit3	ACAGAGCCAGAATAACAGCCG
	GACACCGTCTCCAAGGTGAA
Ebf1	TGCTGGTCTGGAGTGAGTTG
	GATGAATCTGCCTGGTGTCC
Ebf3	AGCAATGGCGTCAGAACAG
	GCACATGATCTCGTGGGTC
Epcam	TGGCAACAAGTTGCTCTCTG
	ATTTCTGCTTTCATCGCCAA
Fbxo15	CTCATCTGTCACGAAGCAGC
	AGGTCACCGCATCCAAGTAA
Fn1	GCTCAGCAAATCGTGCAGC
	CTAGGTAGGTCCGTTCCCACT
Lef1	AGCACGGAAAGAGAGACAGC
	TCTGGGACCTGTACCTGAAGT
Meox1	ACAGCCTTCACCAAGGAGC
	CCCCTTCACACGTTTCCA
Meox2	AGGGGATTATGGCCGTCAAG
	TCCTTCCTAGGTTTGCTGTTCA
Nanog	ACCTGAGCTATAAGCAGGTTAAGAC
	GTGCTGAGCCCTTCTGAATCAGAC
Ocln	TACTGTGTGGTTGATCCCCAG
	TTTCTTCGGGTTTTCACAGC
endogenous *Oct4*	CTGTTCCCGTCACTGCTCTG
	AACCCCAAAGCTCCAGGTTC
Osr2	TGTCCAGCCACATCACATTG
	TGGTTTGATGTCCGCATCTC
Prrx1	TTCAGAACCGAAGAGCCAAG
	GATAATCGGTTGGTCTGGGA
Rex1	TTGATGGCTGCGAGAAGAG
	ACCCAGCCTGAGGACAATC
Smarca2	GGGAAGATTCAGCCAGCACA
	CTGTGGGTGTGGACATCTAGG
Smarcd3	TGACATAGATGTGGAGGTGGAG
	TATGGACTCAATCGTCTCATGG
Snai1	TGTGTCTGCACGACCTGTG
	AGTGGGAGCAGGAGAATGG
Snai2	ACACATTGCCTTGTGTCTGC
	GCCCTCAGGTTTGATCTGTC
endogenous *Sox2*	AGAGAAGTTTGGAGCCCGAG
	ATCTGGCGGAGAATAGTTGG
Tbp	TATCTGCTGGCGGTTTGGC
	TGAAATAGTGATGCTGGGCAC
Tcf7	TACTATGAACTGGCCCGCAA
	TGCATTTCTTTTTCCTCCTGTGG
Tgfb1	TGAGTGGCTGTCTTTTGACG
	GGCTGATCCCGTTGATTTC
Tgfb2	CATCATCCCGAATAAAAGCG
	TAGCAGGAGATGTGGGGTC
Tgfb3	GAAGGCTGCACTCAGGAGAC
	TGAGGACACATTGAAACGAA
Tgfbr1	TGCTCCAAACCACAGAGTAGGC
	CCCAGAACACTAAGCCCATTGC
Tgfbr2	ATGAGCAACTGCAGCATCAC
	GGCAAACCGTCTCCAGAGTA
Tgfbr3	GCCCAAAAGGAATATGGAGC
	ACTCCGCAAGGTAATTGAGC
Vim	GATGCTCCAGAGAGAGGAAGC
	TTCCGTTCAAGGTCAAGACG
Zeb2	GCTAACCCAAGGAGCAGGTAAC
	TGAACTGTAGGACCCAGAATGA
Zic1	ATGAACGTGAACATGGCTGC
	CTCCGGCTCGATCCATTTAC

Table S4. Clustered genes in NMuMG RNA-seq data

Cluster 3-1	Cluster 3-2	Cluster 3-3	Cluster 3-4	Cluster 3-5	Cluster 3-6
Lrrc75b	Dusp8	Fst	Mgst3	Pbxip1	Ube2h
Nrp1	Cnn2	Dtx4	Amacr	Agtrap	Gm47163
Sptbn2	Gm12715	Klhl30	Cyp51	Abcc5	Ms4a4b
Ly75	Kpna3	Plxnd1	Socs3	Cdc42ep1	Npc2
2410131K14Rik	Dusp10	Ramp1	Stt3b	Srpk2	Plpp6
Sssca1	Rnd1	Ccl7	Slc26a2	Unc13a	Slfn2
Sp8	Dync1h1	Myh9	Iqgap2	Lrfn3	Harbi1
Urb1	Flnb	Msrb3	S100a6	Sox9	Bambi
Eif3j1	Myl12a	Vgll3	Nt5c2	Acp2	Zbtb4
Pold2	Mmp24	Tpm1	Fam129a	Ldb1	Zfp113
Nop14	Plxna1	Lims2	Fos	Zfp618	Cirbp
Ccdc137	Gna12	Pde8a	Mettl7a1	Gm20300	Naglu
Efnb2	Rflnb	Itpripl2	Cpn1	Bicc1	Hs1bp3
Ftsj3	Snai1	Ttc12	Aldob	Gm12576	Kank1
Ddx27	AU020206	Pim1	Cyp3a13	1700020I14Rik	Mturn
Nop9	Bnc1	Tln1	Gabarapl1	Tm9sf3	Zfp704
Rpl28	Ogfrl1	Ass1	Kitl	Fjx1	Acot1
Gdf11	Ercc1	Ext1	Angpt2	Pskh1	Ppargc1a
Gm45552	Chsy1	Ldlrad4	Acot13	Enpp5	Syngr1
Ago2	Ahnak	Ccn5	Slc16a10	Gca	Slc39a10
Mcc	Cd109	Itgb1	Shmt1	Nuak2	Crebl2
Dstn	Ctif	Ppp1r13l	Slc18a1	Vamp8	Polr3gl
Crim1	Ranbp2	Ppp1r12b	mt-Rnr1	Onecut2	Rhobtb3
Tbcb	Cdr2	Setd7	Eps8l3	Rbbp9	Slc25a23
Nfil3	Dock5	G930009F2	Tob1	H2afv	Cdkn1b
Mmp10	Rap2b	Mmp14	mt-Tp	Kif3a	Gprc5c
Psd	Krt18	Cpe	Tmem176a	Rbmx	Chd6
Klhl21	Zfp703	Slco3a1	Man1a	Pdk1	Fgfr3
Inf2	Nkrf	Pdgfb	Gm35533	Pilrb2	Tsc22d1
Nup98	Golt1b	Map3k20	Thra	Nectin2	Zfyve27
Naf1	Gadd45g	Castor1	Dqx1	Rab5b	Mxd4
Gm12346	Nipal1	Serpine1	Muc5b	AC149090.1	Apba1
Selenow	Kdelr3	Vash1	Hist1h2bh	Camk2n1	Ypel2
Rock2	Abl2	Hk2	Chka	Efna4	Plekhh2
Rpl23a	Sept11	Prss22	Gm22918	Foxj1	Smim14
Lancl3	Dusp5	Nsmce3	Akr1b7	Tsc22d1	Slc40a1
Ctps	Itprip	Stk17b	Meox2	Fzd8	Firre
Kif4	Map1b	Plxna4	Igfbp5	Tmsb4x	Malat1
Mki67	Kif1b	Crocc2	Pzp	Scara3	Slc6a6
Atp10a	Ptgs2	Tns3	Cpm	Ddx17	Crebrf
Sgo1	Cyp1b1	Dyrk3	Acat1	Gm26115	Mmab
Ckap2l	Mras	Slc9a1	Sgpp2	Ddx17	Hhex
H2afx	Uts2b	Gjb3	Ddit4l	Spaca6	C4b
Bard1	Nfix	Hdac11	Atp1a1	Mrpl24	Kat2b
Kif18b	Ccn2	Lpcat4	C730027H18	Prex2	Manba
Nucks1	St3gal2	Ehbp1l1	Ngef	Plxnb1	Ccdc50
Lmnb1	Sdc3	Cnnm4	Apoa1	Tbc1d2b	Slc35f5
Stk10	Lmcd1	Gm38158	Ugt2b35	Pilrb1	Gm13415
Emp2	Tram2	Parvb	Erbb3	Kdsr	Kiz
Srf	Nectin1	Sh3bgrl2	Cyp2c65	Ogt	Tcp11l2
Clic4	Podxl	Mgat5	Vnn3	Pea15a	Atp1b1
Prr7	Pkp1	Itga2	Nampt	Rnf135	Dbp
Slc20a2	Sh3pxd2a	Chst11	Galm	Amn1	H1f0

Loxl4	Sned1	Ccbe1	Afm	Colgalt1	Hist2h2be
Tbc1d10b	Aif1l	Adgra1	Asb13	Zfp810	Scd2
Gm3226	Tgfb1	Zeb1	Gstp1	Pros1	Mgst2
Plekha3	Bcr	Msn	Tmprss2	Dock8	Ppp1r1b
Usp31	Gm26781	Crlf1	Glul	Cxxc4	1700016C15Rik
Spcs3	Zdhhc18	Fzd1	Dbt	Cfi	Rnf128
Nol10	Erfe	Map3k14	Irf6	Pfkl	Rnf128
Prep	Sox11	Sorcs2	Nfe2l2	Nsdhl	Cdkl5
Igfbp3	Slc4a8	Smad7	Tff3	Selenoi	Strbp
Ywhag	Dusp7	Abca2	Flrt3	Pgap1	Kantr
Pom121	Capn2	Endod1	Sdhd	Elovl7	Map3k1
Sf3a1	Lce1g	Angptl2	Pcbd1	Ralgps2	F5
Slc39a6	Ulbp1	Onecut3	Cab39	Junb	Gas6
F3	F2r	Pmepa1	Lgals4	Spns3	Rassf9
Dhx37	Ackr3	Cldn4	Eef1a1	Rtn4rl1	Dio3os
Sac3d1	Lrrk1	Fam69a	Hadh	Narf	C730027H18Rik
Gm340	Rab11fip5	Runx1	Gpam	Apobec3	S100b
Phlda3	Npc1	Cdk5r2	Cyp4b1	Rufy1	Klhl36
BC005537	Pdk4	B4galt1	Ak3	Dsg2	Palmd
Crip2	Ets1	Pdgfa	Atp1a1	Sppl2a	Fam114a2
Ccne1	Shroom4	Gpbar1	Snora31	C130074G19Ri	Ogt
Sprr1b	Pcdh7	Odaph	Pipox	Cldn2	1810017P11Rik
Haspin	Timp3	5830408C2	Krt19	Megf9	Ehf
Tubb6	Frmd6	Has2	Cyp4a12b	Nck2	Vamp2
Cd3eap	Tpm4	Lgr6	Acaa2	Ctso	Decr1
Foxk2	Litaf	Dpm3	Dio3os	Ormdl1	Mindy2
Melk	Foxf2	Spsb1	Cyp2c67	AC132455.2	Pamr1
Prpf4	Syt12	Elk3	Anxa4	Frk	Tspan9
Ehd2	Mprip	Gm28231	Ier2	Dyrk2	Bcl9l
Mirt1	Amotl1	Qk	Ifit3b	Plin2	Ralgapa2
Cdc20	Tuba1a	Ucn2	Naxe	Capn5	Abcd1
Ercc6l	Ncs1	Actn1	Phyh	Trp53inp2	Spp2
Foxm1	Lrrc8c	Chrna1	Acadm	Arid2	2810013P06Rik
Ints5	Gdnf	Col5a1	Irf2bp2	Lbp	Bnip3
Tmem238	Rdh10	Col5a3	Igbp1	Vps41	Erlin2
Epop	Atxn1	Dll4	Plcl2	Pon2	Ubqln2
Tubb5	Il1rn	Fam167a	Bcam	2010315B03Ril	Gmcl1
Anp32b	Fgd3	Notch2	Alcam	Ttc30b	Slc25a20
Nudc	Bmp2	Tnfrsf1b	Epb41l5	Ggh	Stxbp2
Parp1	Zyx	D630003M2	Cdh1	Prkca	Aldh3b1
Tubg1	Samd4	Coro6	Fah	Mrgpre	Muc1
C3ar1	Tnfrsf23	Ubtd1	Sc5d	Man2b1	Hes1
Asf1b	Vegfc	Glipr2	S100g	Pnisr	Akr1c12
2810408I11Rik	Col27a1	Pcolce2	Ambp	Osbpl3	Nqo2
Prmt5	Gm2115	Sema4f	Tmem135	Tcim	Mrgprb2
Tuba1b	Tagln2	Col1a1	Akr1c19	Zbtb44	Slc25a30
Camk2n2	Plcg2	Rhoq	Sult1d1	Veph1	Naip5
Ccna2	Csf2	Bmpr2	Clrn3	Thbs3	Foxo4
Tubb4b	Nrp2	Pdgfb	Anks4b	Glis3	Paqr7
D10Wsu102e	AC132148.1	Nat8l	Id2	Sh3bgrl	Ivd
Klf16	Klf9	Creb3l1	Agt	Usp53	Rnasel
Cdca7l	Jam2	Il11	Mtss1	Scly	Cmbl
Nomo1	Myo5a	Fn1	Flt1	Ccl2	Tmem51
Htr1b	Gldc	Agpat3	Sfxn1	4930402H24Ri	Prkra
4930523C07Rik	Ccdc88a	Inhba	Stc1	Vgll4	Hes1
Tmem109	Pvr	Rasal2	Scd1	Casp6	Lpar6

Gm4366	Ptprn	Arhgef19	Adamts15	Tgm2	Sptlc2
Mars2	Slc46a1	Usp9x	Mgat3	Tgfb3	Cyp2s1
G3bp1	Zeb2	Pde4d	Hs6st1	Sestd1	Hist1h1d
Rps6	Wnt7a	Abtb2	Ccnd2	Fbxl20	Lactb2
CAAA01118383.1	Vcl	A330074K2	Aqp1	Mmp11	Aldh4a1
Cdca8	Tpm1	Serpine1	Cebpa	Lrp1	Tmbim6
Psme3	Fam126a	Gas1	Alb	Frrs1	Btg2
Cenpq	Hcn4	Tnnt2	Nudt4	Ulk2	Cat
Utp20	Il18rap	Gab2	Id1	Ctnnbip1	C1rl
Brip1	Nrip1	Hsd11b2	Dio3	Lnpep	Lnx2
Gm9825	Map3k20	Spred2	Eif4b	Clu	Macrod1
Anln	Akr1b3	Iqgap1	Cyp2c68	Slc44a1	Zfp369
Igfbp4	Mtpn	Col18a1	Tomm20	Vill	Slc16a12
Mcm4	Gpc1	Sash1	Esrra	Paox	Ctnnb1
Smc3	Acsbg1	Csgalnact1	St3gal4	Enpp1	St8sia4
Rrp12	Actn1	Bhlhe40	Cmpk1	4732440D04Ri	Pxmp4
Ncbp1	Lfng	Nt5e	Hist1h2bc	Rsrp1	Pgpep1
Aunip	Itgb3	Sacs	Id3	Gm20559	Ugt2b36
Nol6	Fosl2	Atrn	Sord	Spns2	Hsd17b2
Kpnb1	Kctd5	Ammecr1	Epas1	Wdr19	Klhdc7a
Rps23		Igsf11	Wwc1	Skap2	Xist
Trdc		Lce1f	Sh2d4a	Chd3	Fem1b
Gm9115		Pitpnc1	Itih2	Dcaf8	Pdk2
Gfod1		Cish	Rassf3	Clu	Klf3
Dhx33		Cplane1	Cyp2c70	Nhsl2	Tmem176a
Eif2s1		Samd14	Glod5	Fam189a2	Crot
Sf3b4		Carhsp1	Aldh1a7	Ptpn3	Masp1
Bysl		Mex3a	Notch1	Camk1	Cpt1a
Rrs1		Irgq	Pim3	1700052K11Ril	Fahd1
Ehd1		Col12a1	Gm7694	Twsg1	Glud1
Oat		Pik3ip1	Cbln3	Pea15a	Ticam1
Lrrc59		Enc1	Ffar4	Fam210b	Lamb2
E2f7		Pla2g16	R3hdml	Spns2	Arfgef1
Nxn		Pkd2	Trim71	Crp	Clec2d
Fbxo5		Gm15867	Nostrin	Card10	Hist1h1c
Mybl2		Ccn4	Ermp1	Cmtm3	Sult1c2
Pbk		AC132253.9	Dhrs9	Peg3	Sdf4
Zmynd19		AU022754	1810019D21	Clmn	Dnase2a
AI506816		Lix1l	Rnd3	Alpl	Chmp4c
Eif3b		Snn	Mettl7b	Foxn3	Hist1h2ac
Ddias		Pkhd1	Esrp2	Parm1	Zfp36
Hells		Fam171a2	Gnai1	Serinc5	Osgin1
Exo1		Snx30	Mal2	Lpin2	Mospd2
Mcm2		Clcf1	Gm2a	Cp	H3f3b
Pcna		Ece1	Atoh8	Slc4a4	C4bp
Hmgb2		Rbms2	Them6	Neurl3	Tmem98
Kif11		Olfml2b	Aass	Phc3	Cyp4a12a
Txn1		Ccdc9b	Tst	Gc	Hist1h3e
Ssr1		Epb41l5	Hprt	Klhl24	Slc3a1
Lgalsl		Nuak1	Rdh11	Sdc4	Tnks2
Ppa1		Mical2	Nceh1	Bckdha	Mpp1
Cactin		Ahr	Vnn1	Hip1r	Akr1c13
Rps10		Gm8113	Kcnk5	Dcaf8	Btf3l4
Itga6		Fzd2	Bace2	Stat6	Anxa13
Rrm2		Ctxn1	Mylk	Cxcl1	2210016L21Rik
Cnot9		Smad3	Gclc	Ubxn7	Gde1

Bms1	A930038B1	Pcyt2	Bmf	Sft2d2
Wdr18	Wnt7b	Afp	D5Ertd579e	Lss
Cgref1	Olr1	Rfk	Ddah1	Pls1
Mfsd5	Itpkb	Prdx3	A430106G13Ri	Pla1a
Pwp2	Slc6a8	Slc16a1	Cyp2j6	Ppm1k
Abcf2	Ptk7	Cdhr2	Tpmt	Lgals3bp
Usp39	Ptgfrn	Plscr4	Cys1	Acsf2
Gltp	Prag1	Coq9	Kcnh7	Gpd1
Slc25a4	Agap1	Slc9a3r1	2310030G06Ri	Rorc
Amd1	Has3	Srd5a1		Atp8b1
Rplp1	Coro6	Gm45330		Neurl1b
Rps19bp1	Marcksl1	Ngef		Habp2
Ak6	Lad1	Map3k5		Amdhd1
Rsl24d1	Gli3	Sod2		Ttr
Pcbp1	Jag1	Uqcrfs1		Frat1
Mettl16	Inava	Atp7b		Akr1c19
Exosc2	Gabre	Sptssb		Ifi27l2b
Gemin6	Rhobtb2	Ctdspl		Dnm3
Arf6	Gm20544	Fbp2		Dgat2
Chchd4	Kctd11	Pgrmc1		Ston2
Eif3d	Fn1	Fam84b		Cx3cl1
Cisd1	Apobr	Fzd5		Ripk4
Mcu	Inhbb	Gm37800		Ugt1a7c
Krt4	Cyth4	Klf4		Insig1
Ctsz	Cyp21a1	Slc10a2		Cyp3a16
Phgdh	Dusp2	Khnyn		Ipcef1
Shb	Adam12	Tmem151a		Tnfsf9
Gm8730	Ivl	Id3		Cmtm8
E2f2	Tmod3	Hpx		Gpd1l
Acan	Zfp760	Fth1		Atp6v1b2
Rcc1l	Clcf1	Btg1		Ddx5
4933440M02Rik	Il13ra1	Pdhb		Degs1
Gfpt1	Loxl2	Vsig1		Slc33a1
Pard6b	Gpr39	Gsta4		mt-Nd4
Hspa9	Irf2bpl	Proser2		mt-Cytb
Etnk1	Ddit4	Cav2		Tcf7l2
Sesn2	Cpd	E330009J07Rik		Nipsnap1
Slc25a48	Zfp36l2	Ces2g		mt-Nd2
Ubl3	Stard4	Dhx40		Cp
Ddit3	Marcks	Frat2		Itga1
Cdc42ep2	Samd9l	Lgals2		Plin3
Fitm2	Cxxc5	G6pdx		Tpp1
Sgms2	Slc2a5	Tcf23		Cp
Adh7	Arl4c	Prdx1		Gm379
Abhd2	Gm30692	Ndufb11		Echdc3
Pttg1ip	Tbc1d16	Smim6		Ggcx
Mydgf	Dtx3l	Mrpl9		Dnajc10
Otud1	Galc	Perp		0610040J01Rik
Foxn2	Gm49708	Bpnt1		AW549877
Ngdn	Plekha2	Cers2		Setbp1
Klf5	Lbp			Scp2
Tiparp	Efnb1			Tgoln1
Plk2	Vdr			Pnrc1
Camk1d	Vasn			Maf
Tigit	Bace1			Agfg1
Slc7a11	Cd47			Dnm3

Slc16a6
Mthfd2
Prelid3b
Trnt1
Ereg
Anxa2
Ccdc117
Angptl8
Slc7a1
Ube2g2
Eaf1
Timm8a1
Nifk
Eif3g
Mrpl46
Grpel1
Clpp
Atf1
Lap3
Anxa10
Ccdc88c
Pgd
Slc5a3
Eif2b1
Mrps28
Drg2
Eif4ebp1
Kmt5a
Eif3c
Atg101
Smim3
Brix1
Eprs
Utp14a
Rplp0
Itgb7
Dhx15
Mrps30
Pwp1
Cdc42ep5
Nudcd1
Eif4e
Yars
Cnih1
Tmem179
F2rl1
Cth
Gm3776
Phlda1
Lonrf3
Rpl36
Anxa10
Spry2
Slc12a2
Emc7
Avpi1
Sh3glb1
Steap4
Sat1
Hoga1
Tgfbr1
Atp6v1g1
Itpr3
Plin2
Scx
Krt20
Il6ra
Egfr
Tbc1d8b
Celsr1
Tenm4
Igsf3
Creb3l2
Add2
Zbtb38
Erap1
Hs2st1
Wipi1
Fam114a1
Sppl3
Stk38l
Hook3
Dusp28
Fgd6
Sept6
Tspo
Cdkn2b
Kcnd1
Ror1
Thbs1
Gm19385
Trim56
Prnp
Cdh6
Sat1
Arhgap42
Pdlim7
Rhob
Rspo3
Ccl9
Fbxo32
Afap1
Lpp
Olfr1372-ps1
Vat1
Dstyk
Gprc5b
Col4a2
Appl2
B2m
Lamp2
Fads3
Vldlr
Ankmy2
Bdh1
Itm2b
Stom
Pten
Cd164
Hdac11
Deptor

Ptpru
Lin7c
Imp3
Cdx2
S100a13
Oxct1
Gm13394
Slc25a5
Mboat1
Mtmr10
Hbegf
Ndufa8
Polr1d
Rab3b
Ldlrap1
Gcnt3
Wdr76
Cmss1
Arl2bp
Samd5
Mrpl18
Me2
Efna5
Pigf
Prkar2a
Hey1
Nanos1
Spire2
Egln3
Got2
Krt23
Crisp1
Gm13420
Tspan15
Psat1
Paip2b
S100a7a
BC030870
Mlph
Barhl2
Slco2a1
Inka2
Vstm5
Ezr
Gm5543
Calr
Gm5117
Dnajb11
Chac1
AC168977.1
Hspa1a
Trib3
Krt76
Npm1
Cpox
Dnajb1
Zc2hc1a
Snx13
Ntn4
Pik3ap1
Zmiz1
Parp14
Ralb
Tlr2

Gm8300
Hspa1b
Zwint
Gnl3
Med13l
Hmox1
Irs2
Gpr137b
Srxn1
Ltv1
Eef1e1
Fosl1
Strap
Nufip1
Klf2
Ctsc
Wincr1
Esf1
Tmed5
Rpl7a
Btaf1
Eif1
Kti12
Gars
Insm1
Nmd3
Slc25a33
Rsl1d1
Nip7
Fmn1
Aars
Mmp13
Gm7901
Abt1
Dlx2
Fbrsl1
Eif4a-ps4
Hspe1
Cacybp
Yrdc
Epha2
Tmx1
Tbc1d2
Gm7993
Dkc1
Prps1
Areg
Abce1
Ddx56
Wdr43
Nop16
Hpdl
Cad
Hsp90aa1
Cldnd1
Zfp64

Gpr137b-ps
Cct6a
Rars
Hsp90ab1
Gm5844
Ccdc85b
Tnfrsf10b
Ero1lb
Psmd3
Pno1
Tnfrsf21
Ehd4
Stip1
Plat
Cltb
Dlk2
Ak5
Tspan4
Tcrg-C4
Upk1b
Cdc42bpg
Fgf13
Clic5
Chst1
Lbhd1
Id4
Npm3
Wdr46
AC124518.1
Hdgf
Tspan13
Thbd
Msln
Gm8126
Mmp3
Sec14l1
Sfta2
Adgrg6
Slc8a1
Psmb3
Tma16
Nme1
Abcc1
Cox10
Rbm22
Sprr2h
Ppp1r2
Pdap1
Ipo7
Ddx20
S100a11
Mak16
Timm50
Dctpp1
S100a10
N4bp3

Wdr55
Hnrnpab
Tuba1c
Wbp11
Ccdc124
Ncapg2
Gm6166
Dhfr
Mcm7
Nup43
Ruvbl1
Dnph1
Polr1b
Sf3b5
Gadd45gip1
Apcdd1
Cstf1
Tmem97
Lamc1
Cry1
Dnttip2
Ascc3
Dis3
Rplp2
Tomm70a
Noc3l
Orc1
Rad23b
Etf1
Rpl3
Nt5dc3
Arhgap31
Ppm1l
Zfp367
Orc2
Chd1l
Rmi2
Rpa2
Slc35g1
Rrn3
Nop2
C1qbp
Ran
Sf3a2
Taf1d
Smg5
Tigar
Ddx18
Trmt10c
Ptges3-ps
Gcsh
Gtf2f1
Ddx21
Rps6ka2
Atic
Hmga1b

Mrps7
Psmd7
Polh
Ncl
Nmt2
Rpl27
Npm1
Eif1ad
Ddx31
Eif2s3x
Slc7a5
Hgh1
Pin1
Thop1
Odc1
Hspd1
Gprc5a
Srm
Krt79

Cluster 9-1	Cluster9- 2	Cluster 9-3	Cluster 9-4	Cluster 9-5	Cluster 9-6
Ormdl1	Pole	Afap1	Kif1b	Ugt1a7c	Agt
Itpa	Prkdc	Ccdc9b	Pcdh7	Cth	Cyp3a13
Pgap1	Pola1	Sat1	Ctif	Stc1	Fos
Serp1	Utp20	Lims2	Prag1	Abcc2	Eps8l3
Cdh17	Anln	Dusp10	Cd109	Slc7a11	Pxmp4
Tmem97	Mcm4	Tpm1	Clstn2	AC117816.	Tmprss2
Lefty1	Rrm1	Cnn2	Flrt2	Rnf128	Hist1h3e
Cs	Zfp36l2	Parp14	Gpx8	Iqgap2	Cyp2c70
Tram1	Aspm	Nfil3	Tmem43	Ripk4	Proser2
Pgam1	Kif18b	Gm12715	Phlda3	mt-Tp	Rorc
Igf2bp1	Ddit4	Clec2e	Rnf145	Acvr2a	Dio3
Polr3k	Lmnb1	Litaf	Tnfrsf23	Mrgprb2	Deptor
Prkca	Kpnb1	Zbtb20	Snn	Setbp1	Slc16a12
Tmem51	Irf2bpl	Dtx4	Loxl4	Slc16a10	Man1a
Ak2	Ykt6	Rab11fip5	Scara3	Muc1	Gm37800
Zfp706	Cda	Npc1	Cpe	Neurl1b	Pamr1
Bag2	Prep	Ahnak	Syt12	Rilpl2	Cyp2c67
Dnajc22	Bub1b	Snai1	Mras	Prdx3	Cab39
Ivd	Rrs1	A330074K:	Ahr	Gpd1l	Eif4b
Aldh9a1	Sh3bgrl2	Bnc1	Plxna1	Pten	Acot13
Tigit	Ckap2l	Eif4e3	Peg13	Lnx2	Dio3os
Ralgps2	Pimreg	Lrrk1	Klf6	Fgd4	Mettl7b
Trib3	H2afx	Spcs3	Dusp8	Spp2	Galm
Thbs3	Ppa1	Rflnb	Ntn4	mt-Rnr2	Pgrmc1
Neurl3	Map2k1	Ackr3	Msrb3	Cmtm8	Acot2
Them6	D630003M	Chsy1	Olfr1372-p	Cd9	1810019D21Rik
Sar1b	Selenot	Arhgef19	4930539E(	Tcf7l2	Acadm
mt-Tl1	Kcnd1	Igfbp3	Nfkbia	mt-Nd2	Irf2bp2
mt-Nd1	Sept6	Tln1	Rnd1	Plcl2	Gm6969
Dnajc10	Ror1	Vcl	Dlgap4	Hprt	Cmpk1
Larp4	Spred2	Zeb2	Stk10	Cdh1	Hdac11
Acsl5	Pigs	Mprip	Lfng	Slc33a1	Phyh
Pfkl	Cdkn2b	Plxnd1	Fosl2	Agfg1	Naxe
Phlda1	Ccdc88a	Map3k14	Farp1	Degs1	C230096K16Rik
Tnfsf9	Hspa4	Sh3pxd2a	Mmp24	Emc7	Hist1h2be
B4galt6	Snx9	Notch2	Gprc5b	Cox14	Cst3
Pkm	Map3k20	Pde8a	Mmp10	Foxo4	Decr1
Slc25a5	Ccbe1	Ass1	Clcf1	Tomm20	Igbp1
Gm4735	Samd9l	Wwc2	Ripor1	Lgals3bp	Dhrs9
Gsr	Dusp2	Tpm4	Olfml2b	Pcdh10	Pcbd1
Rap1gapos	Adam12	Rhob	Col6a1	Akr1c19	AU040320
Ubqln2	Rhobtb2	Fn1	Ptpn14	Dgat2	Avpi1
Shmt1	Cyp21a1	Nfix	Adgrl1	Frat1	Snora31
Mpp1	Bysl	Fzd1	Zbtb8a	Anks4b	Rdh11
S100a7a	Entpd7	Pdk4	Fnbp1	Sult1d1	Krt23
Gpat4	Setx	Sat1	Ptp4a3	Akr1c19	Rpl4
Slc25a10	Ammecr1	Zdhhc8	Sept11	Polr1d	Dhx40
Ranbp2	Olr1	Tnfrsf1b	Gfod1	Akr1c13	S100b
Pwp2	Igsf11	St3gal2	Sned1	Gde1	Oxct1

Fam110c	Tmod3	Prr7	Atl3	Bpnt1	Tmem176a
Rrp12	Il18rap	Fn1	Plekhm3	Pls1	March9
2810025M	Atrx	Lrrc8c	Gdf11	Akr1c12	Dnase2a
Ifi202b	Acsbg1	Tns3	Emp2	Tnks2	Klf3
Tmem167	Rasal2	Clic4	Ehd2	Nipsnap1	Hist1h2ac
Bard1	Pcolce2	Endod1	St8sia2	Sdhd	Hist1h2bg
Lrrc59	Jak1	Timp3	Cdkn2a	2210016L2	Uap1l1
Smc3	Itga2	Crocc2	Il13ra1	Frat2	Acot1
Ccnd1	Parvb	Amotl1	Crip2	Anxa13	Tcp11l2
Top2a	Tmx3	Cyp1b1	Upk1b	Ak3	Slc35f5
Gpr39	Fgd6	Cabin1	Antxr2	G6pdx	Plin3
Cenpe	E2f4	Frmd6	Ascc3	Rpl36	Mospd2
Foxm1	Smc5	Sdc3	Ush1g	Tgoln1	Fahd1
Mtr	Ivl	Tuba1a	Sp8	Slc10a2	Itga1
Ccnf	Sf3a1	B2m	Rap2a	Rassf9	Hist1h2bc
Cenpq	Med14	Gdnf	Slc22a4	Ifi27l2b	Tmem176a
Kif4	Phip	Ccn5	Pik3r3	Flt1	Ube4a
AI506816	Tmed5	Mmp14	Prdx5	Gm35533	Scp2
Mybl2	Socs6	Plcg2	Ipo13	S100g	Fth1
Fbxo5	Cdca8	Csf2	Moxd1	Rfk	Pdk2
Hmmr	Ddx21	Bmp2	Ikzf2	Lss	Khnyn
Ccnb2	Galnt7	Zmiz1	Krt79	Igfbp5	Xist
Hells	Enc1	Itgb1	AU021092	Klhl36	Narf
Nsl1	Vgll3	Foxq1	Nkx3-2	Ppm1k	Bmf
Plk1	Rdh10	Actn1	Gm42047	Ttr	Slc40a1
Sgo1	Col4a2	Il1rn	Gprc5a	Cav2	Bnip3
Spdl1	Col12a1	Cdh6	Fam25c	Clrn3	Fbp2
Spag5	Fgd3	Actn1	Grem1	Pipox	Rnf39
Knstrn	Actr1b	Myh9	Fzd4	Aldh3b1	Angpt2
Haus6	Wnt7a	Dync1h1	S100a11	Krt19	Tmbim6
Ercc6l	Samd4	Usp22	Nfe2l3	Meox2	St8sia4
Mki67	Kpna3	Flnb	Fam3c	Tbc1d15	Anxa4
Eme1	Tcf7l1	Myl12a	Foxd1	Scd2	Gpd1
Tuba1c	Serpinb9g	Zyx	Fam117a	Sod2	Fzd5
Ada	Ece1	Atxn1	Gda	Psat1	Asb13
Tmpo	Ywhag	Itprip	Id4	Slc9a3r1	Apoa1
Nop10	Gas1	Ramp1	P3h4	Tff3	Acsf2
Bop1	Zfp451	Fbxo32	Tspan13	Ston2	Esrra
Snrpd2	Fam167a	Mgat4b	Hpse	Cx3cl1	Sfxn1
Psme3	Aebp2	Ccl7	Exoc4	Ipcef1	Acaa2
Haus1	Nuak1	Abca2	Acss2	Hist2h2be	F5
Tmem158	Sprr2k	Prnp	Slc5a3	Slc26a2	Atp8b1
Uck2	Hcn4	Iglon5	Smad9	Cdx2	Aldh1a7
Gm30692	Gm19385	Fst	Chst1	Slc3a1	Sftpd
Dusp28	Arhgap42	Slco3a1	Scarb2	Kcnk5	Erbb3
Lrp8	Fgd3	AC132253.	Arl6ip5	Stt3b	Ngef
Igfbp4	Rap1b	Basp1	Kank2	Dnm3	Pzp
Cenpf	Scx	Tram2	Vcam1	Atp1a1	Epb41l5
Top2a	Nrp2	Adprh	Vcam1	Nqo2	Vsig1
Dhfr	Col27a1	Coro6	Ier5l	Elovl6	Stxbp2

Cenph	Abl2	Ldlrad4	Foxo3	H1f0	Tmem135
Knl1	Pmepa1	Ppp1r12b	Plat	F2rl1	Cyp2c65
Areg	Sf3b4	Pkp1	Laptm4a	Lgals2	Fth1
Nek2	Ucp2	Ogfrl1	Foxa1	Cdhr2	Id2
Ncapg2	Atp6v1g1	Gna12	Sdc4	Insig1	Ngef
Ahcy	Rspo3	Klhl30	Vcam1	Cyp3a16	C730027H18Rik
Cdc42se2	Anxa8	Aif1l	Bbc3	Gm13420	Ifit3b
Dtymk	Sac3d1	Pdlim7	Cxcl16	Gcnt3	C730027H18Rik
Mmd	Snx15	Sorcs2	Ccdc71l	0610040J0	Gsta4
Ube2c	2900097C:	Ets1	Rtl8a	Glud1	Amdhd1
Dkc1	Csgalnact1	Itgb3	Epb41l4a	mt-Nd4	Mylk
Ska3	Tagln2	Ncs1	Cebpd	mt-Cytb	Mlph
Pclaf	Slc9a5	Bcr	Gm26809	Stom	Acat1
Cks2	Runx1	Gm2115	Igf1r	Tspan9	Cyp51
Tubg1	Uts2b	Nectin1	Serinc5	Arfgef1	Mtmr10
Hmga1b	Kctd5	Ccn2	Col6a2	Ralgapa2	Sgpp2
Eepd1	Epb41l5	Klf9	Plekhf1	Itm2b	Srd5a1
Adss	Nat8l	Rhoq	Mcc	Lactb2	Map3k5
Inpp4b	Ucn2	Setd7	Upk3b	Kitl	Gm45330
G2e3	Itpripl2	Tgfb1	Slc8a1	Cat	Irf6
Tbc1d8b	Il11	Ehd1	Mmp13	Macrod1	Plscr4
Celsr1	Ext1	Gadd45g	Net1	Fam129a	Thra
Mrc1	Tpm1	Zfp703	Anxa5	Ugt2b36	Muc5b
Dock8	Nxpe3	Reep5	Bbx	Cd164	Gm3776
Hspd1	Pkhd1	Ctxn1	Zbtb7c	Gstp1	Crisp1
Atp1b3	Smad7	Plxna4	Foxd2	Btf3l4	Gas6
Coa5	Serpine1	Kdelr3	Trim3	Cmbl	S100a6
Rbl1	Slc20a2	Plek2	Tmeff2	Ehf	Rdh14
Prkg2	Ccn4	Gm26781	Serpina9	Mrpl9	Cox19
Bub1	Prss22	Hsd11b2	Sytl2	Ogt	Adamts15
Esco2	Ubtd1	Gm8113	Magel2	Idh3b	Hs6st1
Hspa4l	Gpc1	Coro6	Ddx5	Lgals4	Cbln3
Hmgn5	Msn	Marcksl1	Lama5	Afp	Hes1
C130074G	Stk38l	Nipal1	Tfcp2l1	Tst	Barhl2
Stip1	Zbtb38	Slc4a8	2310022B(	Prdx1	E330009J07Rik
Mtap	Thbs1	Gabre	Pappa2	Eef1a1	Eef2
Krt20	Akr1b3	B4galt1	Clec3b	Uqcrfs1	Lpar6
Ddah1	Zeb1	Angptl2	Nr2f2	L2hgdh	Slco2a1
Gm28809	Bmpr2	Atrn	Rnf150	Mdh1	Ces2g
Pdk1	Erap1	Sox11	Plxnb1	Cers2	Tob1
Snai3	Onecut3	Cish	Sbk1	Gpam	Ifnlr1
Nbeal1	Capn2	Gpbar1	Lrrc75b	Hibadh	Neu1
Spns2	Pvr	Slc46a1	Gxylt2	Ndufa13	Ddit4l
Fjx1	Cd3eap	Vash1	Pik3ap1	Dio3os	Nostrin
Eaf1	Tlnrd1	Slc9a1	Pik3ip1	Pim3	Ermp1
Tmem65	Adgra3	Jam2	Tubb2b	Gclc	Cyp4b1
Lbp	Cyth4	Serpine1	Rhou	Hes1	Mcu
Pon2	Akr1b3	Hdac11	Mark1	Hao1	Ctdspl
Nhsl2	Plekha3	Pde4d	Timp2	Ugt2b35	Tspan15
Thbs3	Phlpp1	Nol10	Fscn1	Ambp	Ffar4

Omp	Wnt7b	Itpkb	Lrp1	Habp2	Dqx1
Spats2l	Sppl3	Ptgfrn	Ptpn13	Hist1h2bh	Scd1
Ddx19a	Ctdp1	Vegfc	Elmo1	Vldlr	Kantr
Acadl	Inhbb	Kcnk12	Hipk3	Grpel2	Pnrc1
Prpf40a	4930471E1	Lce1g	Tubb2a	Aldob	Osgin1
Ifi204	Steap4	Map3k20	Sec14l1	Mettl7a1	Kif5c
Nop2	Hacd2	Erfe	Pgm5	Glul	Tle1
Atic	Dip2b	Lgr6	Adgrg6	Dbt	Slc25a30
Pno1	Fam126a	Col1a1	Mmp3	Hadh	Gm7694
Met	Mtpn	Bhlhe40	Tgfb3	Btg1	Chka
Dctpp1	Slc41a1	Nt5e	Vtcn1	Atp1a1	Klf5
Zfp106	Gab2	Cldn4	Thsd7a	Pdhb	Ddit3
Megf9	Hook3	Shroom4	Osmr	Vhl	Vstm5
Nedd1	Srf	AC132148.	Il6st	Sc5d	Dio1
Fam210b	Grk5	Angel1	Pag1	mt-Rnr1	Rps4x
Cldn2	Add2	Castor2	Sptbn2	Sft2d2	Palmd
Padi2	Bag3	Cxxc5		Flrt3	Fah
Nck2	Podxl	Trim56		Kif12	Nfe2l2
Capn5	Pcdh1	Pdgfb		Coq9	Akr1b7
Actr2	Agap1	Fam69a		S100a13	Tmprss2
Sh3bgrl	Gm20544	Sash1		Pcyt2	Trim71
Lpin2	Ptprn	Chst11		Fundc2	Nt5c2
Ppbp	Abtb2	Ppp1r13l		Mgst3	Egr2
Dyrk2	Qk	Dusp7		Gm22918	Mgat3
Twsg1	Pim1	Stk17b		Ndufb11	Nceh1
Card10	Dll4	Castor1		Rps3a3	Vnn1
1110002E2	Gm28231	Dpm3		Tcf23	Mapt
Crp	Sept6	Inhba		Gm12191	Rundc3b
Ptpn3	Sgo2a	Ptgs2			Bcam
Clcn5	Usp9x	Col5a3			Ier2
Ptar1	Fbln2	Tnnt2			Bace2
Glrp1	Rbms2	Spsb1			Slc18a1
Esf1	Rasa1	Map1b			Id1
Zfp994	Ssc5d	Lpgat1			Pla1a
Cdc73	Tnnt2	Adgra1			Atp7b
Vamp7	Foxk1	Kctd11			Sptssb
Map3k2	Jag1	Smad3			Tiparp
Fam126b	Kremen1	Fzd2			Perp
Eea1	Thap12	Tns3			Cyp2c70
Gch1	Nacc1	Dusp5			Cpm
Egfr	Gldc	Creb3l2			Map3k1
Itpr3	Igsf3	Cplane1			Esrp2
Galnt3	Pdgfa	Col5a1			Nfe2l2
Trdv4	Hnrnpa0	G930009F23Rik			Syngr1
Aff4	F2r	Foxf2			Fam84b
Hs2st1	AU020206	Mical2			Hpgds
Tgfbr1	Gjb3	Pdgfb			Sult1c2
Tenm4	Iqgap1	Creb3l1			Zfp704
Sos1	Relt	Lmcd1			Gnai1
Plin2	Ehbp1l1	Crlf1			St3gal4

Denr
Tspo
Arl4c
Sacs
Sh3glb1
Ddx52
Selenof
Ern1
Zmym2
Ccl9
Mal
Ctps
Gclm
Zfp760
Uba6
Cdc27
Minpp1
Gm30246
Ghr
Pkp2
Pspc1
AU022754

Gm38158
Myo5a
Has2
Nrip1
5830408C22Rik
Slc6a8
Slc9a5
Mgat5
Gm14002
Efhd2
Krt8
Tubb6
Inava
Golt1b
Cdk5r2
Myh15
Zdhhc18
Dusp18
Heatr5a
Krt8-ps
Dynap
Gli3
Fcrlb
Nol6
Has3
Cnnm4
Pitpnc1
Nsmce3
Col18a1
Ptprn
Odaph
Sema4f
Cenpc1
Pgm2l1
Chrna1
Hk2
Elk3
Cdr2
Dyrk3
Lpcat4
Lad1
Ulbp1

Vps26c
Cp
Clec2d
Npc2
Slc30a4
Snx2
Pnrc1
Crot
Rora
Masp1
Rhobtb3
Ticam1
Gpt2
Ghdc
Tpt1-ps3
C1rl
Grpel2
Cebpa
Aqp1
Pgpep1
Cxadr
Alcam
Prkcz
Cpn1
Mtss1
Gm3716
Pik3r1
Id3
Hpx
Sord
Mme
Itih2
Alb
Nudt4
Rnd3
Klf4
Gata6
Cdh13
Fem1b
Susd6
Zfp36
Nicn1
Aass
Masp1
Hsd17b2
Nampt
Afm
Cyp2c68
Cyp4a12a
Cyp4a12b

Sh2d4a
Id3
Ezr
Epas1
Rassf3
Wwc1
Btg2
Vnn3
Kif16b
H3f3b
Lamb2
Abca5
Arhgef26
Cyp2s1
Maoa
Mturn
Kank1
Crebl2
Mal2
Arl4a
Ube2h
Dnajc5
Klhl24
Ano3
Jund
Mbip
Rasgef1a
Syngap1
Cirbp
Slc25a23
Smad6
Slc39a10
Zbtb4
Atp6v1b2
Firre
Smpd1
Nedd4
Pttg1ip
Cltb
Fam69b
Ctsz
Vat1l
Ppp1r3c
Gm2a
Tmem98
Slc37a3
Gm15222
C4bp
Mindy2
Foxa2

Adh7
Chmp4c
Ccnd2
Jun
Fgb
Atoh8
Ets2
Dusp1
C4b
Fgfr3
Dusp1
Cfi
Mboat1
Fam131c
Amacr
Atp1b1
Rpl3-ps1
Slc16a1
Egln3
Socs3
Hbegf
1700025G04Rik
Dbp
Uqcc3
Cd24a
Tinagl1
Serpina1d
Thra
Got2
Snx27
Smim6
Slc7a5
Mboat2
Ppfibp2
Isoc2a
Kidins220
Rasl11a
Nr4a1
Psrc1
Smpd3
Tgfbr3
Gm49654
Rab3b
Hap1
Tbl1x
Fut2
Ptpru
Snapc5
Hpgds
Chka

Trib1
Cdc42bpg
Wdr6
Fzd7
Suox
Slc36a4
Me2
Hey1
Efna5
Atp2b1
Mpeg1
Klhdc7a
Lyst
Sorl1
Notch1
Inka2
Gm44066
BC030870
Ppl
Vopp1
Glod5
5430403N17Rik
C9
Actg1
Grb14
Krt4
Pygb
AC124518.1
Lmo4
Asap3
Gkn2
Slc25a48
Car13
Sema3f
Trib1
Gsto1
Prdx5
Lifr
Gstm2
Ccdc88c
Gm8730
Cd14
Cln6
Tgfbr2
Malat1
Mdm4
Sesn3
Sv2a
Fbxw8
Ypel3

Clic5
Tmem178
Ak5
Gfpt1
Cxcl15
Upk1b
Dpysl3
Cdc42ep2
Sgms2
Hs3st3b1
Thbd
Igf2r
Fam43a
Nipal3
Arid5b
Mgmt
AC100212.9
Kcnj11
Abcc5
Lurap1l
Abcc5
Mxd4
Klf11
Epdr1
Cdk6
Myo1d
Ppp4r1l-ps
Rab6b
Cxadr
Tmem151a
Adamts1
Casz1
Ifit2
Mxd1
Hp
Mcl1
Lynx1

Table S5. Enriched pathways for each cluster in NMuMG RNA-seq data

Control; low - Day3; high - TGFb; low

	Term	Adjusted P-valu	Overlap	Genes
1	Retinoblastoma Gene in Cancer WP2446	2,32E-05	14/87	BARD1;PCNA;RRM2;MCM7;HMGB2;RPA2;SMC3;CCNA2;DHFR;ANLN;ORC1;CCNE1;MCM4;E2F2
2	Cytoplasmic Ribosomal Proteins WP477	1,12E-04	13/89	RPL3;RPLP1;RPLP0;RPS6;RPL23A;RPL7A;RPS6KA2;RPL36;RPLP2;RPL27;RPS10;RPL28;RPS23
3	Translation Factors WP107	1,17E-04	10/52	EIF4EBP1;EIF3G;ETF1;EIF2B1;EIF3C;EIF4E;EIF2S1;EIF3D;EIF1;EIF3B
4	Parkin-Ubiquitin Proteasomal System pathway WP2359	2,03E-04	11/70	HSPA9;TUBA1C;TUBB6;TUBA1B;PSMD7;CCNE1;PSMD3;UBE2G2;TUBB4B;HSPA1B;HSPA1A
5	DNA Replication WP466	9,84E-04	8/42	PCNA;MCM7;ORC1;ORC2;POLD2;RPA2;MCM4;MCM2
6	Amino Acid metabolism WP3925	1,82E-03	11/91	OAT;PPM1L;RARS;MARS2;CTH;CAD;ODC1;GOT2;EPRS;ADH7;SRM
7	NRF2 pathway WP2884	1,83E-03	14/146	HSP90AA1;HSP90AB1;SRXN1;SLC7A11;PGD;ADH7;SLC5A3;DNAJB1;SLC39A6;HMOX1;FGF13;EPHA2;HBEGF;HSPA1A
8	DNA IR-damage and cellular response via ATR WP4016	2,12E-03	10/80	BARD1;BRIP1;PCNA;PARP1;EXO1;H2AFX;RPA2;FOXM1;EEF1E1;MCM2
9	G1 to S cell cycle control WP45	2,24E-03	9/64	PCNA;MCM7;ORC1;CCNE1;ORC2;MCM4;E2F2;RPA2;MCM2
10	Cell Cycle WP179	3,16E-03	12/120	CDC20;CCNA2;PCNA;ORC1;MCM7;CCNE1;ORC2;MCM4;E2F2;SMC3;YWHAG;MCM2
11	Nucleotide Metabolism WP404	4,22E-03	5/19	DHFR;PRPS1;RRM2;MTHFD2;SRM
12	Nuclear Receptors Meta-Pathway WP2882	1,05E-02	20/319	HSP90AA1;HSP90AB1;SRXN1;PLK2;ABHD2;IRS2;SLC7A11;ADH7;PGD;SLC5A3;SLC7A5;THBD;DNAJB1;SEC14L1;SLC39A6;HMOX1;FGF13;EPHA2;HBEGF;HSPA1A
13	Pathogenic Escherichia coli infection WP2272	1,89E-02	7/55	TUBA1C;TUBB6;TUBA1B;ROCK2;NCL;EZR;TUBB4B
14	Trans-sulfuration and one carbon metabolism WP2525	3,75E-02	5/31	DHFR;MTHFD2;PSAT1;CTH;PHGDH
15	VEGFA-VEGFR2 Signaling Pathway WP3888	4,14E-02	15/236	HSP90AA1;ROCK2;SRF;RPS6;SHB;F3;MMP10;SLC8A1;NCL;PBK;EZR;EIF4E;HBEGF;ARF6;HSPA1A
16	mRNA Processing WP411	4,85E-02	10/126	SF3B4;PRPF4;SF3B5;SF3A1;SF3A2;NCBP1;CSTF1;DHX15;DDX20;HNRNPAB
17	Transcriptional cascade regulating adipogenesis WP4211	1,13E-01	3/13	KLF5;DDIT3;KLF2
18	Photodynamic therapy-induced unfolded protein response WP3613	1,28E-01	4/27	DDIT3;DNAJB11;TRIB3;CALR
19	Pyrimidine metabolism WP4022	1,54E-01	7/85	RRM2;POLR1B;CAD;POLD2;POLR1D;DCTPP1;NME1
20	Gastric Cancer Network 1 WP2361	1,57E-01	4/29	RUVBL1;MCM4;MYBL2;E2F7

Control; low - Day3; high - TGFb; high

	Term	Adjusted P-value	Overlap	Genes
1	VEGFA-VEGFR2 Signaling Pathway WP3888	1,47E-03	10/236	NRP2;ITGB3;GPC1;CAPN2;ACKR3;FLNB;PTGS2;ETS1;VCL;RND1
2	Focal Adhesion WP306	1,04E-02	8/198	ACTN1;ITGB3;CAPN2;ZYX;VEGFC;FLNB;VCL;MYL12A
3	MAPK Signaling Pathway WP382	3,12E-02	8/246	TGFB1;DUSP10;MRAS;GNA12;MAP3K20;FLNB;DUSP8;DUSP7
4	Epithelial to mesenchymal transition in colorectal cancer WP4239	4,90E-02	6/159	NRP2;ZEB2;TGFB1;SNAI1;PKP1;WNT7A
5	Primary Focal Segmental Glomerulosclerosis FSGS WP2572	1,14E-01	4/72	TGFB1;PODXL;ITGB3;VCL
6	Integrin-mediated Cell Adhesion WP185	1,79E-01	4/101	ITGB3;CAPN2;ZYX;VCL
7	Aryl Hydrocarbon Receptor WP2586	1,92E-01	3/46	NRIP1;CYP1B1;PTGS2
8	Mammary gland development pathway - Embryonic development (Stage 1 of 4) WP2	1,94E-01	2/15	ZEB2;TGFB1
9	Hepatitis C and Hepatocellular Carcinoma WP3646	2,04E-01	3/49	TGFB1;PODXL;PTGS2
10	Estrogen Receptor Pathway WP2881	2,07E-01	2/13	PDK4;CYP1B1
11	TGF-B Signaling in Thyroid Cells for Epithelial-Mesenchymal Transition WP3859	2,14E-01	2/18	TGFB1;SNAI1
12	Vitamin D Receptor Pathway WP2877	2,21E-01	5/182	TGFB1;DUSP10;TPM1;NRIP1;TIMP3
13	Regulation of Actin Cytoskeleton WP51	2,28E-01	5/150	MRAS;ACTN1;F2R;GNA12;VCL
14	Simplified Interaction Map Between LOXL4 and Oxidative Stress Pathway WP3670	2,32E-01	2/18	BMP2;TGFB1
15	Ebola Virus Pathway on Host WP4217	3,08E-01	4/129	NPC1;ACTN1;ITGB3;FLNB
16	TGF-beta Signaling Pathway WP366	3,12E-01	4/132	ZEB2;TGFB1;ITGB3;ETS1
17	Cytokines and Inflammatory Response WP530	3,18E-01	2/26	CSF2;TGFB1
18	Chromosomal and microsatellite instability in colorectal cancer WP4216	3,26E-01	3/73	TGFB1;PTGS2;GADD45G
19	Selective expression of chemokine receptors during T-cell polarization WP4494	3,72E-01	2/29	CSF2;TGFB1
20	Matrix Metalloproteinases WP129	3,77E-01	2/30	MMP24;TIMP3

Control; low - Day3; low - TGFb; high

	Term	Adjusted P-value	Overlap	Genes
1	Focal Adhesion WP306	3,72E-04	14/198	ITGB1;ACTN1;ITGA2;PDGFB;FN1;PDGFA;PARVB;THBS1;EGFR;COL1A1;COL4A2;COL5A3;TLN1;PPP1R12B
2	Epithelial to mesenchymal transition in colorectal cancer WP4239	5,84E-04	12/159	NOTCH2;FZD1;DLL4;CLDN4;SMAD3;FZD2;JAG1;ZEB1;COL4A2;WNT7B;FN1;TGFBR1
3	Differentiation Pathway WP2848	6,77E-04	7/48	IL11;NT5E;FST;WNT7B;PDGFB;PDGFA;INHBA
4	miRNA targets in ECM and membrane receptors WP2911	1,04E-03	5/22	COL5A1;COL4A2;COL5A3;FN1;THBS1
5	TGF-beta Receptor Signaling WP560	1,14E-03	7/54	SMAD3;FST;SERPINE1;INHBA;THBS1;TGFBR1;SMAD7
6	Senescence and Autophagy in Cancer WP615	1,29E-03	9/105	SH3GLB1;COL1A1;MMP14;SMAD3;SERPINE1;LAMP2;FN1;INHBA;THBS1
7	Focal Adhesion-PI3K-Akt-mTOR-signaling pathway WP3932	1,69E-03	15/303	ITGB1;ITGA2;PDGFB;FN1;PDGFA;THBS1;EGFR;COL1A1;COL4A2;COL5A1;PIK3IP1;CREB3L1;COL5A3;CREB3L2;DDIT4
8	Nanoparticle-mediated activation of receptor signaling WP2643	2,27E-03	5/28	ITGB1;COL1A1;FN1;TLN1;EGFR
9	Canonical and Non-Canonical TGF-B signaling WP3874	4,01E-03	4/17	SMAD3;BMPR2;TGFBR1;LOXL2
10	TGF-beta Signaling Pathway WP366	4,72E-03	9/132	ITGB1;CDKN2B;SMAD3;ZEB1;ITGA2;FN1;THBS1;TGFBR1;SMAD7
11	Neovascularisation processes WP4331	7,89E-03	4/21	DLL4;SMAD3;JAG1;TGFBR1
12	ESC Pluripotency Pathways WP3931	8,83E-03	8/116	FZD1;FZD2;BMPR2;WNT7B;PDGFB;PDGFA;EGFR;SMAD7
13	PI3K-Akt Signaling Pathway WP4172	1,17E-02	14/340	ITGB1;ITGA2;PDGFB;FN1;PDGFA;THBS1;EGFR;COL1A1;COL4A2;CREB3L1;CREB3L2;DDIT4;PIK3AP1;TLR2
14	Notch Signaling WP268	1,33E-02	5/45	NOTCH2;DLL4;JAG1;DTX3L;DTX4
15	Inflammatory Response Pathway WP453	2,40E-02	4/30	COL1A1;FN1;TNFRSF1B;THBS1
16	Osteoclast Signaling WP12	3,65E-02	3/16	ATP6V1G1;PDGFB;SLC9A1
17	Regulation of Actin Cytoskeleton WP51	3,65E-02	8/150	ACTN1;PDGFB;FN1;PDGFA;MSN;IQGAP1;EGFR;SLC9A1
18	TYROBP Causal Network WP3945	3,78E-02	5/61	CREB3L2;TNFRSF1B;TGFBR1;ZFP36L2;IL13RA1
19	miR-509-3p alteration of YAP1/ECM axis WP3967	3,92E-02	3/17	COL1A1;COL5A1;FN1
20	NOTCH1 regulation of human endothelial cell calcification WP3413	4,14E-02	3/17	DLL4;JAG1;SAT1

Control; high - Day3; high - TGFb; low

	Term	Adjusted P-value	Overlap	Genes
1	Selenium Micronutrient Network WP15	1,70E-02	7/86	PRDX3;RFK;PRDX1;ALB;DIO3;APOA1;SOD2
2	Photodynamic therapy-induced NFE2L2 (NRF2) survival signaling WP3612	2,61E-02	4/24	GCLC;GSTP1;FOS;NFE2L2
3	One carbon metabolism and related pathways WP3940	3,48E-02	5/52	GCLC;PCYT2;CHKA;SHMT1;SOD2
4	Folate Metabolism WP176	4,55E-02	5/66	RFK;SHMT1;ALB;APOA1;SOD2
5	Oxidative Stress WP408	4,66E-02	4/33	GCLC;FOS;SOD2;NFE2L2
6	Nuclear Receptors Meta-Pathway WP2882	4,93E-02	11/319	SLC26A2;GCLC;GPAM;GSTA4;FTH1;MGST3;PRDX1;GSTP1;APOA1;ACADM;NFE2L2
7	ID signaling pathway WP53	5,61E-02	3/16	ID2;ID1;ID3
8	NRF2 pathway WP2884	5,62E-02	7/146	GCLC;GSTA4;FTH1;MGST3;PRDX1;GSTP1;NFE2L2
9	miR-517 relationship with ARCN1 and USP1 WP3596	5,74E-02	2/5	ID2;ID1
10	let-7 inhibition of ES cell reprogramming WP3299	7,70E-02	2/6	TRIM71;KLF4
11	Hair Follicle Development: Cytodifferentiation (Part 3 of 3) WP2840	1,00E-01	5/87	KRT19;NOTCH1;IGFBP5;PERP;FOS
12	Adipogenesis WP236	1,04E-01	6/130	SOCS3;CEBPA;EPAS1;NAMPT;ID3;AGT
13	Preimplantation Embryo WP3527	1,21E-01	4/58	ESRRA;CDH1;ATP1A1;KLF4
14	Mammary gland development pathway - Involution (Stage 4 of 4) WP2815	1,60E-01	2/10	SOCS3;CDH1
15	SRF and miRs in Smooth Muscle Differentiation and Proliferation WP1991	1,70E-01	2/11	CCND2;KLF4
16	Fatty Acid Beta Oxidation WP143	1,74E-01	3/34	ACADM;HADH;ACAT1
17	Nonalcoholic fatty liver disease WP4396	1,74E-01	6/155	SOCS3;CEBPA;NDUFB11;UQCRFS1;SDHD;MAP3K5
18	Kennedy pathway from Sphingolipids WP3933	2,12E-01	2/13	PCYT2;CHKA
19	Role of Osx and miRNAs in tooth development WP3971	2,41E-01	2/15	NOTCH1;KLF4
20	Amino Acid metabolism WP3925	2,44E-01	4/91	ACADM;HADH;FAH;GLUL

Control; high - Day3; low - TGFb; high

	Term	Adjusted P-value	Overlap	Genes
1	Endochondral Ossification WP474	4,97E-01	4/64	KIF3A;ENPP1;ALPL;SOX9
2	Association Between Physico-Chemical Features and Toxicity Associated Pathways W	8,68E-01	3/66	TMSB4X;FZD8;CAMK1
3	T-Cell Receptor and Co-stimulatory Signaling WP2583	8,70E-01	3/29	DYRK2;PRKCA;PDK1
4	Human Complement System WP2806	8,75E-01	4/97	CRP;PROS1;CFI;PRKCA
5	Fibrin Complement Receptor 3 Signaling Pathway WP4136	9,20E-01	2/37	CCL2;LBP
6	Spinal Cord Injury WP2431	9,41E-01	4/118	CCL2;PRKCA;CXCL1;SOX9
7	ErbB Signaling Pathway WP673	9,43E-01	3/91	NCK2;PRKCA;PDK1
8	Insulin Signaling WP481	9,65E-01	4/160	PFKL;KIF3A;ENPP1;PRKCA
9	Photodynamic therapy-induced HIF-1 survival signaling WP3614	9,68E-01	2/37	PFKL;TGFB3
10	Target Of Rapamycin (TOR) Signaling WP1471	9,72E-01	2/36	ULK2;PRKCA
11	LncRNA involvement in canonical Wnt signaling and colorectal cancer WP4258	9,76E-01	3/94	CTNNBIP1;FZD8;CXXC4
12	Platelet-mediated interactions with vascular and circulating cells WP4462	1,00E+00	2/17	TGFB3;CCL2
13	Regulation of Wnt/B-catenin Signaling by Small Molecule Compounds WP3664	1,00E+00	2/17	LRP1;FZD8
14	Complement and Coagulation Cascades WP558	1,00E+00	3/58	PROS1;CFI;CLU
15	Wnt Signaling WP428	1,00E+00	4/115	CTNNBIP1;FZD8;PRKCA;CXXC4
16	Oncostatin M Signaling Pathway WP2374	1,00E+00	3/65	CCL2;PRKCA;JUNB
17	PDGFR-beta pathway WP3972	1,00E+00	2/29	STAT6;PRKCA
18	Oligodendrocyte Specification and differentiation(including remyelination), leading t	1,00E+00	2/30	CXCL1;SOX9
19	Ectoderm Differentiation WP2858	1,00E+00	4/138	TSC22D1;FZD8;CCL2;OGT
20	Fluoropyrimidine Activity WP1601	1,00E+00	2/33	ABCC5;GGH

Control; high - Day3; low - TGFb; low

	Term	Adjusted P-value	Overlap	Genes
1	DNA Damage Response (only ATM dependent) WP710	8,44E-03	8/110	TCF7L2;FRAT1;CDKN1B;MAP3K1;SCP2;CAT;PTEN;CTNNB1
2	Mitochondrial LC-Fatty Acid Beta-Oxidation WP368	1,59E-02	4/17	CPT1A;SCP2;SLC25A20;ACSF2
3	PTF1A related regulatory pathway WP4147	3,46E-02	3/11	KAT2B;CTNNB1;HES1
4	Sudden Infant Death Syndrome (SIDS) Susceptibility Pathways WP706	2,04E-01	7/158	C4B;CPT1A;CTNNB1;HES1;GPD1L;PPARGC1A;VAMP2
5	Circadian rhythm related genes WP3594	2,47E-01	8/201	CPT1A;DDX5;DBP;NAGLU;RORC;PTEN;PPARGC1A;OGT
6	Nuclear Receptors Meta-Pathway WP2882	2,77E-01	10/319	SLC6A6;KAT2B;CPT1A;CDKN1B;SCP2;MGST2;SLC39A10;STOM;HES1;PPARGC1A
7	Endometrial cancer WP4155	2,95E-01	4/63	TCF7L2;PTEN;CTNNB1;FGFR3
8	Factors and pathways affecting insulin-like growth factor (IGF1)-Akt signaling WP385	2,99E-01	3/31	PTEN;TNFSF9;PPARGC1A
9	Fatty Acid Beta Oxidation WP143	3,11E-01	3/34	CPT1A;SLC25A20;DECR1
10	PI3K-AKT-mTOR signaling pathway and therapeutic opportunities WP3844	3,11E-01	3/30	CDKN1B;PTEN;FOXO4
11	Oxidative Damage WP3941	4,44E-01	3/40	C4B;CDKN1B;MAP3K1
12	NOTCH1 regulation of human endothelial cell calcification WP3413	6,08E-01	2/17	ITGA1;FGFR3
13	TYROBP Causal Network WP3945	7,13E-01	3/61	MAF;NPC2;SFT2D2
14	Breast cancer pathway WP4262	7,27E-01	5/154	TCF7L2;FRAT1;PTEN;CTNNB1;HES1
15	Complement and Coagulation Cascades WP558	7,31E-01	3/58	C4B;MASP1;F5
16	Triacylglyceride Synthesis WP325	7,40E-01	2/24	DGAT2;GPD1
17	PPAR Alpha Pathway WP2878	7,42E-01	2/26	CPT1A;SCP2
18	miRNA targets in ECM and membrane receptors WP2911	7,47E-01	2/22	LAMB2;ITGA1
19	Wnt Signaling Pathway WP363	7,61E-01	3/52	TCF7L2;FRAT1;CTNNB1
20	Neural Crest Differentiation WP2064	7,69E-01	4/101	HDAC11;CTNNB1;HES1;FGFR3

Control; high - Day9; low - TGFb; high

	Term	Adjusted P-value	Overlap	Genes
1	Trans-sulfuration and one carbon metabolism WP2525	4,78E-03	5/31	DHFR;AHCY;SHMT1;MTR;GCLM
2	One Carbon Metabolism WP241	8,09E-03	5/30	DHFR;AHCY;ATIC;SHMT1;MTR
3	ErbB Signaling Pathway WP673	1,00E-02	7/91	CCND1;NCK2;PRKCA;SOS1;AREG;EGFR;PDK1
4	Trans-sulfuration pathway WP2333	1,73E-02	3/10	AHCY;MTR;GCLM
5	Retinoblastoma Gene in Cancer WP2446	2,29E-02	6/87	TOP2A;BARD1;DHFR;CCNB2;CCND1;SMC3
6	Cell Cycle WP179	2,42E-02	7/120	CCNB2;RBL1;CCND1;CDC27;PLK1;SMC3;BUB1
7	Gastric Cancer Network 1 WP2361	2,53E-02	4/29	TOP2A;CENPF;UBE2C;MYBL2
8	Disorders of Folate Metabolism and Transport WP4259	2,69E-02	3/13	DHFR;ATIC;MTR
9	Regulation of sister chromatid separation at the metaphase-anaphase transition WP4240	2,80E-02	3/15	CENPE;SMC3;BUB1
10	TGF-beta Signaling Pathway WP366	3,00E-02	7/132	CCNB2;RBL1;CCND1;SOS1;MET;TGFBR1;PDK1
11	Non-small cell lung cancer WP4255	3,07E-02	5/66	CCND1;PRKCA;SOS1;EGFR;PDK1
12	Folate Metabolism WP176	3,35E-02	5/66	CRP;DHFR;AHCY;SHMT1;MTR
13	Methionine De Novo and Salvage Pathway WP3580	6,21E-02	3/22	MTAP;AHCY;MTR
14	One carbon metabolism and related pathways WP3940	8,46E-02	4/52	SHMT1;GSR;MTR;GCLM
15	Nanoparticle-mediated activation of receptor signaling WP2643	1,09E-01	3/28	SOS1;AREG;EGFR
16	T-Cell Receptor and Co-stimulatory Signaling WP2583	1,13E-01	3/29	DYRK2;PRKCA;PDK1
17	Gastric Cancer Network 2 WP2363	1,15E-01	3/31	TOP2A;UBE2C;EGFR
18	Extracellular vesicle-mediated signaling in recipient cells WP2870	1,17E-01	3/30	MET;EGFR;TGFBR1
19	Ethanol effects on histone modifications WP3996	1,22E-01	3/31	DHFR;AHCY;MTR
20	Methionine metabolism leading to Sulphur Amino Acids and related disorders WP4292	1,45E-01	2/11	AHCY;MTR

Control; low - Day9; low - TGFb; high

	Term	Adjusted P-value	Overlap	Genes
1	PDGF Pathway WP2526	4,30E-02	5/39	MAP2K1;SRF;RASA1;PDGFA;JAK1
2	Epithelial to mesenchymal transition in colorectal cancer WP4239	4,83E-02	8/159	DLL4;MAP2K1;NRP2;JAG1;ZEB1;COL4A2;WNT7B;WNT7A
3	ESC Pluripotency Pathways WP3931	5,39E-02	7/116	MAP2K1;BMPR2;WNT7B;PDGFA;WNT7A;SMAD7;JAK1
4	Retinoblastoma Gene in Cancer WP2446	5,44E-02	6/87	ANLN;POLA1;RRM1;PRKDC;MCM4;POLE
5	TGF-beta Signaling Pathway WP366	6,64E-02	7/132	MAP2K1;CDKN2B;ZEB1;ITGA2;E2F4;THBS1;SMAD7
6	ncRNAs involved in STAT3 signaling in hepatocellular carcinoma WP4337	6,69E-02	3/13	IL11;ZEB1;JAK1
7	PDGFR-beta pathway WP3972	8,40E-02	4/29	MAP2K1;SRF;RASA1;JAK1
8	Mesodermal Commitment Pathway WP2857	8,66E-02	7/147	EXT1;EPB41L5;CCDC88A;TCF7L1;BMPR2;AEBP2;SRF
9	VEGFA-VEGFR2 Signaling Pathway WP3888	8,68E-02	9/236	RAP1B;DLL4;NRP2;MAP2K1;JAG1;GPC1;SRF;CAPN2;IQGAP1
10	Interleukin-11 Signaling Pathway WP2332	9,29E-02	4/44	IL11;MAP2K1;ITGA2;JAK1
11	Imatinib and Chronic Myeloid Leukemia WP3640	9,41E-02	3/20	SPRED2;PIM1;GAB2
12	Focal Adhesion WP306	9,80E-02	8/198	RAP1B;MAP2K1;COL4A2;ITGA2;CAPN2;PDGFA;PARVB;THBS1
13	TGF-beta Receptor Signaling WP560	1,27E-01	4/54	SERPINE1;THBS1;JAK1;SMAD7
14	ncRNAs involved in Wnt signaling in hepatocellular carcinoma WP4336	1,28E-01	5/86	TCF7L1;WNT7B;KREMEN1;WNT7A;ROR1
15	LncRNA involvement in canonical Wnt signaling and colorectal cancer WP4258	1,62E-01	5/94	TCF7L1;WNT7B;KREMEN1;WNT7A;ROR1
16	Signaling of Hepatocyte Growth Factor Receptor WP313	2,19E-01	3/34	RAP1B;MAP2K1;RASA1
17	Focal Adhesion-PI3K-Akt-mTOR-signaling pathway WP3932	2,66E-01	9/303	MAP2K1;PHLPP1;COL4A2;ITGA2;DDIT4;F2R;PDGFA;THBS1;JAK1
18	Serotonin Receptor 4/6/7 and NR3C Signaling WP734	2,72E-01	2/19	MAP2K1;SRF
19	Genes targeted by miRNAs in adipocytes WP1992	2,76E-01	2/13	HCN4;SRF
20	IL-3 Signaling Pathway WP286	2,79E-01	3/49	MAP2K1;GAB2;JAK1

Control; low - Day9; high - TGFb; high

	Term	Adjusted P-value	Overlap	Genes
1	Focal Adhesion WP306	3,86E-06	14/198	ITGB1;ACTN1;ITGB3;PDGFB;FN1;VEGFC;MYL12A;COL1A1;COL5A3;ZYX;FLNB;TLN1;PPP1R12B;VCL
2	Senescence and Autophagy in Cancer WP615	9,61E-05	9/105	COL1A1;BMP2;MMP14;TGFB1;SMAD3;IGFBP3;SERPINE1;FN1;INHBA
3	TGF-B Signaling in Thyroid Cells for Epithelial-Mesenchymal Transition WP3859	9,67E-05	5/18	CDH6;TGFB1;SMAD3;FN1;SNAI1
4	Epithelial to mesenchymal transition in colorectal cancer WP4239	1,00E-04	11/159	FOXQ1;NOTCH2;FZD1;CLDN4;ZEB2;TGFB1;SMAD3;FZD2;FN1;SNAI1;PKP1
5	Mammary gland development pathway - Embryonic development (Stage 1 of 4) WP	9,97E-04	4/15	ITGB1;CLDN4;ZEB2;TGFB1
6	TGF-beta Receptor Signaling WP560	1,03E-03	6/54	ZEB2;TGFB1;SMAD3;FST;SERPINE1;INHBA
7	Neural Crest Differentiation WP2064	3,77E-03	7/101	CDH6;NOTCH2;ITGB1;HDAC11;SNAI1;ETS1;RHOB
8	Primary Focal Segmental Glomerulosclerosis FSGS WP2572	4,06E-03	6/72	ITGB1;TGFB1;ITGB3;MYH9;TLN1;VCL
9	Differentiation Pathway WP2848	5,09E-03	5/48	NT5E;TGFB1;FST;PDGFB;INHBA
10	Nanoparticle-mediated activation of receptor signaling WP2643	6,78E-03	4/28	ITGB1;COL1A1;FN1;TLN1
11	TGF-beta Signaling Pathway WP366	1,17E-02	7/132	ITGB1;ZEB2;TGFB1;SMAD3;ITGB3;FN1;ETS1
12	Osteoblast Signaling WP322	1,28E-02	3/14	COL1A1;ITGB3;PDGFB
13	Osteoclast Signaling WP12	1,64E-02	3/16	ITGB3;PDGFB;SLC9A1
14	VEGFA-VEGFR2 Signaling Pathway WP3888	1,66E-02	9/236	ITGB1;MMP14;ITGB3;MYH9;ACKR3;FLNB;PTGS2;ETS1;VCL
15	miR-509-3p alteration of YAP1/ECM axis WP3967	1,71E-02	3/17	COL1A1;COL5A1;FN1
16	Simplified Interaction Map Between LOXL4 and Oxidative Stress Pathway WP3670	1,91E-02	3/18	BMP2;TGFB1;FN1
17	Focal Adhesion-PI3K-Akt-mTOR-signaling pathway WP3932	2,08E-02	10/303	COL1A1;ITGB1;COL5A1;CREB3L1;COL5A3;ITGB3;CREB3L2;PDGFB;FN1;VEGFC
18	miRNA targets in ECM and membrane receptors WP2911	3,12E-02	3/22	COL5A1;COL5A3;FN1
19	MicroRNAs in cardiomyocyte hypertrophy WP1544	3,29E-02	5/84	FZD1;TGFB1;FZD2;CISH;MAP3K14
20	Ebola Virus Pathway on Host WP4217	3,58E-02	6/129	ITGB1;NPC1;ACTN1;ITGB3;FLNB;RHOB

Control; low - Day9; high - TGFb; low

	Term	Adjusted P-value	Overlap	Genes
1	Matrix Metalloproteinases WP129	1,93E-03	5/30	MMP24;MMP13;MMP3;TIMP2;MMP10
2	Oncostatin M Signaling Pathway WP2374	4,44E-02	5/65	NFKBIA;MMP13;MMP3;OSMR;IL6ST
3	Endochondral Ossification WP474	2,91E-01	4/64	MMP13;PLAT;NKX3-2;IGF1R
4	DNA Damage Response (only ATM dependent) WP710	3,96E-01	4/110	CDKN2A;PIK3R3;FOXO3;BBC3
5	miRNA targets in ECM and membrane receptors WP2911	4,04E-01	2/22	COL6A2;COL6A1
6	Chemokine signaling pathway WP3929	4,05E-01	5/164	NFKBIA;ELMO1;PIK3R3;FOXO3;CXCL16
7	Focal Adhesion-PI3K-Akt-mTOR-signaling pathway WP3932	4,14E-01	7/303	FOXA1;LAMA5;PIK3IP1;COL6A2;FOXO3;OSMR;IGF1R
8	Senescence and Autophagy in Cancer WP615	4,23E-01	4/105	CDKN2A;PLAT;IL6ST;IGF1R
9	Platelet-mediated interactions with vascular and circulating cells WP4462	4,35E-01	2/17	VCAM1;TGFB3
10	Simplified Interaction Map Between LOXL4 and Oxidative Stress Pathway WP3670	4,38E-01	2/18	ANXA5;LOXL4
11	Vitamin D Receptor Pathway WP2877	4,41E-01	5/182	CDKN2A;ID4;TIMP2;GXYLT2;SLC8A1
12	TP53 Network WP1742	4,42E-01	2/19	CDKN2A;BBC3
13	PI3K-Akt Signaling Pathway WP4172	4,63E-01	8/340	LAMA5;COL6A2;COL6A1;PIK3R3;FOXO3;OSMR;PIK3AP1;IGF1R
14	Non-small cell lung cancer WP4255	4,64E-01	3/66	CDKN2A;PIK3R3;FOXO3
15	Canonical and Non-Canonical TGF-B signaling WP3874	4,89E-01	2/17	GREM1;LOXL4
16	Apoptosis Modulation and Signaling WP1772	5,16E-01	4/91	NFKBIA;CDKN2A;PTPN13;BBC3
17	Adipogenesis WP236	5,44E-01	4/130	KLF6;CEBPD;AHR;IL6ST
18	PI3K-AKT-mTOR signaling pathway and therapeutic opportunities WP3844	5,84E-01	2/30	PIK3R3;FOXO3
19	Apoptosis WP254	5,84E-01	4/84	NFKBIA;CDKN2A;BBC3;IGF1R
20	Signal transduction through IL1R WP4496	6,06E-01	2/33	NFKBIA;TGFB3

Control; high - Day9; low - TGFb; low

	Term	Adjusted P-value	Overlap	Genes
1	Amino Acid metabolism WP3925	1,40E-02	6/91	GLUD1;HIBADH;MDH1;CTH;HADH;GLUL
2	Nuclear Receptors Meta-Pathway WP2882	1,42E-02	11/319	FGD4;SLC26A2;GCLC;ABCC2;GPAM;MGST3;PRDX1;GSTP1;STOM;HES1;SLC7A11
3	Selenium Micronutrient Network WP15	1,71E-02	6/86	PRDX3;RFK;PRDX1;CTH;CAT;SOD2
4	Pathways in clear cell renal cell carcinoma WP4018	2,40E-02	6/85	FLT1;MDH1;PSAT1;PTEN;ALDOB;VHL
5	Photodynamic therapy-induced NFE2L2 (NRF2) survival signaling WP3612	2,48E-02	4/24	NQO2;GCLC;ABCC2;GSTP1
6	Metabolic reprogramming in colon cancer WP4290	3,85E-02	4/42	GLUD1;PSAT1;PDHB;ALDOB
7	One carbon metabolism and related pathways WP3940	7,45E-02	4/52	GCLC;PCYT2;CTH;SOD2
8	NRF2 pathway WP2884	1,07E-01	6/146	GCLC;ABCC2;MGST3;PRDX1;GSTP1;SLC7A11
9	Sterol Regulatory Element-Binding Proteins (SREBP) signalling WP1982	1,14E-01	4/69	MDH1;GPAM;INSIG1;LSS
10	Oxidative Stress WP408	1,17E-01	3/33	GCLC;CAT;SOD2
11	DNA Damage Response (only ATM dependent) WP710	1,21E-01	5/110	TCF7L2;FRAT1;CAT;PTEN;SOD2
12	Folate Metabolism WP176	1,26E-01	4/66	RFK;CTH;CAT;SOD2
13	Trans-sulfuration and one carbon metabolism WP2525	1,30E-01	3/31	GCLC;PSAT1;CTH
14	Cysteine and methionine catabolism WP4504	2,18E-01	2/14	GCLC;CTH
15	Phytochemical activity on NRF2 transcriptional activation WP3	2,19E-01	2/15	GCLC;SLC7A11
16	Cholesterol Biosynthesis Pathway WP197	2,33E-01	2/15	SC5D;LSS
17	Amplification and Expansion of Oncogenic Pathways as Metastatic Traits WP3678	2,64E-01	2/17	TCF7L2;VHL
18	TCA Cycle (aka Krebs or citric acid cycle) WP78	2,79E-01	2/18	IDH3B;SDHD
19	Breast cancer pathway WP4262	2,86E-01	5/154	TCF7L2;FRAT1;FRAT2;PTEN;HES1
20	Preimplantation Embryo WP3527	3,37E-01	3/58	CDX2;CDH1;ATP1A1

Control; high - Day9; high - TGFb; low

	Term	Adjusted P-value	Overlap	Genes
1	Transcriptional cascade regulating adipogenesis WP4211	1,38E-02	4/13	CEBPA;EGR2;KLF5;DDIT3
2	Nuclear Receptors Meta-Pathway WP2882	1,40E-02	18/319	GSTM2;JUN;JUND;ABCC5;SLC39A10;APOA1;ADH7;TGFBR2;TGFBR3;SLC7A5;THBD;SCP2;GSTA4;FTH1;HES1;ACADM;HBEGF;NFE2L2
3	Adipogenesis WP236	1,47E-02	11/130	SOCS3;CEBPA;EGR2;KLF5;EPAS1;DDIT3;NAMPT;ID3;RORA;LIFR;AGT
4	IL-2 Signaling Pathway WP49	1,52E-02	6/42	SOCS3;JUN;CCND2;PIK3R1;FOS;MAPT
5	Complement and Coagulation Cascades WP558	1,59E-02	7/58	C4B;FGB;THBD;C9;CFI;MASP1;F5
6	Mesodermal Commitment Pathway WP2857	1,63E-02	11/147	TRIM71;EPB41L5;ARL4A;KLF5;FZD5;GATA6;ARID5B;SMAD6;KLF4;NFE2L2;FOXA2
7	Photodynamic therapy-induced AP-1 survival signaling. WP3611	1,83E-02	7/50	JUN;BMF;FOS;MAP3K5;HBEGF;MCL1;NFE2L2
8	White fat cell differentiation WP4149	2,20E-02	6/32	CEBPA;EGR2;KLF5;DDIT3;RORA;KLF4
9	Vitamin D Receptor Pathway WP2877	2,48E-02	12/182	SULT1C2;THBD;CEBPA;CYP2S1;ID1;HSD17B2;S100A6;CD14;ATP2B1;EFNA5;MXD1;KLF4
10	Nuclear Receptors WP170	5,28E-02	5/38	ESRRA;NR4A1;THRA;RORC;RORA
11	Notch Signaling Pathway WP61	6,74E-02	6/61	TLE1;NOTCH1;HEY1;HES1;MAPT;PIK3R1
12	Physiological and Pathological Hypertrophy of the Heart WP1528	7,27E-02	4/25	JUN;LIFR;FOS;AGT
13	Heart Development WP1591	7,93E-02	5/44	NOTCH1;HEY1;ERBB3;GATA6;FOXA2
14	Selenium Metabolism and Selenoproteins WP28	8,39E-02	5/46	JUN;DIO1;DIO3;FOS;NFE2L2
15	PDGFR-beta pathway WP3972	8,79E-02	4/29	JUN;MAP3K1;PIK3R1;FOS
16	Aryl Hydrocarbon Receptor Pathway WP2873	8,99E-02	5/46	SLC7A5;JUN;JUND;HES1;NFE2L2
17	Human Complement System WP2806	9,66E-02	7/97	FGB;C9;CFI;ALB;APOA1;MASP1;CPN1
18	miR-517 relationship with ARCN1 and USP1 WP3596	9,91E-02	2/5	ID2;ID1
19	let-7 inhibition of ES cell reprogramming WP3299	1,01E-01	2/6	TRIM71;KLF4
20	TGF-beta Receptor Signaling WP560	1,01E-01	5/54	TGFBR3;JUN;FOS;SMAD6;TGFBR2